OCT 2 2 1923

Eighth Annual Meeting, Optical Society of America
Cleveland, Ohio, October 25, 26, 27, 1923

Volume 7 Number 10

Journal of the Optical Society of America and Review of Scientific Instruments

EDITOR-IN-CHIEF: PAUL D. FOOTE
BUREAU OF STANDARDS, WASHINGTON, D. C.

ASSISTANT EDITOR-IN-CHIEF AND BUSINESS MANAGER: F. K. RICHTMYER
CORNELL UNIVERSITY, ITHACA, N. Y.

CONSULTING BUSINESS MANAGER, M. E. LEEDS, PHILADELPHIA, PA.

Associate Editors:

Term Ending Dec. 31, 1927	Term Ending Dec. 31, 1925	Term Ending Dec. 31, 1923
H. D. CURTIS	G. K. BURGESS	W. T. BOVIE
E. P. HYDE	K. T. COMPTON	H. G. GALE
PAUL E. KLOPSTEG	L. R. INGERSOLL	HERBERT E. IVES
L. SILBERSTEIN	C. E. K. MEES	W. B. LANCASTER
L. T. TROLAND	C. E. MENDENHALL	F. G. NUTTING
F. E. WRIGHT	D. C. MILLER	J. P. C. SOUTHALL

OCTOBER, 1923

The Formation of Interference Figures. A Study of the Phenomena Exhibited by Transparent Inactive Crystal Plates in Convergent Polarized Light 779
F. E. WRIGHT

Stages in the Excitation of the Spectra of Thallium 819
F. L. MOHLER and ARTHUR E. RUARK

INSTRUMENT SECTION

An Instrument for the Testing of Prisms 831
G. W. MOFFITT

A Spectrometer Table 853
B. J. SPENCE

An Apparatus for Testing the Perception of Depth 857
HERMANN KELLNER

Longitudinal Aberration in Aspherical Optical Systems 861
IRWIN ROMAN

Some Properties of Atoms and Electrons as Measured by Students 873
FREDERIC PALMER, JR.

A New Ocular Micrometer 889
HERMANN KELLNER

A Photometric Sectored Disk, Variable and Electrically Readable While in Rotation 893
ENOCH KARRER

Some Laboratory Notes 901
H. W. FARWELL

Design of a Kundt's Tube 905
OTTO STUHLMAN, JR.

A Constant Pressure Blowpipe 907
H. G. BECKER

Notes 818, 829, 830, 852, 856, 872, 887, 891, 899, 900, 906, 912

Reviews 888, 892, 903, 904

Index to Advertisers XXXV

Published Monthly by the
OPTICAL SOCIETY OF AMERICA

OFFICE OF PUBLICATION:
GEORGE BANTA PUBLISHING COMPANY
450-454 Ahnaip St.,
MENASHA, WISCONSIN

Entered as second-class matter May 31, 1921 at the postoffice at Menasha, Wis., under the act of March 3, 1879

Journal
of the
Optical Society of America
and
Review of Scientific Instruments

Published monthly beginning May 1922.
Annual Subscription $5.00

The JOURNAL of the Optical Society of America was first published in January 1917. Four separate issues appeared in 1917, and two issues in 1919. During the years 1920 (Vol. IV) and 1921 (Vol. V) the JOURNAL was published bi-monthly. Copies of back numbers may be secured from the Business Manager for $1.00 each. The total charge for all numbers from Vol. I to Vol. V, 1921 inclusive, is $16.00. Only a small stock of the earlier issues remains. The six numbers comprising Vols. I to III will not be sold except in complete sets with Vol. IV and V.

By cooperation with the Association of Scientific Apparatus Makers of the United States of America the scope of the JOURNAL was enlarged beginning January 1922. As indicated by the present title the JOURNAL now publishes original papers on instruments of every description as well as papers on experimental and applied optics. The new JOURNAL is published monthly beginning May 1922, making 10 issues for 1922.

Annual Subscription $5.00 dating from January of the current year. Single copies $0.60. Remittances for subscriptions and back numbers should be made to "F. K. Richtmyer, Manager," Cornell University, Ithaca, N. Y.

All correspondence on the following subjects must be made with the Business Manager: (1) Application for, and checks in payment of annual subscriptions other than those of members of the Optical Society; (2) Change in mailing address; (3) Missing numbers: these will be replaced free of charge only when notification is made within 30 days from date of the immediately succeeding issue; (4) All advertising accounts and applications for space and rates.

THE OPTICAL SOCIETY OF AMERICA

President—L. T. TROLAND,
Harvard University,
Cambridge, Mass.

Vice-President—H. E. IVES,
Western Electric Co.,
New York, N. Y.

Secretary—IRWIN G. PRIEST,
Bureau of Standards,
Washington, D. C.

Treasurer—ADOLPH LOMB,
Rochester, New York.

The Council consists of the above officers, the Editor-in-Chief and the Assistant Editor-in-Chief and Business Manager of the JOURNAL, the past President, James P. C. Southall, Columbia University, and the following elected members: Adelbert Ames, Dartmouth College, H. G. Gale, University of Chicago, Ernest Merritt, Cornell University and W. E. Forsythe, Nela Research Laboratories.

The object of the Optical Society of America is to serve the interests of all who are engaged in any branch of optics from fundamental research to the manufacture of optical goods.

The Constitution provides that anyone who has contributed materially to the advancement of optics shall be eligible to regular membership in the Society with the privilege of voting and holding office. Any individual or corporation interested in optics is eligible to associate membership. Annual dues including subscription to the JOURNAL are five dollars for individual membership and fifty dollars for corporation membership. Further information may be obtained from the Secretary.

Journal
of the
Optical Society of America
and
Review of Scientific Instruments

Vol. 7 OCTOBER, 1923 Number 10

THE FORMATION OF INTERFERENCE FIGURES A STUDY OF THE PHENOMENA EXHIBITED BY TRANSPARENT INACTIVE CRYSTAL PLATES IN CONVERGENT POLARIZED LIGHT

By F. E. Wright

Of the many phenomena observed by the student in crystal optics the most impressive and fascinating are interference figures. They present a remarkable combination of color display and symmetry of arrangement, which satisfies the eye and at once excites the student's interest. Early in the last century the essential features of interference figures were described and explained through the efforts of Fresnel, MacCullagh, F. E. Neumann, Hamilton, Sylvester, Cauchy, Plücker, Biot, Lloyd, and others. The connection between type of interference figure and crystal system of the crystal plate under observation was first noted by Brewster in 1819. After the application of polarized light to the study of minerals and rocks by H. Clifton-Sorby in 1858, the interference figures from minerals in the thin section furnished important diagnostic features in determinative work with the petrographic microscope. At the present time rock making minerals are classified in text books on microscopical petrography according to the type of interference figure they present. It might seem, therefore, that the phenomena exhibited by interference figures and the principles underlying their formation are thoroughly known in detail and that further work in this field is unnecessary. A review of the literature shows, however, that there is still lacking a coordinated presentation of the subject in which the influence of the many factors that enter into the formation of an interference figure is considered from a quantitative viewpoint. The present paper seeks to cover part of this field; in the course of the presentation certain novel lines of approach to

the subject are followed which have the advantage of simplicity and are applicable directly to the development of methods for the measurement of optic axial angles.

The index ellipsoid and index surface. In crystal optics a number of surfaces of reference have been derived and are described in the text books to aid the student in visualizing the spacial geometrical relations involved; but if presented one after another in rapid succession, as is commonly the case, they tend to confuse and to bewilder him; he finds it difficult to distinguish between them and to realize the significance of each; and, as a result, may fail to obtain a clear idea of any part of the subject. The remedy is obvious, namely, select the particular surface of reference best suited to the purpose at hand and adhere to it strictly to the practical exclusion of the other surfaces. In petrographic microscope work the interest centers chiefly in the effects produced on plane polarized waves on transmission through a crystal plate; this means primarily a consideration of wave fronts, wave normals, and refractive indices; for this purpose the index ellipsoid and the surface derived from it, the index surface, furnish the most direct mode of presentation. To employ any but the simplest possible surface of reference would appear to add to the difficulty of forming a mental picture of the optical and crystallographical relations. Once the simplest surface has been thoroughly mastered by the student it is easy for him to add other surfaces and to perceive their significance. It is believed that by thus reducing to a minimum the geometrical conceptions required by the petrographer a real advance can be made in the presentation of the subject.

The equation of a central ellipsoid of principal axes α, β, γ, $(\alpha < \beta < \gamma)$ and referred to these axes is

$$\frac{x^2}{\alpha^2} + \frac{y^2}{\beta^2} + \frac{z^2}{\gamma^2} = 1 \qquad (1$$

In problems in crystal optics this index ellipsoid is the surface of reference for a biaxial mineral having the principal refractive indices α, β, γ; it reduces to a rotation ellipsoid or spheroid in case $\alpha = \beta$ or $\beta = \gamma$ (uniaxial minerals) and to a sphere for $\alpha = \beta = \gamma = \rho$ (isotropic minerals). From the shape of the ellipsoid and its position within the crystal the optical behavior of the crystal can be ascertained.

The equation of a central sphere of radius ρ is

$$\frac{x^2}{\rho^2} + \frac{y^2}{\rho^2} + \frac{z^2}{\rho^2} = 1 \qquad (2)$$

On subtracting equation (2) from (1) we obtain

$$x^2\left(\frac{1}{\alpha^2}-\frac{1}{\rho^2}\right)+y^2\left(\frac{1}{\beta^2}-\frac{1}{\rho^2}\right)+z^2\left(\frac{1}{\gamma^2}-\frac{1}{\rho^2}\right)=0 \qquad (3)$$

which is, for a given ρ, a homogeneous equation of the second degree; it represents a central cone passing through the curve of intersection of the sphere with the index ellipsoid. Curves of intersection of a central sphere with a central quadric are called *spheroconics* and Salmon[1] has shown how the properties of spherical curves are readily obtained from the equations of the cones which join them to the center. With the aid of these curves many of the relations in crystal optics are rendered clear and readily grasped, and the derivation of the standard formulas in use in microscopical petrography is greatly simplified. In the following paragraphs the first attempt is made, so far as the writer is aware, thus to use spheroconics.

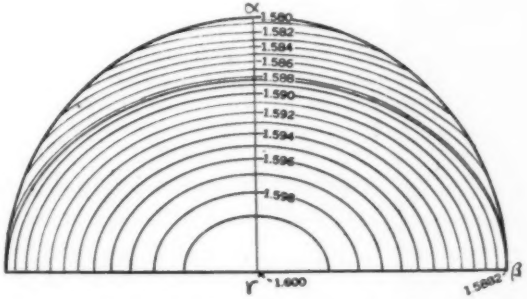

FIG. 1. *Orthographic projection of the equivibration curves (spheroconics) of a crystal having the principal refractive indices: $\alpha=1.580$, $\beta=1.5882$, $\gamma=1.600$. Only half of the projection is shown. The curve labeled 1.592 shows, for example, the positions in space of all radii vectors (vibration directions) of the index ellipsoid of length 1.592. Similarly for the other curves. The contour interval between two successive curves is 5 per cent of the difference, $\gamma-\alpha$.*

To find the locus of all radii of given length ρ_1, add the subscript to the ρ of equation (3); the curve thus represented is the desired curve; it is actually the curve of intersection of the ellipsoid with a sphere of radius ρ_1. For example by assigning different values of ρ in equation (3) for an index ellipsoid having the principal axes $\alpha=1.5800$, $\beta=1.5882$, $\gamma=1.6000$, we obtain a series of curves the orthographic projections of which on the x, y plane are shown in Fig. 1.

[1] Analytic Geometry of Three Dimensions, Fifth Edition, Revised by R. A. P. Rogers. I, Chapter X. London, 1912.

One of these curves is of special interest, namely, that for which $\rho=\beta$. In this case (3) reduces to the form

$$x^2\left(\frac{1}{\alpha^2}-\frac{1}{\beta^2}\right)-z^2\left(\frac{1}{\beta^2}-\frac{1}{\gamma^2}\right)=0 \tag{4}$$

or

$$\left(x\sqrt{\frac{1}{\alpha^2}-\frac{1}{\beta^2}}+z\sqrt{\frac{1}{\beta^2}-\frac{1}{\gamma^2}}\right)\left(x\sqrt{\frac{1}{\alpha^2}-\frac{1}{\beta^2}}-z\sqrt{\frac{1}{\beta^2}-\frac{1}{\gamma^2}}\right)=0 \tag{4a}$$

Equation (4a) is obviously the equation of two planes passing through the y-axis. The curve of intersection of each of these planes with the sphere is a circle and the planes are therefore called the planes of circular section or the cyclic planes. Equation (4a) can be written in the form

$$(lx+nz)\ (lx-nz)=0 \tag{4b}$$

wherein l and n are the direction cosines of the normals to the planes and are equal to

$$l=\frac{\sqrt{\frac{1}{\alpha^2}-\frac{1}{\beta^2}}}{\sqrt{\frac{1}{\alpha^2}-\frac{1}{\gamma^2}}};\quad n=\frac{\sqrt{\frac{1}{\beta^2}-\frac{1}{\gamma^2}}}{\sqrt{\frac{1}{\alpha^2}-\frac{1}{\gamma^2}}} \tag{5}$$

Let $n=\cos\ V_s$; then $l=\cos(90^\circ-V_s)$ and $2V_s$ is the angle between the normals to the two cyclic sections (optic axial angle). Equation (5) becomes

$$\sin^2V_s=\frac{\frac{1}{\alpha^2}-\frac{1}{\beta^2}}{\frac{1}{\alpha^2}-\frac{1}{\gamma^2}};\quad \cos^2V_s=\frac{\frac{1}{\beta^2}-\frac{1}{\gamma^2}}{\frac{1}{\alpha^2}-\frac{1}{\gamma^2}};\quad \tan^2V_s=\frac{\frac{1}{\alpha^2}-\frac{1}{\beta^2}}{\frac{1}{\beta^2}-\frac{1}{\gamma^2}} \tag{6}$$

The spheroconics represented by equation (3) are the curves of intersection of the index ellipsoid with a sphere of radius ρ. If now, for any given spheroconic, radii vectors be drawn from the origin to all points of the spheroconic, these radii vectors describe a central cone and equation (3) may be considered to represent this cone. A tangent plane to this central cone through any given point of the spheroconic is obviously a diametral plane whose curve of intersection with the index ellipsoid is an ellipse. The radius vector to the given point on the spheroconic is, moreover, one of the two principal axes of this ellipse, because it is normal to the spheroconic and therefore, as follows from the definition of the tangent plane, to the ellipse at this point.

The equation of the plane tangent to the central cone (3) at a point x', y', z' of the spheroconic is

$$xx'\left(\frac{1}{a^2}-\frac{1}{\rho^2}\right)+yy'\left(\frac{1}{\beta^2}-\frac{1}{\rho^2}\right)+zz'\left(\frac{1}{\gamma^2}-\frac{1}{\rho^2}\right)=0 \tag{7}$$

The equation of any diametral plane whose direction cosines are l, m, n is

$$lx+my+nz=0 \tag{8}$$

The conditions that this plane shall coincide with the tangent plane are, if k is the proportionality factor:

$$l=k\cdot x'\left(\frac{1}{a^2}-\frac{1}{\rho^2}\right);\quad m=ky'\left(\frac{1}{\beta^2}-\frac{1}{\rho^2}\right);\quad n=k\cdot z'\left(\frac{1}{\gamma^2}-\frac{1}{\rho^2}\right) \tag{9a}$$

or

$$\frac{l}{\sqrt{\frac{1}{a^2}-\frac{1}{\rho^2}}}=k\cdot x'\sqrt{\frac{1}{a^2}-\frac{1}{\rho^2}};\quad \frac{m}{\sqrt{\frac{1}{\beta^2}-\frac{1}{\rho^2}}}=k\cdot y'\sqrt{\frac{1}{\beta^2}-\frac{1}{\rho^2}};$$

$$\frac{n}{\sqrt{\frac{1}{\gamma^2}-\frac{1}{\rho^2}}}=k\cdot z'\sqrt{\frac{1}{\gamma^2}-\frac{1}{\rho^2}} \tag{9b}$$

On squaring and adding the last three expressions we find by noting equation (3)

$$\frac{l^2}{\frac{1}{a^2}-\frac{1}{\rho^2}}+\frac{m^2}{\frac{1}{\beta^2}-\frac{1}{\rho^2}}+\frac{n^2}{\frac{1}{\gamma^2}-\frac{1}{\rho^2}}=0 \tag{10}$$

This is the equation of the index surface. It can also be expressed in the form

$$\frac{1}{\rho^4}-\frac{1}{\rho^2}\left(\frac{l^2+m^2}{\gamma^2}+\frac{m^2+n^2}{a^2}+\frac{n^2+l^2}{\beta^2}\right)+\frac{a^2l^2+\beta^2m^2+\gamma^2n^2}{a^2\beta^2\gamma^2}=0 \tag{10a}$$

which is a quadratic equation in $\frac{1}{\rho^2}$; if, therefore, $\frac{1}{\rho_1{}^2}, \frac{1}{\rho_2{}^2}$ be the two roots of equation (10a), we have

$$\frac{1}{\rho_1{}^2}+\frac{1}{\rho_2{}^2}=\frac{l^2+m^2}{\gamma^2}+\frac{m^2+n^2}{a^2}+\frac{n^2+l^2}{\beta^2} \tag{10b}$$

$$\frac{1}{\rho_1{}^2}\times\frac{1}{\rho_2{}^2}=\frac{a^2l^2+\beta^2m^2+\gamma^2n^2}{a^2\beta^2\gamma^2} \tag{10c}$$

From these equations together with the equation, $l^2+m^2+n^2=1$, the direction cosines l, m, n of the section whose ellipse axes are ρ_1, ρ_2 can

be computed. For the section for which $\rho_1=\rho_2=\beta$, we find $m=0$ and $\frac{l^2}{\frac{1}{\alpha^2}-\frac{1}{\beta^2}}+\frac{n^2}{\frac{1}{\gamma^2}-\frac{1}{\beta^2}}=0$ from which we obtain directly expressions (6) for the value of the optic axial angle. Similarly for the case $\rho_1=\alpha$ and $\rho_2=\gamma$ we find $l=0$, $n=0$, $m=1$.

For any point (x, y, z) on the surface of the index ellipsoid we have $x=l\cdot\rho$, $y=m\cdot\rho$, $z=n\cdot\rho$ and the equation may be written

$$\frac{x^2}{\frac{1}{\alpha^2}-\frac{1}{\rho^2}}+\frac{y^2}{\frac{1}{\beta^2}-\frac{1}{\rho^2}}+\frac{z^2}{\frac{1}{\gamma^2}-\frac{1}{\rho^2}}=0 \tag{11}$$

which is, for a given ρ, a homogeneous equation of the second degree and therefore that of a central cone. It should be noted that in this form wherein ρ is considered a constant, equation (11), although similar to (10) in form, is not the equation of the index surface but that of a central cone. The intersection of this cone with a concentric sphere is a spheroconic which is the locus of the poles of all sections one of whose ellipse axes is ρ. It is easy to show by a comparison of the equation of the tangent plane of this cone, $\left(\frac{xx'}{\frac{1}{\alpha^2}-\frac{1}{\rho^2}}+\frac{yy'}{\frac{1}{\beta^2}-\frac{1}{\rho^2}}+\frac{zz'}{\frac{1}{\gamma^2}-\frac{1}{\rho^2}}=0\right.$, analogous to equation 7) with that of a central diametral plane (as in 8, 9a, 9b) that the two cones (3) and (11) bear reciprocal relations; in other words, every edge of the one is perpendicular to a tangent plane of the second; the cone (11) may be looked upon as the cone generated by perpendiculars erected at the vertex of (3) to its several tangent planes.

It is thus possible with the aid of the equations (3) and (11) which represent central cones, to draw for a crystal of refractive indices α, β, γ a series of spheroconics (curves of intersection of these cones with a concentric sphere of unit radius) one set (equation 3) of which gives the actual positions of all vibration directions of radius vector equal to a given ρ, while the second set gives the positions of the normals to the sections one of whose ellipse axes is equal to ρ (equation 11). Each curve of the first set is the locus of all radii vectors of the index ellipsoid of length ρ. Each curve of the second set is the locus of the normals of all diametral sections one of whose ellipse axes has the length ρ. Considered from the viewpoint of crystal optics each curve of the second set is the locus of all directions of wave propagation, within

the crystal, of refractive index ρ; each curve of the first set is the locus of all vibration directions of length ρ. To each given point on a spheroconic of the second set there corresponds a point on the first set; this point is distant 90° from the given point and is the vibration direction of one of the two possible waves propagated along the direction indicated by the given point. The curves of the second set are essentially refractive index curves and may be called for convenience *equirefringence* curves. The curves of the first set have to do with vibration directions and may be called *equivibration* curves. To find the vibration directions for any given direction of propagation it is not necessary, however, to draw the equivibration curves. It is shown above that the cones (3) and (11) bear reciprocal relations. The tangent plane therefore to the cone of an equirefringence curve (equation 11) is the desired vibration plane. From equirefringence curves alone it is therefore possible to ascertain not only the refractive indices of the two waves propagated along any given direction but also their vibration directions.

The projections of the equirefringence curves on the principal sections are readily found by rearranging equation (11) to the following forms, if we consider the spheroconics to be located on the sphere of unit radius ($x^2+y^2+z^2=\rho^2=1$)

$$x^2+y^2+z^2 = x^2\frac{\frac{1}{\alpha^2}-\frac{1}{\beta^2}}{\frac{1}{\alpha^2}-\frac{1}{\rho^2}}+z^2\frac{\frac{1}{\gamma^2}-\frac{1}{\beta^2}}{\frac{1}{\gamma^2}-\frac{1}{\rho^2}}=1 \qquad (12a)$$

$$= y^2\frac{\frac{1}{\beta^2}-\frac{1}{\gamma^2}}{\frac{1}{\beta^2}-\frac{1}{\rho^2}}+x^2\frac{\frac{1}{\alpha^2}-\frac{1}{\gamma^2}}{\frac{1}{\alpha^2}-\frac{1}{\rho^2}}=1 \qquad (12b)$$

$$= z^2\frac{\frac{1}{\gamma^2}-\frac{1}{\alpha^2}}{\frac{1}{\gamma^2}-\frac{1}{\rho^2}}+y^2\frac{\frac{1}{\beta^2}-\frac{1}{\alpha^2}}{\frac{1}{\beta^2}-\frac{1}{\rho^2}}=1 \qquad (12c)$$

These curves of projection are different in type for different values of ρ. Thus for $\rho=\alpha'$, $(\rho<\beta)$, (12a) is an ellipse; (12b), an hyperbola; (12c), an ellipse; for $\rho=\gamma'$, $(>\beta)$ (12a) is an ellipse; (12b), an ellipse; (12c), an hyperbola.

In similar manner the orthographic projections of the equivibration spheroconics (equation 3) on the principal planes are the following:

$$x^2+y^2+z^2 = x^2\frac{\frac{1}{\beta^2}-\frac{1}{\alpha^2}}{\frac{1}{\beta^2}-\frac{1}{\rho^2}}+z^2\frac{\frac{1}{\beta^2}-\frac{1}{\gamma^2}}{\frac{1}{\beta^2}-\frac{1}{\rho^2}}=1 \tag{13a}$$

$$= y^2\frac{\frac{1}{\gamma^2}-\frac{1}{\beta^2}}{\frac{1}{\gamma^2}-\frac{1}{\rho^2}}+x^2\frac{\frac{1}{\gamma^2}-\frac{1}{\alpha^2}}{\frac{1}{\gamma^2}-\frac{1}{\rho^2}}=1 \tag{13b}$$

$$= z^2\frac{\frac{1}{\alpha^2}-\frac{1}{\gamma^2}}{\frac{1}{\alpha^2}-\frac{1}{\rho^2}}+y^2\frac{\frac{1}{\alpha^2}-\frac{1}{\beta^2}}{\frac{1}{\alpha^2}-\frac{1}{\rho^2}}=1 \tag{13c}$$

These curves of projection are different in type for different values of ρ. For $\rho=\alpha'$, $(\rho<\beta)$, (13a) is an hyperbola; (13b), an ellipse; (13c), an ellipse; for $\rho=\gamma'$ $(\rho>\beta)$, (13a) is an hyperbola; (13b), an ellipse; (13c), an ellipse.

Equation (3) can be written in the form

$$\left(x\sqrt{\frac{\frac{1}{\alpha^2}-\frac{1}{\beta^2}}{\frac{1}{\alpha^2}-\frac{1}{\gamma^2}}}+z\sqrt{\frac{\frac{1}{\beta^2}-\frac{1}{\gamma^2}}{\frac{1}{\alpha^2}-\frac{1}{\gamma^2}}}\right)\left(x\sqrt{\frac{\frac{1}{\alpha^2}-\frac{1}{\beta^2}}{\frac{1}{\alpha^2}-\frac{1}{\gamma^2}}}-z\sqrt{\frac{\frac{1}{\beta^2}-\frac{1}{\gamma^2}}{\frac{1}{\alpha^2}-\frac{1}{\gamma^2}}}\right)=\rho^2\frac{\frac{1}{\rho^2}-\frac{1}{\beta^2}}{\frac{1}{\alpha^2}-\frac{1}{\gamma^2}} \tag{13'a}$$

in which each expression in parenthesis is clearly the length of the perpendicular from a given point x, y, z, on one of the two cyclic planes. The expression states that the product of the perpendiculars from any point of a spheroconic to the two cyclic planes of (3) is constant. But each perpendicular is equal to the product of the radius vector to the given point into the sine of the angle which this radius vector makes with a cyclic plane. If the angles included between the radius vector and the two cyclic planes be D_1 and D_2 respectively, equation (13'a) can be written

$$\frac{1}{\rho^2}-\frac{1}{\beta^2}=\left(\frac{1}{\alpha^2}-\frac{1}{\gamma^2}\right)\sin D_1 \sin D_2 \tag{13''a}$$

This equation applies to vibration directions primarily, but from it the corresponding equation for the equirefringence spheroconics can

be readily deduced. In Fig. 2 let ρ_1, ρ_2 be the given vibration directions, *BEB* and *BFB*, the two cyclic planes, A_1, A_2 the two normals to the cyclic planes (optic binormals), $\rho_1 a_1 \rho_2$, the plane tangent to the vibration spheroconic at ρ_1; P the pole of the tangent plane $\rho_1 a_1 \rho_2$; $\rho_1 A'_1 = D_1$, $\rho_1 A'_2 = D_2$, the perpendiculars from ρ, to the two cyclic planes; $A_1 Z = A_2 Z = V_a$, half the angle between the binormals $A_1 A_2$.

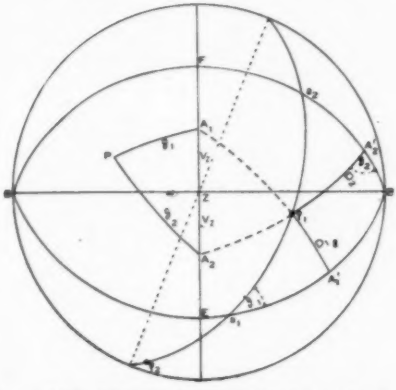

FIG. 2. *In this figure BEB, BFB are the two cyclic planes; A_1, A_2, two optic axes; Z the acute bisectrix; ρ , ρ_2, the two vibration directions of the diametral plane $\rho_2 a_1 \rho_1 a_2$, of which P is the pole; $\rho_1 A'_1 = D_1$ and $\rho_1 A'_2 = D_2$, perpendiculars let fall from ρ_1 on BEB and BFB respectively; $PA_1 = \theta_1$, $PA_2 = \theta_2$, the angular distances of P from A_1 and A_2 respectively.*

In the triangles $\rho_1 a_1 A'_1$, $\rho_1 a_2 A'_2$ we have $\rho_1 a_1 = \rho_1 a_2$ because in an ellipse a principal axis (ρ_1 or ρ_2) bisects the angle between any two radii vectors of equal length, a_1 and a_2 (radii of circular sections); also

$$\sin D_1 = \sin \rho_1 a_1 \sin \theta_1$$
$$\sin D_2 = -\sin \rho_1 a_2 \sin \theta_2$$

$$\text{Therefore } \sin D_1 \cdot \sin D_2 = -\sin^2 \rho_1 a_1 \sin \theta_1 \sin \theta_2 = \frac{\frac{1}{\rho^2} - \frac{1}{\beta^2}}{\frac{1}{a^2} - \frac{1}{\gamma^2}} \tag{14}$$

Passing now to the polar triangle PA_1A_2 we have $A_1PA_2 = 180° - a_1 a_2$, $PA_2 = \theta_2$, $PA_1 = \theta_1$; substituting these values in (14) we get

$$\cos^2 \tfrac{1}{2} A_1 PA_2 \cdot \sin \theta_1 \cdot \sin \theta_2 = \frac{\frac{1}{\beta^2} - \frac{1}{\rho^2}}{\frac{1}{a^2} - \frac{1}{\gamma^2}} \tag{14a}$$

Let half the sum of the sides in triangle PA_1A_2 be $S=\frac{\theta_1+\theta_2+2V_s}{2}$.

Then from trigonometry we have in triangle PA_1A_2

$$\cos^2\tfrac{1}{2}A_1PA_2\sin\theta_1\sin\theta_2=\sin S\sin(S-V_s)$$

$$=\sin^2\frac{\theta_2+\theta_1}{2}-\sin^2V_s$$

$$=\sin^2\frac{\theta_2+\theta_1}{2}-\frac{\frac{1}{\alpha^2}-\frac{1}{\beta^2}}{\frac{1}{\alpha^2}-\frac{1}{\gamma^2}}$$

This equation combined with (14a) yields, for $\rho_1=\gamma'$ or $(\rho_1>\beta)$, the expression,

$$\frac{1}{\alpha^2}-\frac{1}{\gamma'^2}=\left(\frac{1}{\alpha^2}-\frac{1}{\gamma^2}\right)\sin^2\frac{\theta_2+\theta_1}{2},\text{ or }\frac{1}{\gamma'^2}-\frac{1}{\gamma^2}=\left(\frac{1}{\alpha^2}-\frac{1}{\gamma^2}\right)\cos^2\frac{\theta_2+\theta_1}{2}\quad(15a)$$

For the second vibration direction, $\rho_2=\alpha'$ or $(\rho_2<\beta)$ we find in similar manner

$$\frac{1}{\alpha^2}-\frac{1}{\alpha'^2}=\left(\frac{1}{\alpha^2}-\frac{1}{\gamma^2}\right)\sin^2\frac{\theta_2-\theta_1}{2},\text{ or }\frac{1}{\alpha'^2}-\frac{1}{\gamma^2}=\left(\frac{1}{\alpha^2}-\frac{1}{\gamma^2}\right)\cos^2\frac{\theta_2-\theta_1}{2}\quad(15b)$$

From these two equations the lengths of the ellipse axes of any section whose normal includes the angles θ_1 and θ_2 with the optic binormals can be computed directly.

Subtracting (15b) from (15a) we obtain

$$\frac{1}{\alpha'^2}-\frac{1}{\gamma'^2}=\left(\frac{1}{\alpha^2}-\frac{1}{\gamma^2}\right)\sin\theta_1\cdot\sin\theta_2\quad(16a)$$

or approximately

$$\gamma'-\alpha'=(\gamma-\alpha)\sin\theta_1\sin\theta_2\quad(16b)$$

Equations 15a to 16b are standard equations, though derived elsewhere by different methods.

Equations (11), (12a) to (12c) can be expressed in different form by substituting in them $\cos^2 V_s$ (equation 6), $\sin^2\frac{\theta_2+\theta_1}{2}$, $\cos^2\frac{\theta_2+\theta_1}{2}$, $\sin^2\frac{\theta_2-\theta_1}{2}$, $\cos^2\frac{\theta_2-\theta_1}{2}$ (equations 15*a*, 15*b*)

and thus obtaining for $\rho=\gamma'$, $(\rho>\beta)$ the expressions:

$$\frac{x^2}{\sin^2\frac{1}{2}(\theta_2+\theta_1)}+\frac{y^2}{\cos^2V_s-\cos^2\frac{1}{2}(\theta_2+\theta_1)}-\frac{z^2}{\cos^2\frac{1}{2}(\theta_2+\theta_1)}=0\quad(17)$$

and for $\rho_2 = \alpha'$, $(\rho < \beta)$

$$\frac{x^2}{\sin^2\frac{1}{2}(\theta_2-\theta_1)} + \frac{y^2}{\cos^2 V_z - \cos^2\frac{1}{2}(\theta_2-\theta_1)} - \frac{z^2}{\cos^2\frac{1}{2}(\theta_2-\theta_1)} = 0 \qquad (18)$$

The projection equations (12a), (12b), (12c) for $\rho_1 = \gamma'$ now read

$$x^2 \frac{\sin^2 V_z}{\cos^2\frac{1}{2}(\theta_2+\theta_1)} + z^2 \cdot \frac{\cos^2 V_z}{\sin^2\frac{1}{2}(\theta_2+\theta_1)} = 1 \qquad (17a)$$

$$y^2 \frac{\cos^2 V_z}{\cos^2 V_z - \sin^2\frac{1}{2}(\theta_2+\theta_1)} + x^2 \frac{1}{\cos^2\frac{1}{2}(\theta_2+\theta_1)} = 1 \qquad (17b)$$

$$z^2 \frac{1}{\sin\frac{1}{2}(\theta_2+\theta_1)} + y^2 \frac{\sin^2 V_z}{\sin^2 V_z - \cos^2\frac{1}{2}(\theta_2+\theta_1)} = 1 \qquad (17c)$$

and for $\rho_2 = \alpha'$, $(\rho_2 < \beta)$

$$x^2 \cdot \frac{\sin^2 V_z}{\cos^2\frac{1}{2}(\theta_2-\theta_1)} + z^2 \frac{\cos^2 V_z}{\sin^2\frac{1}{2}(\theta_2-\theta_1)} = 1 \qquad (18a)$$

$$y^2 \frac{\cos^2 V_z}{\cos^2 V_z - \sin^2\frac{1}{2}(\theta_2-\theta_1)} + x^2 \frac{1}{\cos^2\frac{1}{2}(\theta_2-\theta_1)} = 1 \qquad (18b)$$

$$z^2 \frac{1}{\sin^2\frac{1}{2}(\theta_2-\theta_1)} + y^2 \frac{\sin^2 V_z}{\sin^2 V_z - \cos^2\frac{1}{2}(\theta_2-\theta_1)} = 1 \qquad (18c)$$

Expressions (17) to (18c) were first derived by Bobek[2], but by a different method, and used by him and by Becke in the derivation of the projection equations (17a, b, c and 18a, b, c). These curves of projection of the equirefringence curves were called skiodromes by Becke and used by him in the investigation of phenomena observed in interference figures, especially the course of the curves of extinction or isogyres. In the following paragraphs the investigation is carried a step beyond that taken by Becke and not only are the extinction positions derived but also the isochromatic curves in the interference figure obtained from a section in any position as seen in convergent polarized light. For this purpose equation (11) is better adapted than (17) or (18).

The projections of the equirefringence spheroconics as they appear on the three principal sections are shown in Figs. 3 to 12. These curves

[2] F. Becke, Denkschriften d. k. Akad. d. Wissen zu Wien, Math.-Wissensch. Kl. *75*, p. 68; 1904. A. Beer in 1852 considered briefly in his Einleitung in die höhere Optik analogous cones and called them Geschwindigkeitskegel erster und zweiter Art. He bases his conclusions, however, on equations analogous to 15a and 15b and not to 3 and 11.

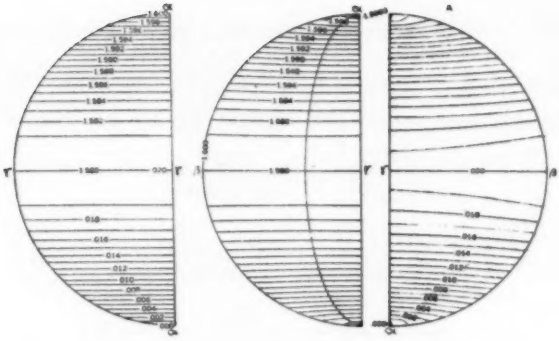

FIG. 3 FIG. 4

FIG. 3. *Upper half: Equirefringence curves in orthographic projection on the xy plane of a crystal having the principal refractive indices* $\alpha = 1.580$, $\beta = \gamma = 1.600$, $2V_Z = 180°$. *The curve, 1.586, gives, for example, the position in space of all directions of propagation having the refractive index 1.586; similarly for the other curves. The contour interval between any two successive curves is 5 per cent of* $\gamma - \alpha$. *Lower half: Equibirefringence curves for same crystal in the same projection. The curve, .012, for example, passes through all directions within the crystal for which the birefringence is .012; likewise the remaining curves. The interval between any two successive curves is 5 per cent of the total birefringence,* $\gamma - \alpha$. *The letters* α, β, γ *indicate the directions of the principal axes of the index ellipsoid.*

FIG. 4. *Left half: Equirefringence curves, projected as in Fig. 3, of a crystal having* $\alpha = 1.580$, $\beta = 1.5993$, $\gamma = 1.600$, $2V_Z = 160°$. FIG. 4A. *Equibirefringence curves for same crystal and in the same projection.*

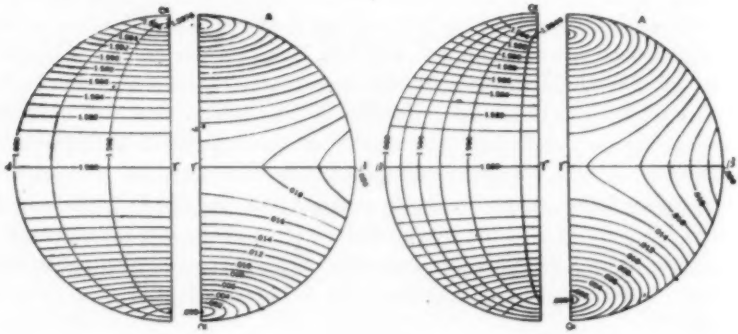

FIG. 5 FIG. 6

FIG. 5. *Equirefringence curves in orthographic projection as in Fig. 3 for a crystal having* $\alpha = 1.580$, $\beta = 1.5976$, $\gamma = 1.600$, $2V_Z = 140°$. FIG. 5A. *Equibirefringence curves for same crystal and in same projection.*

FIG. 6. *Equirefringence curves in orthographic projection as in Fig. 3 for a crystal for which* $\alpha = 1.580$, $\beta = 1.5949$, $\gamma = 1.600$, $2V_Z = 120°$. FIG. 6A. *Equibirefringence curves for same crystal and in same projection.*

are drawn in orthographic projection on the $\beta-\gamma$ plane for an average mineral $\alpha=1.5800$, $\beta=1.6000$, 1.5993, 1.5976, 1.5949, 1.5916, 1.5882, 1.5849, 1.5823, 1.5806, 1.5800 and $\gamma=1.6000$, corresponding to the following values of the optic binormal angle $2V_Z=180°$, 160°, 140°, 120°, 100°, 80°, 60°, 40°, 20°, 0°. The equirefringence spheroconics

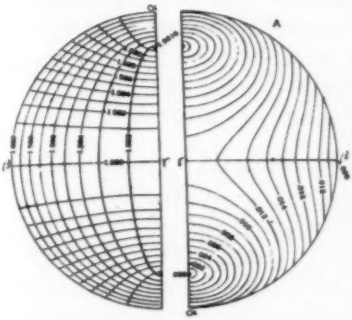

FIG. 7

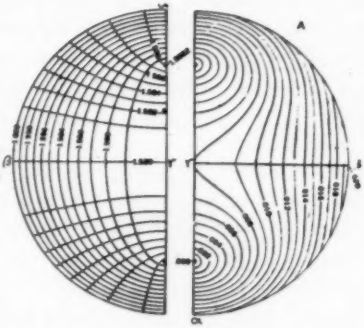

FIG. 8

FIG. 7. *Equirefringence curves in orthographic projection as in Fig. 3 for a crystal for which* $\alpha=1.580$, $\beta=1.5916$, $\gamma=1.600$, $2V_Z=100°$. FIG. 7A. *Equibirefringence curves for same crystal and in same projection.*

FIG. 8. *Equirefringence curves in orthographic projection as in Fig. 3 for a crystal for which* $\alpha=1.580$, $\beta=1.882$, $\gamma=1.600$, $2V_Z=80°$. FIG. 8A. *Equibirefringence curves for same crystal and in same projection.*

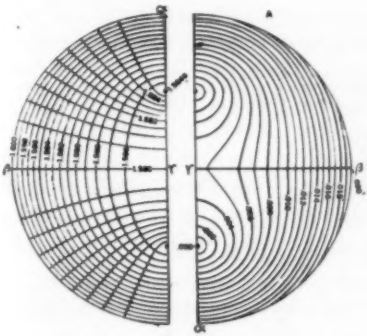

FIG. 9

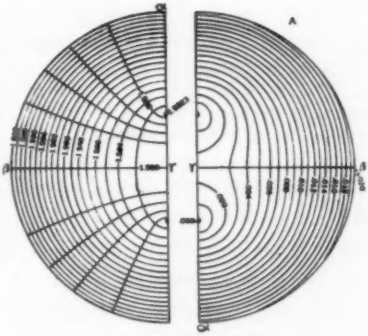

FIG. 10

FIG. 9. *Equirefringence curves in orthographic projection, as in Fig. 3, for a crystal for which* $\alpha=1.580$, $\beta=1.5849$, $\gamma=1.600$, $2V_Z=60°$. FIG. 9A. *Equibirefringence curves for same crystal and in same projection.*

FIG. 10. *Equirefringence curves in orthographic projection, as in Fig. 3, for a crystal having refractive indices* $\alpha=1.580$, $\beta=1.5823$, $\gamma=1.600$, $2V_Z=40°$. FIG. 10A. *Equibirefringence curves for same crystal and in same projection.*

of the figure function as contour lines and indicate the refringence values for every point on the surface of the sphere. Each point on the sphere may be considered to mark the position of the direction of propagation of two waves (α', γ') through the crystal. The two equirefringence curves (α', γ') through this point state the refractive indices (α', γ') of the two waves thus propagated. The birefringence in this case is $\gamma'-\alpha'$. Similarly the birefringence for any other direction can be read off directly. By connecting points of equal birefringence, we thus obtain a series of equibirefringence curves (Figs. 3A to 12A) in which the contour interval between successive curves is 5 per cent of

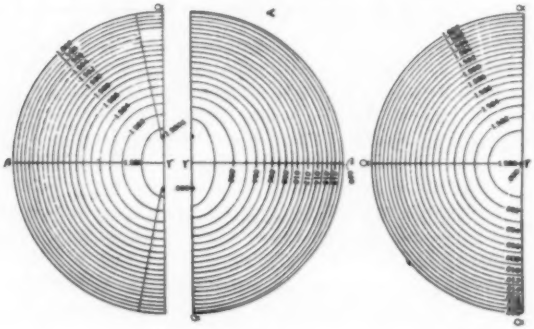

FIG. 11 FIG. 12

FIG. 11. *Equirefringence curves in orthographic projection, as in Fig. 3, for a crysal for which* $\alpha=1.580$, $\beta=1.5806$, $\gamma=1.600$, $2V_Z=20°$. FIG. 11A. *Equibirefringence curves for same crystal and in same projection.*

FIG. 12. Upper half. *Equirefringence curves in orthographic projection, as in Fig. 3, for a crystal for which* $\alpha=\beta=1.5800$, $\gamma=1.600$, $2V_Z=0°$. Lower half. *Corresponding equibirefringence curves in the same projection.*

the total maximum birefringence, $\gamma-\alpha$. From these curves in turn the isochromatic curves as they actually appear in the interference figure from a section cut in any given direction through the crystal, can be deduced graphically.

The analytical expression for the equibirefringence curves is readily derived from equations (10*a* to 10*c* and 11).

In equations (10b, 10c) let $\rho_2=\alpha'$ and $\rho_1=\alpha'+d$ wherein $d=\gamma-\alpha$, is the birefringence. Substituting these values in (10a) and (10b) and, for brevity, calling the right sides of (10b) and (10c) K and C^2 respectively, we find on eliminating α' between them

$$K-d^2C^2-2C=0$$

$$\text{or} \quad [a^2x^2(\beta^2+\gamma^2-d^2)+\beta^2\gamma^2(\gamma^2+a^2-d^2)+\gamma^2z^2(a^2+\beta^2-d^2)]^2-4a^2\beta^2\gamma^2 (a^2x^2+\beta^2y^2+\gamma^2z^2)=0 \qquad (20)$$

a quadratic equation in x^2, y^2, z^2 and containing d, the birefringence as the constant for each one of the successive equibirefringence curves.

Equation (20) can be written in another form, namely:

$$d^2=\frac{K-2C}{C^2} \quad \text{or}$$

$$d^2=\frac{a^2\beta^2(l^2+m^2)+\beta^2\gamma^2(m^2+n^2)+\gamma^2a^2(n^2+l^2)-2a\beta\gamma\sqrt{a^2l^2+\beta^2m^2+\gamma^2n^2}}{a^2l^2+\beta^2m^2+\gamma^2n^2} \qquad (20a)$$

From this equation the birefringence, $d=\gamma'-a'$, of any section whose direction cosines, l, m, n are given can be computed directly. For most purposes, however, the graphical method is simpler and sufficiently accurate. The equibirefringence curves as projected on the principal sections are shown in Figs. 3A to 12A. Equibirefringence curves are inscribed on the surface of a sphere and may be considered to indicate, for the different directions, the relative path differences for light waves transmitted normally through plane parallel plates of unit thickness (radius of sphere).

From the equirefringence and equibirefringence curves the isochromatic curves and the isogyres of interference figures obtained from plane parallel plates in convergent polarized light can be readily deduced. The more important of the factors which effect the change from equibirefringence curves to isochromatic curves of the interference figure are: (a) refraction of the waves at the surfaces of the p ate under observation; and (b) increase in length of path within the crystal with increase in inclination of the direction of propagation.

The changes in direction of the wave normals at the surface of the crystal can be ascertained graphically by means of a diagram of the type illustrated by Fig. 13. In one quadrant of this plot concentric arcs spaced 1° apart in orthographic projection ($r=\sin i$) are drawn; in the diagonally opposite quadrant are drawn the same concentric arcs but corrected for refraction ($r=n\sin i$) in which n is the given refractive index. Each equirefringence spheroconic can be plotted accurately by this method, if the correct refractive index for each refrirgence curve be used. In the case of a weakly birefracting mineral a single diagram with an average refractive index suffices for all curves, but for a strongly birefracting mineral, such as calcite or aragonite several diagrams may be required. These are, however, easily prepared; a set drawn at re-

fringence intervals of 1 or 2 in the second decimal place may well be prepared once for all.

To correct for refraction at the surface of the crystal plate, the diagram (on tracing paper) of the equirefringence spheroconics in orthographic projection, as viewed from the direction of the normal to the given section, is placed over the refraction diagram (Fig. 13) and the equirefringence curves are redrawn, so that to every point in the original diagram there is a corresponding point in the new diagram whose distance from the center is n times that of the original; n is the refractive index of the given equirefringence curve. From the equire-

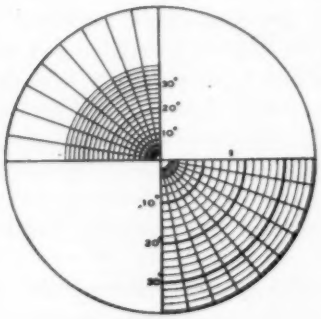

FIG. 13

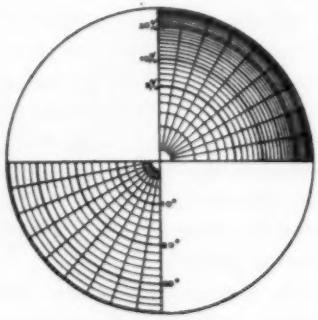

FIG. 14

FIG. 13. *Plot for converting graphically directions observed in an interference figure from a crystal plate of average refractive index n = 1.59 and weak to medium birefringence, to corresponding directions within the crystal plate or vice versa. The radii vectors in the* S.E. *quadrant are* n *times the lengths of the corresponding radii vectors in the* N.W. *quadrant.*

FIG. 14. *Graphical plot for correcting for change in length of path of waves transmitted through a crystal plate at an angle with the normal to the plate. In the* N.E. *quadrant the percentage increase in length of path for a given inclination whose angular value is shown in the* S.W. *quadrant.*

fringence curves in the projection the isogyres for any given position of the vibration plane of the polarizer can be drawn in directly. In each case the plane of vibration for a given direction of propagation is tangent to the equirefringence curve.

The corresponding isochromatic curves can now be found from the graphical plot of the equirefringence curves; to transform the equibirefringence curves into equipath difference curves (isochromatic curves of the interference figure) the increase in path for all inclined wave normals must be taken into account. This is readily done with the aid of a diagram (Fig. 14) from which the percentage increases in paths for the different inclinations can be read off directly, and which is corrected

for refractive index n. The radii of the concentric circles of Fig. 14 (orthographic projection) are found for directions within the crystal itself from the equation

$$1 = \sec \alpha$$

For an increase of 5 per cent sec $\alpha = 1.05$, which corresponds to an angle $\alpha = 17°46'$ within the crystal; the radius of the circle in the plot is sin $17°46'$; this direction in turn corresponds to a definite direction after refraction at the upper surface of the plate; for this direction the path difference is 5 per cent greater than the birefringence. In this manner we pass from the equibirefringence curves of the sphere to the equipath-difference curves of a crystal plate and these are actually the isochromatic curves of the interference figure.

In this connection there are certain features of an interference figure which may be deduced from the foregoing presentation and which should be noted. Strictly speaking, the birefringence of any point in an interference figure, except the center, does not correspond exactly with that of the diametral section of the index ellipsoid it is supposed to represent. Thus when a beam of polarized light enters the crystal plate at an angle with the normal to the plate, it is, by refraction, broken into two waves whose normals follow slightly different paths because of the different refractive indices γ' and α'. These two directions cannot both be normal to any one central section and γ' and α' do not, therefore, belong to the same section, with the result that their planes of vibration are not exactly at right angles. On emerging from the crystal plate these directions of propagation are again made parallel and in the analyzer are brought to interference because of the differences in path through the crystal. In crystals of weak birefringence, the order of magnitude of these differences in direction is slight and they may be generally neglected, but in minerals of strong birefringence they are appreciable and may not be disregarded. This is clearly proved by the data for a crystal plate of aragonite inclined at an angle of 30° with the acute bisectrix a, and parallel with β. The refractive indices for sodium light for aragonite are $\alpha = 1.5301$; $\beta = 1.6816$; $\gamma = 1.6859$. For a beam of light incident at an angle $i = 63°43.6'$ in a plane normal to the principal γ or plane of the index ellipsoid we find by computation, on using the index surface as a basis:[3] $r_1 = 32°10'$; $r_2 = 33°58.5'$; $r_2 - r_1 = 1°48.5'$; $\gamma' = 1.6843$, $\alpha' = 1.6046$; the azimuth angles with reference to the plane of incidence, of the planes of vibration of r_1 and r_2 are $\delta_1 =$

[3] For a summary of these methods of computation, which are standard, see F. E. Wright, The transmission of light, etc. Am. J. Sci., (4) *31*, pp. 157-211; 1911.

$46°42.8'$, $\delta_2 = -44°38.2'$; the azimuth angles of the corresponding emerging waves are $\epsilon_1 = 42°08.1'$, $\epsilon_2 = -41°58.5'$, the angle between the planes of vibration after emergence of the two waves from the crystal is $84°06.59'$. The angles between the wave normals r_1 r_2 and the corresponding two rays are respectively $s_1 = 0°13.2'$, $s_2 = -5°28.1'$. These results of computation prove that in the case of aragonite which is strongly birefracting the angle between the planes of vibration of the emergent waves is noticeably different from a right angle.

The direction of an inclined beam of light is changed on transmission through a microscope objective, so that it nearly coincides with the normal to the crystal plate. The question arises "How does this change of direction affect the azimuth of the plane of vibration?" To answer this question let us consider a plane polarized beam of light which is incident on the surface of an isotropic substance at an appreciable angle with the normal to the surface and whose plane of vibration does not coincide with the plane of incidence. In Fig. 15, let *AO* be the in-

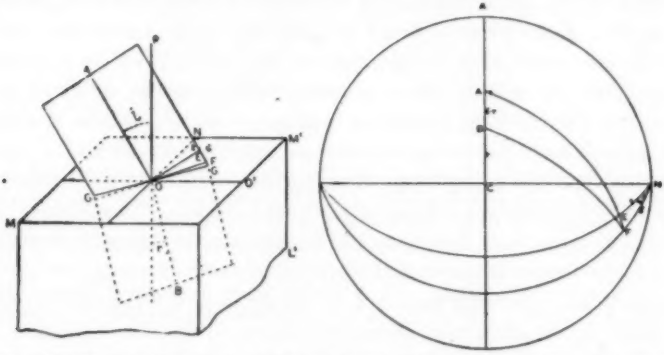

FIG. 15. *Diagram to illustrate the change in azimuth angle of the plane of vibration of a plane polarized beam of light on entering an isotropic substance* LMM'L *at the plane surface* MO'M'. FIG. 15A. *The geometrical relations of Fig. 15 represented in stereographic projection.*

cident beam, *MLL'M'* the isotropic substance, *AOP* the plane of incidence, *AOE* the plane of vibration of the incident beam, $NOE = \epsilon$ the azimuth of the plane of vibration, *OB* the direction of the refracted beam, *BOF* the plane of vibration of the refracted beam. In an isotropic medium there are no preferred directions as in an anisotropic crystal and the vibrations in the wave front may take place in any azimuth; moreover a beam of light whose vibrations are restricted to one plane (plane polarized light) maintains the same plane of vibration

throughout its passage through the isotropic medium. In passing from one isotropic medium to a second the wave encounters no forces which tend to divert the line of vibration from its original plane. The direction of propagation of the wave, and with it the wave-front, is changed on entering the second medium but the plane of vibration remains unaltered; the line of vibration of the refracted wave is accordingly the line of intersection of the original plane of vibration with the new wave-front. In Fig. 14 this line is OF. In the spherical triangle NEF Fig. 15A let angle $NOE=\epsilon$, $NOF=\delta$; then $EOF=i-r$ and NEF is a right angle; accordingly

$$\tan\delta=\cos(i-r)\cdot\tan\epsilon \tag{21}$$

This is the fundamental formula of Fresnel for waves transmitted through an isotropic plate, who, however, obtained the equation by an entirely different method.[4] In 1838 J. MacCullagh stated the above rule in terms of transversals and arrived at the result through a geometrical interpretation of the Fresnel equation 21. See *Collected Papers*, 1880. With the aid of this concept or rule, that plane polarized light waves in passing from one isotropic medium to a second are refracted but the line of vibration of the refracted wave is contained in original plane of vibration, it is easy graphically, or with the aid of equation (21) by computation, to ascertain the azimuth of the plane of vibration of the refracted wave. Equation (21) shows that for $\epsilon=0$, $\delta=0$, and for $\epsilon=90°$, $\delta=90°$; in both these cases $\epsilon-\delta=0$ and there is no change in azimuth of the plane of vibration on refraction. The greatest change in azimuth angle occurs for the value $\tan^2\epsilon=\dfrac{1}{\cos(i-r)}$ or $\tan^2\delta=\cos(i-r)$ from which we find

$$\tan(\epsilon-\delta)=\frac{1-\cos(i-r)}{2\sqrt{\cos(i-r)}} \tag{22}$$

From this formula it is evident that with increase in $(i-r)$, either as a result of greater inclination of incident beam or of greater difference in refringence between the two media, the change in azimuth angle increases.

In order to test the validity of the Fresnel formula (2) and the mode of its derivation given above, a prism of variable angle was constructed as indicated in Fig. 16 and mounted on a spectrometer. The prism is made of a cylinder of brass 2 inches in diameter, closed at the ends

[4] See F. E. Wright, The methods of petrographic microscope research. Carnegie Institution of Washington, Pub. *158*, pp. 75-76; 1911.

and with two segments cut out. A plane parallel plate of borosilicate glass of refractive index $n_D = 1.5087$ is cemented over the one segment and forms the base of the prism which is filled with a liquid of the same refractive index. A beam of plane polarized light is sent through the prism at a definite inclination and with its vibration plane including a definite angle with the plane of incidence. The azimuth of the plane of vibration of the wave emerging from the prism perpendicular to the surface of the liquid is then measured. By setting the polarizer

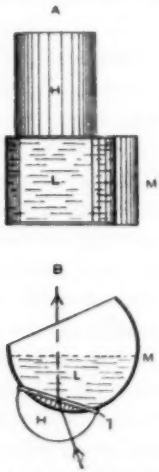

FIG. 16. A. *Top view and* B, *side view of a liquid prism of variable angle.* M, *segment of a brass cylinder, 6 cm diameter and 4 cm high. The ends are sealed by brass disks and out of the brass box thus formed two segments are cut off. One of these openings is again sealed by cementing over it a plane parallel piece of optical glass, as indicated in Fig. 16.I.* H *is a brass cylinder soldered to* M; *it slips over the central bearing of the spectrometer and serves as support for* M. *The liquid with horizontal surface is shown at* L.

at different azimuth angles, ϵ, for the same angles of incidence the azimuth angle, δ, of the vibration plane of the emergent beam is read off directly from the position of the analyzer, in front of which a biquartz wedge plate was inserted to increase the accuracy of the individual settings. In Table 1 are listed the averages of a series of readings, on a graduated circle with vernier reading to 0.1°, of the angle δ for an angle $i - r = 30°$. The agreement between observed and computed values is excellent and proves the validity of the Fresnel equation.

In Table 2 are listed the computed azimuth angles, with reference to the plane of incidence, of the vibration planes of light beams after

TABLE 1. *Rotation of vibration plane of beam of light on refraction at a single surface of glass. $n=1.5087$; $i-r=30°$; ϵ=azimuth of vibration plane of incident wave; δ=azimuth of vibration plane of refracted wave.*

ϵ	δ observed	δ computed	$\delta-\epsilon$
0	0	0	0
10	8.7	8.7	1.3
20	17.55	17.5	2.5
30	26.6	26.6	3.4
40	36.0	36.0	4.0
50	45.8	45.9	4.1
60	56.2	56.3	3.7
70	67.15	67.2	2.8
80	78.45	78.5	1.5
90	90.0	90.0	0

TABLE 2. *In this table $i-r$ is the angle between the incident and the refracted beam; ϵ is the azimuth angle of the plane of vibration of the incident beam; δ, that of the beam after refraction at a single surface; δ', that after transmission through a plane parallel plate.*

$i-r$	10°	20°	30°	40°	50°	60°	70°	80°
ϵ	δ	δ	δ	δ	δ	δ	δ	δ
0°	0°00′	0°00′	0°00′	0°00′	0°00′	0°00′	0°00′	0°00′
10	9°51.1	9°24.5	8°41.0	7°41.6	6°28.0	5°02.3	3°27.1	1°45.2
20	19 43.2	18 52.9	17 29.7	15 34.5	13 10.1	10 18.9	7 05.8	3 37.0
30	29 37.4	28 28.8	26 33.9	23 51.5	20 21.6	16 06.1	11 10.2	5 43.5
40	39 34.1	38 15.4	36 00.3	32 43.9	28 20.5	22 45.6	15 00.8	8 17.4
50	49 34.1	48 14.3	45 54.3	42 23.7	37 27.3	30 47.5	22 10.7	11 41.6
60	59 37.2	58 26.0	56 18.6	52 59.9	48 04.3	40 53.7	30 38.6	16 44.4
70	69 43.0	68 49.6	67 12.3	64 35.4	60 28.8	53 56.9	43 13.2	25 30.3
80	79 51.8	79 22.3	78 29.5	77 02.2	74 39.7	70 34.5	62 43.6	44 33.7
90	90 00	90 00	90 00	90 00	90 00	90 00	90 00	90 00
	δ'	δ'	δ'	δ'	δ'	δ'	δ'	δ'
0°	0°00′	0°00′	0°00′	0°00′	0°00′	0°00′	0°00′	0°00′
10	9 42.3	8 51.0	7 31.0	5 54.4	4 10.0	2 31.4	1 10.9	0 18.3
20	19 26.6	17 49.0	15 16.1	12 03.4	8 33.2	5 11.9	2 26.3	0 37.7
30	29 14.8	27 10.8	23 24.8	18 43.0	13 25.0	8 13.0	3 51.8	0 59.8
40	39 08.3	36 32.2	32 11.0	26 12.9	19 07.3	11 50.9	5 36.4	1 27.0
50	49 08.1	46 27.7	41 47.9	34 58.1	26 13.0	16 35.5	7 56.4	2 03.5
60	59 14.1	56 49.4	52 24.8	45 28.0	35 35.4	23 24.8	11 27.3	2 59.3
70	69 25.7	67 36.0	64 06.8	58 11.5	48 37.4	34 29.1	17 49.0	4 44.1
80	79 41.8	78 42.5	76 46.2	73 16.6	66 53.5	54 48.3	33 33.7	9 42.4
90	90 00	90 00	90 00	90 00	90 00	90 00	90 00	90 00

refraction at a single surface and after refraction at two plane parallel surfaces, as encountered on transmission through a plane parallel plate.

The results of Table 2 are illustrated graphically in orthographic projection in Fig. 17. They show that with increase of angle of inclination, $i-r$, the amount of rotation of the plane of vibration increases, except for the two principal planes of the crossed nicols.

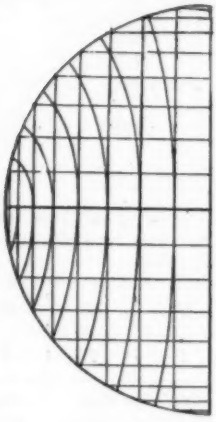

FIG. 17

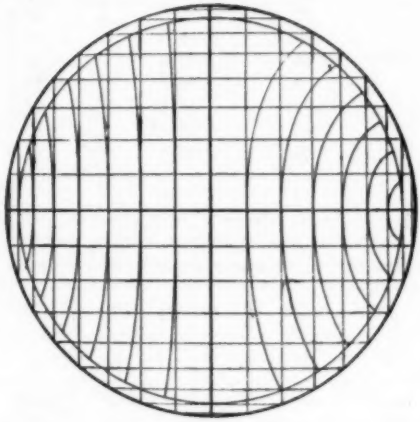

FIG. 18

FIG. 17. *Orthographic projection of the computed (equations 21, 21a) azimuth angles which the planes of vibration make with the plane of incidence after refraction at a single surface (lower half of Fig. 17) and after refraction at two plane parallel surfaces (upper half of Fig. 17) as encountered on transmission through an isotropic glass plate. In the figure the straight* E-W *and* N-S *lines are small circle coordinates spaced 10° apart. The initial plane of vibration is represented by the* N-S *line. It should be noted that the distances from the pole (center of projection) represent the angles (i-r).*

FIG. 18. *Curves in orthographic projection representing data of observation of Table 4 on the rotation of the plane of vibration of a beam of plane polarized light in mercury light (546μμ) on transmission through the condenser (aplanatic) and objective (4 mm apochromatic) of the microscope* (N.W.) *quadrant; through the above lens system plus an intervening cover glass mounted with Canada balsam on an object glass* (S.W. *quadrant); through lens system plus 6 unmounted cover glasses between objective and condenser* (S.E. *quadrant); through lens system plus 12 unmounted cover glasses* (N.E. *quadrant). The slope angles in the projection are the angles of inclination of the points observed in the conoscopic field.*

Observations prove that, if the analyzer is rotated to the position of darkness for a point in the interference figure field, absolute darkness is not attained. In the case of a plane parallel plate a certain amount of light reflected from the surfaces of the plate is added to the direct beam. Thus a certain amount of light is reflected from each of the two surfaces of the plate; that which is reflected from the second surface

travels in the plate back to the first surface whence a small fraction is again reflected and finally emerges from the plate parallel with the direct beam. The amount of light reflected increases with the refringence of the glass, with the angle of incidence, and with the azimuth angle of the plane of vibration with reference to the plane of incidence; thus for a glass plate of refractive index $n=1.51$, and an angle of incidence $i=51°24'$, $r=31°24'$; $i-r=20$, 11.88 per cent of the incident light is reflected when the plane of vibration is normal to the plane of incidence and only 3.07 per cent is reflected when the vibration plane is contained in the plane of incidence. This amount of light is sufficient to cause an appreciable effect in lowering the degree of darkness of the extinction position for all points outside the principal planes of the two nicols. The angle included between the plane of vibration of the beam transmitted directly through the above glass plate incident of the angle $i=51°24'$ and its weakened, twice reflected component is found directly from the equation which is readily derived by application of the above principle

$$\tan \delta'_R = \cos^2(i-r)\cdot\cos^2 2r\cdot\tan \epsilon \qquad (23)$$

The results of the computations are tabulated in Table 3 and show how large the angular rotation for certain azimuths of the plane of

TABLE 3. *In this table ϵ is the azimuth angle of the plane of vibration of a beam incident on a glass plate ($n=1.51$) under an angle, $i=51°24'$; δ', the corresponding azimuth angle after transmission through the glass plate; δ'_R, the azimuth angle for the twice reflected, emergent beam.*

ϵ	δ'	δ'_R	$\delta'-\delta'_R$
0	0°00′	0°00′	0°00′
10	8°51.0	1°51.8	6°59.2
20	17 49.0	3 50.5	13 58.5
30	27 10.8	6 04.8	21 06.0
40	36 32.2	8 48.0	27 44.2
50	46 27.7	12 24.1	34 03.6
60	56 49.4	17 43.4	39 06.0
70	67 36.0	26 52.8	40 33.2
80	78 42.5	46 17.8	32 24.7
90	90	90	0

incident vibration may be. The results prove that in the conoscopic field there is no position of real darkness except along the principal nicol planes. The differences in rotation experienced by the different beams transmitted through the optical system and converging to the same point in the interference figure are also appreciable and tend again to reduce the degree of darkness of any given point in the interference figure.

This phenomenon of the rotation of the plane of vibration of obliquely transmitted waves gives rise in the microscope to the well known faint uniaxial figure between crossed nicols. The black cross can be rendered sharper and more distinct by placing between the condenser and the objective a pile of thin cover glasses. The following series of measurements were made of the positions of extinction of different points in the interference figure. For the purpose a strong quartz mercury arc with ray filter for the wave length 546$\mu\mu$ was used as source of illumination; the lens system consisted of an aplanatic condenser and a dry 4 mm apochromatic objective. In the rear focal plane of the condenser a substage apertometer was placed, so ruled that the coordinate lines, which were imaged together with the interference field in the upper focal plane of the objective, were spaced 10° apart and appear as small circle coordinates in the orthographic projection of the interference field. In Table 4 the values in column N refer to the ordinates; those in column E to the abscissae; the readings in columns I were made with lens system alone; in II with lens system plus the clear part of a microscope slide (cover glass mounted on object with Canada balsam) inserted between condenser and objective; in III, 6 unmounted cover glasses were inserted between condenser and objective; in IV, 12 unmounted cover glasses were inserted between condenser and objective.

TABLE 4.[1] *Observed angular rotations of the plane of vibration for different points in the conoscopic field of the microscope for : I. Lens system (aplanatic condenser and 4 mm objective) alone; II. Lens system + mounted cover glass; III. Lens system + 6 unmounted cover glasses; IV. Lens system + 12 unmounted cover glasses.*

N	E	I	II	III	IV	N	E	I	II	III	IV
0°	0°	0°	0°	0°	0°	30°	10	1·°	2°	7°	12:°
10°	10	.5°	.75	3	4		20	2:	4	13	24
	20	1.	1·	5·	7		30	4.	6:	19	30
	30	1:	2.	7	9:		40	6.	9:	24·	38·
	40	2.	3.	10·	12						
	50	2:	3·	—	—						
20°	10	1	1.	5·	6:	40	10	1:	4	12	17·
	20	1:	2·	8·	13·		20	4	6:	20	46·
	30	2·	3·	12·	19:		30	6.	10:	27·	56
	40	3:	6	16	23·		40	8.	15·	35·	—
	50	4:	8:	—	—						

[1] In this table dots are used after a number to signify additional quarters of a unit; thus 1.=1.25, 1·=1.50, 1:=1.75.

This table proves that even with the lens system alone there is an appreciable rotation of the plane of vibration, sufficient to give rise to a distinct cross in the field. The angular values are increased somewhat on the insertion of a microscope thin section mount and still more if unmounted cover glasses are used. With each boundary surface there is an increase in rotation such that the values in columns III and IV are approximately four and six times, respectively, the values in column I, and the cross is accordingly much more sharply marked than that produced by the lenses alone. In no case are dark extinctions obtained, but rather a fairly wide band of approximate extinction. The readings are therefore only approximately correct. They are reproduced graphically by the curves of Fig. 18 in which the N.W. quadrant of the orthographic projection represents the average data for the lens system alone; the S.W. quadrant, the data for the lens system plus the microscope slide; the S.E. quadrant, the average values for lens system plus 6 unmounted cover glasses; and the N.E. quadrant, the values for lens system plus 12 unmounted cover glasses.

The amount of rotation produced by any number, n, of unmounted plates can be computed from the equation

$$\tan \delta'_n = \cos^{2n}(i-r) \tan \epsilon$$

Thus we find for a single plate for $\epsilon = 40°$, $i-r = 30°$, $\delta' = 32°11'$; for a pile of 5 plates $\delta_5' = 11°15.7'$ and $\epsilon - \delta_5' = 28°44.3'$ instead of $7°49.0'$ for the single plate.

It may be noted that the angular rotation for the lens system alone is less than one might expect from the steep angles of incidence; this follows from the fact that these angles are obtained by a series of refractions at the several lens surfaces of condenser and objective for which angle $(i-r)$ is relatively small.

Comparison of the corresponding values of Tables 3 and 4 and of the curves of Figs. 17 and 18 proves clearly the step down effect of the lens system of the microscope on the degree of rotation of the plane of vibration of steeply inclined rays. This can be shown directly in projection or by an equation. Thus for a ray inclined at a given angle to the microscope axis the azimuth angle for the plane of vibration, in case the rays suffers only a single refraction at the condenser lens and a single refraction at the microscope case, would be

$$\tan \delta' = \cos^2(i-r) \cdot \tan \epsilon \qquad (21a)$$

$i-r$ being the angle of inclination and ϵ the azimuth of the plane of vibration of the polarizer with reference to the plane of incidence. In case the angle of maximum inclination is attained not by a single

refraction but by a series of n refractions, each equal to a definite angle $\frac{i-r}{n}$ the angle δ' is then found from the equation

$$\tan \delta'_n = \cos^{2n}\frac{i-r}{n} \cdot \tan \epsilon \qquad (24)$$

Thus if $\epsilon = 45°$ and $i-r = 40°$ and $n = 4$, $\delta' = 30°24.3'$, $\delta'_n = 41°30.0'$; $\epsilon - \delta' = 14°35.7'$; $\epsilon - \delta'_n = 3°30'$. If in its passage through the microscope lens system and microscope slide the beam is deflected by a series of refractions through the successive angles A, B, C, N, then the azimuth angle δ'_N is given by the equation

$$\tan \delta'_N = \cos A \cdot \cos B, \cos C, \ldots \cos N \cdot \tan \epsilon$$

In every case the effect of repeated refractions of small angular deflections is to produce a relatively small change in the azimuth angle of the plane of vibration. The effect of a very large number of small refractions is to produce zero rotation of the plane of vibration.

It should be noted that the angle of maximum rotation and hence of field illumination is not precisely 45° but always somewhat less, as indicated by equation (22). Values computed by means of this equation are listed in Table 5 for a single refraction (ϵ, δ) and for a plane parallel plate (ϵ', δ').

TABLE 5. *In this table the angles of maximum rotation of the plane of vibration for different slope-difference angles, i-r and for both incident and refracted beams on refraction at a single surface (ϵ and δ respectively) and after transmission through a plane parallel plate (angles ϵ' and δ').*

$i-r$	ϵ	δ	ϵ'	δ'
0°	45°00′	45°00′	45°00′	45°00′
5	45 03.3	44 56.7	45 06.6	44 53.4
10	45 13.2	44 46.8	45 26.3	44 33.7
15	45 29.8	44 30.2	45 59.6	44 00.4
20	45 53.4	44 06.6	46 46.9	43 13.1
25	46 24.5	43 35.5	47 48.8	42 11.2
30	47 03.5	42 56.5	49 06.4	40 53.6
35	47 51.2	42 08.8	50 40.6	39 19.4
40	48 48.4	41 11.6	52 32.8	37 27.2
45	49 56.3	40 03.7	54 44.4	35 15.6

The effect of this change in the azimuth of the plane of vibration with increase in inclination of the rays is to cause an unequal distribution of intensity of illumination in different octants of the field. This gives rise, in turn, to the phenomenon observed when either the polarizer or analyzer is rotated slightly from the crossed position;

namely, the dark cross appears to open out and to recede from the center as do the hyperbolae of a biaxial interference figure of a section normal to a bisectrix. In each case the diametral line drawn through the dark hyperbola bars in the diagonal position is normal to the plane of vibration of the nicol which has been rotated. For example, if the plane of the polarizer is $N-S$, and it is rotated to the right to a $NE-SW$ position, the hyperbolic bars are seen to move out from the center along the diagonal of the $NW-SE$ quadrants. This test furnishes a simple and direct method for ascertaining the position of the plane of vibration of the polarizer or analyzer.

A parallel beam of plane polarized light on entering the condenser lens is converted into a sharply convergent cone. In the foregoing paragraphs we have found how the plane of vibration of each single ray can be determined. This cone becomes a sharply divergent cone, enters the objective and is there converted again to a parallel beam; but the planes of vibration of the several component rays are no longer strictly parallel. Only those rays which are contained in the diametral planes parallel and normal to the original plane of vibration have retained the original plane of vibration. For all other rays the plane of vibration has been rotated somewhat and in different degrees depending on the distance from the center of the beam and on the azimuth of the ray. These effects are due solely to the influence of the lens and glass plate surfaces traversed by the rays and cannot be eliminated. They are superimposed, as it were, on the interference phenomena produced on the waves transmitted through a crystal plate whose interference figure is being observed. With these factors in mind let us now pass to the consideration of the plane of vibration represented by a dark point in the interference figure from a crystal plate.

In an interference figure a point is dark because the beam it represents vibrates parallel with the vibration plane of the polarizer and at right angles with that of the analyzer. The exact position of any point in the interference figure can be accurately determined either in terms of small circle coordinates or of polar distance and azimuth of the beam which it represents. All the rays of light, moreover, from the interference figure converge at such a small angle to the eye of the observer ($\frac{1}{2}°$ or less) that they may be considered practically parallel. It is a simple task to transfer the observed data (position of vibration plane of polarizer, positions of all observed dark points) and to determine the plane of vibration for any obliquely transmitted beam represented by a dark point in the interference figure.

If A in the orthographic projection Fig. 19 represents a dark point in an interference figure and OC, the plane of vibration of the polarizer, then the plane of vibration for the inclined beam A is the plane AHC, the great circle passing through A and C. The point H is the vibration direction of the wave propagated along A; to find the direction of propagation B within the crystal and its plane of vibration it is necessary first either to compute or to ascertain graphically from the equirefringence curves, the required refractive index, α' or γ', and then to determine the angle OB in the plane of incidence OA. The plane of vibration of the wave B is then, as a first approximation, the plane BD, the point D being the intersection of the great circle BH and the polar

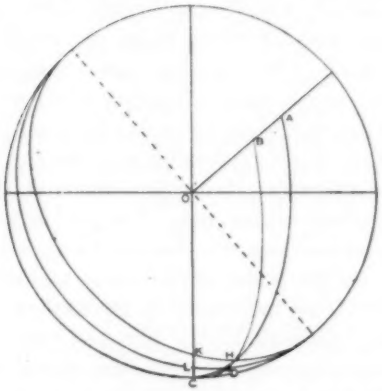

FIG. 19. *Diagram showing in stereographic projection the planes of vibration of a dark point,* A, *in the interference figure and the corresponding beam,* B, *within the crystal plate.* OC *is the plane of vibration of the polarizer,* AHC *the plane of vibration of the dark point* A, *and* BHD *the plane of vibration of the corresponding beam within the crystal plate.*

circle to B. The reason why this mode of construction is only a first approximation is the fact that the rule given above that the line of vibration of the refracted wave is in the original plane is not strictly correct for birefracting crystals, because in them the ray does not in general coincide with the wave normal and there are present in the crystal vectorial forces which cause the direction of vibration of the refracted wave to depart somewhat from the original plane of vibration. The mathematical expression for this case is no longer equation (21), but the following

$$\cot \delta_h = \cos(i-r) \cot \delta_h \pm \frac{\sin^2 r_h \tan s_h}{\sin(i+r_h) \sin \epsilon_h} \qquad (24)$$

in which ϵ_h, δ_h, i, r_h have the same significance as in equation (21); the subscript h may be 1, or 2 and indicates the two waves propagated along a given direction within the crystal; the angle s_h is the angle between the wave normal and the ray direction; this is very small for crystals of weak to medium birefringence and even in strongly birefracting crystals, such as aragonite it rarely exceeds 5 or 7°. Equation (24) may accordingly be looked upon as equation (21) to which a small correction term has been added. In crystals of weak to medium birefringence the term is so small that it may commonly be neglected altogether; in strongly birefracting minerals it is still small for points near the center of the field. In general it may be stated that the rule given above for finding the vibration plane of a point in the interference field holds not only for isotropic plates but also for birefracting crystals for points not too far removed from the center of the field. For points near the margin of the field the rule is not strictly correct; but for these points other factors enter, some of which have already been noted and which tend to mask the phenomena and to render measurements at best approximations only.

With the foregoing considerations in mind we may now discuss the several methods which have been suggested for finding the position of the plane of vibration of a dark point in the interference figure and about which there has been and still is a difference of opinion. In 1904 F. Becke[5] proposed a method for ascertaining the optic axial angle of a crystal by measuring the degree of curvature of the hyperbolic brush (zero isogyre). His method for finding the plane of vibration of the beam defined by a given point in the interference figure is to plot the point in *stereographic* projection, to pass a line through the point parallel to the plane of vibration of the polarizer and to find the great circle which is tangent to this line. This circle is then the plane of vibration (Fig. 20). In 1907 the writer[6] proposed another method; namely, plot the point in projection (orthographic, stereographic, or any other); then the plane which passes through the given point and the intersection of its polar plane with the vibration plane of the polarizer is the plane of vibration. (Fig. 21).

In 1909 F. Becke[7] criticized the writer's method on the ground that for a given direction of propagation as indicated by a point in the inter-

[5] Denkschriften der K. K. d. Wissenschaften. Wien. Math.-Naturwissen. Klasse, *70;* 1904.

[6] Am. J. Sci. (4) *24*, p. 336; 1907.

[7] Tschermak's Min. Petrogr. Mitteil. N. F. *28*, pp. 290-293; 1909.

ference figure, the two planes of vibration should be normal the one to the other; whereas in the writer's construction this angle is somewhat less than 90°. By adopting the angle-true stereographic projection plot and his method ascertaining the plane of vibration Becke was able to preserve this relation. He also simplified his method of ascertaining the vibration direction on the projection plot.

In 1911 the writer[8] considered the general problem of the transmission of light through inactive crystal plates with special reference to certain

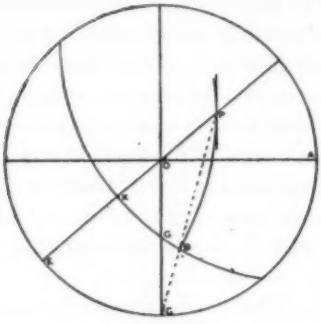

FIG. 20

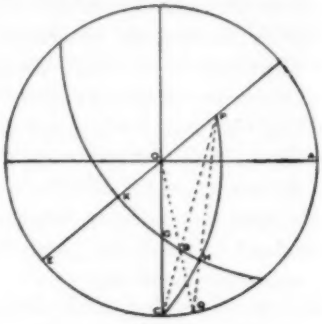

FIG. 21

FIG. 20. *Diagram illustrating Professor Becke's method for ascertaining the direction of vibration* B *of a dark point* P *in the interference figure. The great circle* PB *in stereographic projection is tangent to the dark point* P. B *is on the great circle* KG *polar to* P. B *is also at the intersection of the polar circle* KG *and the straight line* PC; OC *is the plane of vibration of the polarizer.*

FIG. 21. *Diagram illustrating the writer's first method for ascertaining the direction of vibration of the dark point* P. *This direction is represented by* G, *at the intersection of the plane of vibration,* OC, *of the polarizer and the great circle* KB, *polar to* P. *This point, however, is the point of vibration for a wave traveling in reverse direction, namely, from the observer down through the crystal plate. The point* H *at the intersection of the polar circle* PC *and the polar circle* KB *is the direction of vibration for waves which travel toward the observer from the crystal plate.* H *is also at the intersection of the polar plane* KB *and the straight line from* P *to* Q, *where* Q *is the end of the radius* OBQ.

disturbing factors, such as rotation of the plane of vibration at the boundary surfaces of the crystal plate and of the lens and glass surfaces between the polarizer and analyzer, the addition of reflected light to the directly refracted light, and emphasized the fact that, because of these factors the results obtained can at best be only first approximations. Results of series of measurements on isotropic, uniaxial, and biaxial plates were given to indicate the order of magnitude of the errors produced by several factors involved.

[8] Am. J. Sci., *4*, pp. 157-211; 1911.

In 1913 P. Kaemmerer[9] reviewed the situation and on the basis of certain simplifying assumptions concluded that Professor Becke's method is theoretically correct, that of the writer incorrect. His assumptions are: 1. That the principal refractive indices of a crystal plate may be replaced by a single average refractive index. 2. That the rotation of the vibration plane at all boundary surfaces (lenses and plate) may be disregarded. 3. That the convergent cone which, on passing through the objective, is brought to a point in rear focal plane of the objective may be replaced by a single plane wave whose front is normal to the given point; that the plane of incidence and the polarization azimuth of this wave are identical with the plane of incidence and polarization azimuth of the corresponding wave within the crystal. 4. That from each point of the conoscopic figure a plane wave passes parallel to the microscope axes through the analyzer. 5. That these assumptions are valid also for the lens system of the microscope and for any glass surfaces of the mount.

In 1914 V. Souza-Brandao[10] pointed out that Kaemmerer, by virtue of his assumption, was led to his conclusion regarding the validity of the Becke method, but that these assumptions are by no means self evident or justified; that both methods are probably in error and that further theoretical considerations and actual measurements are needed before a method, that takes into account the many factors, can be suggested.

This brief sketch of the literature suffices to show that even at the present time some uncertainty persists regarding the correct procedure for finding the plane of vibration of a point on a dark brush of an interference figure. In the light of the evidence presented in this paper we are able to analyze the problem in greater detail and to ascertain the exact status of each method.

It is evident that, if the assumptions of Kaemmerer are accepted, namely, that each wave normal, through its entire course through the crystal and lens system to the analyzer, behaves as if its vibration planes were rigidly attached to it in such a manner that throughout the course the azimuth angles of these planes with reference to the plane of incidence remain unchanged, then the construction of Professor Becke is correct. Thus in Fig. 20, the azimuth angle, KB, of the vibration plane PB is equal to the azimuth angle CE of the vibration plane OE,

[9] Fortschritte der Mineralogie, *3*, pp. 141-158; 1913.

[10] Uber die Becke-Wright'sche Streitfrage. ZS. f. Krystallogr. *54*, pp. 113-119; 1914.

and the great circle *PBE* is tangent to the line through *P* parallel to the line *OE*. In the Becke method all boundary effects are disregarded, both of lens system and of crystal plate and mount; also the birefringence within the crystal plate. To neglect these effects does not lead to large errors within the field of observation of the conoscopic figure; nevertheless theoretically the method is to that extent incorrect and can only yield results that are approximately correct.

In the writer's method the effect of the lens system was also disregarded, but not so the rotation at the boundary of the crystal plate, mounted and unmounted. Moreover the method applies to incoming waves and not to waves emerging from the crystal plate. In Fig. 20 the point *G*, which is the intersection of *OE* and the polar circle *KB* to *K*, represents the direction of vibration for rays entering the crystal plate (disregarding the correction term of equation 24). The point *H* represents the direction of vibration for waves emerging from the crystal plate and refracted by a single refraction from *P* to *O*. In the writer's method neglect of the effect of the lens system results in an overemphasis of the effect of rotation at the crystal plate and the method is to that extent in error. In neither Professor Becke's nor the writer's method are the results attained better than first approximations. Both are theoretically incorrect because in each one or more factors is disregarded which rotates the plane of vibration and this introduces an error, which may under certain conditions be appreciable.

Thus the rotation due to a single plane glass surface may be several degrees for a ray incident at an angle of 50°. (Table 2 above.) Measurements and computations by the writer on different substances, such as calcite, nephelite, muscovite, aragonite,[11] also computations on page 799 above prove that the angle included between the planes of vibration of the two emergent waves is not exactly 90°, as assumed by Becke, but it may be noticeably different, namely, 84°06.59′, in the case of the aragonite plate noted above. On the other hand, it is not advisable to consider only this rotation, as was done by the writer, and to neglect the stepping-down of this rotation as a result of the repeated refractions through the lens system. The influence of this factor varies of course from objective to objective, depending on the number of lens elements in the system; also with mount of the crystal plate. The dependence of the position of the zero isogyre of an interference figure on the number of boundary surfaces traversed can be

[11] Am. J. Sci., (4), *31*, pp. 186-197; 1911.

shown by noting its shift where a bare cover glass is inserted between the plate and the objective lens. This shift is not great but it is noticeable.

The question arises "Is it possible to devise a method which takes these many factors into account better than has been done either in the Becke method or in the writer's method?" Obviously the Becke method represents one extreme in that it disregards all boundary effects on the rotation of the plane of vibration; the writer's method represents another extreme in that only the rotation of the crystal plate for incoming waves is considered and the effects of the lens system of the objective are disregarded. It would seem, therefore, that some point between H and B of Fig. 21, possibly midway, should yield slightly more accurate results than either H, B, or G.

In Fig. 21 the point G is at the intersection of KB, the polar of P, with $O\,E$, the vibration plane of the polarizer, and of the great circle P through P tangent to the small circle through P which is parallel to the vibration plane $O\,E$. The angle $K\,G = \text{arc}\,C\,D$. The point B is at the intersection of $K\,B$, of the great circle tangent to the line through P parallel to $O\,E$, and of the line $P\,E$. The point H is at the intersection of $K\,B$, of the great circle $P\,E$ and the straight line $P\,F$.

In this renewed consideration of the subject the writer has arrived again at his original conclusion that the point P of a zero isogyre of an interference figure is dark because the plane of vibration of the wave it represents, traveling (as a narrow cone) practically parallel to the axis of the microscope is normal to the principal plane of the analyzer. To pass from this direction and to follow the cone of rays from this point through the objective into the crystal plate through a series of successive refractions it is necessary at each refraction to realize that although the line of vibration remains in the vibration plane of the incident beam, this plane is rotated slightly with each refraction. It is not permissible to overlook these refractions, as was done by the writer in his first method, and to pass directly from the point in the interference figure to the direction within the crystal and to consider the rotation thereby attained to be correct, which in fact is too large. Nor is one justified in disregarding not only rotation of objective lenses but also of crystal plate and mount as is the case in the Becke method. To state, as Kaemmerer has done, that the azimuth of the plane of vibration of the wave within the crystal plate is exactly that of the corresponding point of the interference figure and then to base his criticism of the two methods on this assumption and to con-

clude from this that the Becke method is theoretically correct and that of the writer is theoretically incorrect, simply means a failure on Kaemmerer's part to analyze the situation adequately, as Souza-Brandao has pointed out. Both methods are in fact theoretically incorrect; but both lead to results that are of about the same degree of accuracy.

Examined from a somewhat different viewpoint it is evident that the essential difference between the two methods centers in the mode of changing the direction of the inclined beam emerging from the crystal plate to a direction practically parallel with the microscope axis. In the writer's method this was supposed to be accomplished by a single refraction, in the Becke method by an infinite number of infinitely small refractions. Obviously the better plan is to realize that in the microscope objective alone 6 to 20 refractions take place and that, as a result, a value intermediate between the values obtained by these two methods is more nearly correct.

This is illustrated in Fig. 22, left side, in which the path of a ray from the crystal plate through an objective lens system is traced schematically. In this hypothetical case each refraction is supposed to cause a change in direction of 10° and there are 5 such refractions ($i=50°$); in Fig. 22 right side each refraction is supposed to cause a change of direction of 5° and there are 10 such refractions. In both cases the change in azimuth of the plane of vibration with each refraction is determined by applying the Fresnel-MacCullagh rule. Thus the successive positions of the direction of vibration are represented by the points shown in the stereographic projection. We find the rotation of the plane of vibration of the beam on emergence from the crystal plate, wherein $r=30°$, $i-r=20°$, by applying the same rule, but we realize that in the case of birefracting minerals this rule is only approximately correct. By this procedure we arrive at the points M and M' as marking the vibration direction within the crystal which corresponds to the dark point P of the interference figure. These points are situated between N and N' respectively, and the corresponding points located by the Becke method; N and N' are the points located by the writer's method applied to emergent waves. The exact positions of L and L' between D and H, and D' and H' respectively are different for different sections and slope and azimuth angles. This illustration may suffice to show how the two methods are to be modified in order to make the vibration directions conform more nearly to those in the crystal.

If this improved method be applied by using directly the two principal nicol planes we find that the corresponding vibration planes within the crystal are not 90° apart. Both observation and computations show, however, that the positions of extinction for a dark point on the zero isogyre of the interference are not exactly 90° apart, nor are the planes of vibration of the two waves, δ_1, δ_2 formed on refraction of a plane polarized wave incident at an angle, i.

Possibly the simplest method is to proceed as follows: Plot the

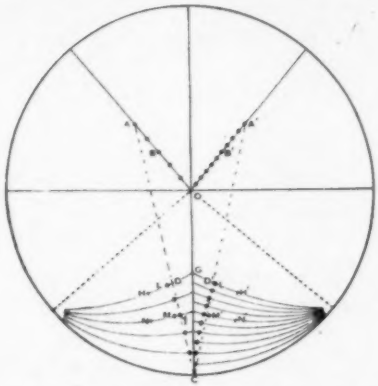

FIG. 22. *Diagram illustrating the step-down effect of the microscope lens system on the rotation of the plane of vibration on a transmitted beam of plane polarized light.* OC *is the plane of vibration of the polarizer.* A *and* A′ *observed dark points in an interference figure. On the left side of the figure the inclination* A *is supposed to have been reached by a succession of 5 refractions of 10° each* (i−r=10°); *on the right side of the figure the slope angle* A′ *is supposed to have been reached by 10 successive refractions of 5° each* (i−r=5°). *By the process the direction of vibration for* A *is found to be at* L, *for* A′ *at* L′, *whereas for a single refraction of 50°* (i−r=50°) H *and* H′ *are found to be the two vibration directions;* D *and* D′ *are the vibration directions as determined by the Becke method which presupposes an infinite number of very small refractions. The arc* LD *is greater than the arc* L′D′ *corresponding to the smaller number of refraction. By this method the vibration directions for* B *and* B′ *are indicated by the points* M *and* M′ *respectively. For the case of a single refraction they are at* N *and* N′.

given point P in stereographic projection (Fig. 23). Draw the circle polar to P, draw a straight line connecting P and C, the end of the radius marking the vibration plane of the polarizer. The intersection of this line with the polar circle is the point B of the Becke method. Connect P and Q, the end of the radius OBQ, and note its intersection H with the polar circle; this point is the writer's point for emergent waves. Some point N on the great circle between B and H is the desired point. For practical purposes the point midway between the

two is probably the most suitable. Experience has shown that the results obtained are at best only approximate and that it makes but little difference whether N, B, H, or G is used, provided the average of several different sets of measurements is taken.

Several of the above difficulties have been eliminated by the modification of the Becke method which was proposed by H. Collingridge[12] in 1913. Instead of determining the position of any convenient point on the zero isogyre, he selects a unique point, namely, that in the center of the field, and determines its position of extinction by observing the section in parallel polarized light and turning it to the position of extinction.

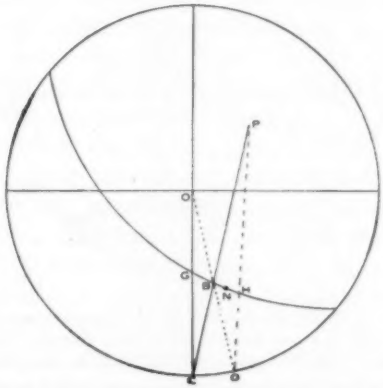

FIG. 23. *New method proposed for ascertaining the vibration direction of a dark point* P *in the interference figure.* OC *in stereographic projection is the plane of vibration of polarizer,* GH *polar circle to* P; B *is the intersection of the straight line* PC *with* GH; H *is the intersection of the polar circle* GH *and the straight line from* P *to* Q *at the end of the radius* OB. *The desired point* N *is then somewhere between* B *and* H *and, as a first approximation midway between them. In the case of a number of refractions (apochromatic objective) it is nearer* B *than* H.

This method, however, has one disadvantage; the radius vector drawn to the second optic axis intersects the plane of the optic axes at such an acute angle that a slight error in the direction of the radius vector may result in an appreciable shift in the position of the optic axis, A_2; if, moreover, the plane of the optic axes coincides with a principal nicol plane the method cannot be used. In certain cases, however, it furnishes excellent results and is free, as Collingridge notes, from certain of the troubles of the foregoing methods.

[12] Mineralogical Magazine, *16*, pp. 347-351; 1913.

SUMMARY

The phenomena observed in interference figures from crystal plates in convergent polarized light are the most beautiful and complex encountered in the study of crystal optics. Experience has proved that in order for the student to grasp the spacial relations involved and to maintain a clear picture of them, it is well for him to adhere strictly to a single surface of reference and to derive from it, step by step, the several relations presented by crystals in polarized light. If this be done in orderly sequence, the complexity which confronts him at the outset disappears and gives way to a sense of pleasure and admiration at the simplicity back of the intricate patterns exhibited by interference figures.

For the petrologist whose work is largely with thin sections of rocks, the interest centers chiefly in wave normals and refractive indices, not in ray directions, and for the treatment of this phase of the subject, the index ellipsoid is the simplest surface of reference, especially if the derived index surface be included. With the aid of these two surfaces, all the relations in the optics of transparent inactive crystal plates can be deduced. In the present paper the attempt has been made to derive the standard equations required by the petrologist by simple, direct methods, which are based on the conceptions of spheroconics and are for the most part new.

A spheroconic is simply the curve of intersection of an ellipsoid with a concentric sphere of given radius ρ. Radii vectors, drawn to the points of this curve, form a central cone, the intersection of which with a sphere of unit radius marks the position in space of all radii vectors of the ellipsoid of length ρ. Experience has shown that, irrespective of the particular theory of light adopted (whether mechanical or electromagnetic), the behavior of a wave of light on passage through a crystal in a given direction can be accurately predicted by considering the diametral plane of the index ellipsoid, normal to this direction. Along the principal axes of the ellipse made by the intersection of this plane with the index ellipsoid, the vibrations take place and the refractive indices of the two waves formed are directly proportional to the length of these axes. The spheroconic, ρ, marks the positions in space of all vibration directions along the radii vectors of length ρ. For this reason the name *equivibration curve* is suggested to designate each one of the series of spheroconics formed in this manner and represented by equation (3) of the central cone wherein ρ signifies a definite value.

To find the direction of wave normal propagation, corresponding to a given vibration direction and represented by a point on a given spheroconic, pass through the given point a plane tangent to the central cone which passes through the given spheroconic. The normal to this diametral plane is then the desired direction while the plane itself is the wave front. By this operation we pass directly to the equation of the index surface whose radii vectors are proportional to the refractive indices (reciprocals of the velocities) of the wave-normals. For a given refractive index, ρ, the equation of the index surface can be interpreted as that of a central cone, the intersections of which with a sphere of unit radius form a spheroconic, which represents the positions in space of all wave normals of refractive index ρ. These spheroconics may therefore be appropriately called *equirefringence curves*. From the properties of these equirefringence curves, the phenomena observed both in parallel polarized light and in convergent polarized light on inactive transparent crystal planes can be deduced. From them the fundamental rules and equations of crystal optics needed by the petrologist are derived directly in the body of this paper. It is believed that by thus attacking the problems from a suitable viewpoint, a degree of simplicity and directness has been attained which is not possible by other methods.

Having prepared for a given mineral a set of equirefringence curves in orthographic or stereographic projection, the observer can determine directly from the curves or from the general equation, the refractive indices for a wave propagated along any given direction. From the set of equirefringence curves the *birefringence* of a plate cut normal to any given direction can be ascertained by inspection. By passing curves through all points of equal birefringence it is possible for the student to prepare a set of *equibirefringence curves* from which the birefringence of any given direction can be read off directly.

To apply these concepts to a discussion of the interference figure exhibited by a given crystal plate it is necessary to consider the refractions at the surface of the crystal plate and also the increase in path for inclined waves. These two factors are readily taken into account by graphical plots and from them the courses of the *isochromatic curves* observed in the interference figure from a crystal plate cut in any given direction can be ascertained. Thus far the method is straightforward and simple.

Difficulties arise when it is desired to find the positions of points on the black brushes (zero isogyres) of the interference figure. The

difficulties appear because of the rotatory effects on the plane of vibration of all boundary surfaces (crystal plate, glass mount of plate, microscope lens system) between polarizer and analyzer. The amount of the rotation at any given boundary surface depends on the inclination and azimuth of the given beam of light and also on the refringence of the medium if it is isotropic; and if anisotropic, on other factors in addition. These factors are discussed in some detail in the paper because they are essential to an understanding of the differences between the methods proposed by F. Becke and the writer for finding the direction of vibration of a point on a zero isogyre of the interference figure. This has been a mooted point in the literature for many years and opinions regarding the validity of either method are not yet in accord. An analysis based on the factors just cited proves, however, as Souza-Brandao first surmised, that both methods are incorrect, the method by Becke disregarding the rotation at boundary surfaces altogether, that of the writer overemphasizing the rotation produced by the crystal plate and neglecting the step-down effect on the rotation produced by the microscope lens system.

An improved method is suggested which takes into account more satisfactorily these boundary effects, and with it somewhat more accurate results can be obtained. The analysis proves, however, that a theoretically correct method is not possible under the circumstances and that, at best, accurate measurements are not possible because of the indistinctness of the phenomena observed, and hence the Becke method, the writer's first method, and likewise the improved method suggested in this paper all furnish results that are only approximately correct. It is wise in all cases, as Becke suggested in his first paper, to measure a number of points on the dark brush in the interference figure and to average the results of the series of measurements. If this be done and the improved method of plotting be adopted, results of a satisfactory degree of accuracy for practical purposes can be obtained; but they are never so exact as the measurement of the optic axial angle made under ideal conditions with the two opic axes visible in the field.

GEOPHYSICAL LABORATORY,
CARNEGIE INSTITUTION OF WASHINGTON,
WASHINGTON, D. C.,
JUNE, 1923.

Super Spark Spectra.—The earliest distinction between arc lines and spark lines was based on their localization in the spark between electrodes, the arc lines being visible all the way from one electrode to the other, the spark lines fading or disappearing in the middle of the gap. L. and E. Bloch have photographed the spectrum of mercury vapor rendered luminous by the high frequency field of the "electrodeless" discharge. Ten turns of wire are wrapped around an arm of the silica tube containing the vapor, and the secondary of a transformer with shunted condenser and adjustable voltage is discharged through the wire. At low voltages the arc lines are perceived stretching completely across the field of vision, the spark lines are concentrated at the sides of the field. As the voltage is increased the arc lines fade, the spark lines extend across the field, and a new set of lines makes its appearance gradually; these are the ones which the Blochs regard as super spark spectra or spark spectra of higher order, emitted by atoms lacking two or more of their normal quota of electrons. [L. and E. Bloch, C.R., *176*, pp. 833–835; 1923.] K. K. DARROW

Stoke's Law of Fall Completely Corrected.—A summary of the results of studies, both experimental and theoretical, by the author and his collaborators, the full details of which will appear later in a series of articles in the Physical Review. The law of motion of small particles in a medium is found to be given by

$$F=\frac{6\pi\eta\, a\, v}{1+A'\frac{l}{a}}$$

where F is the force acting, η the coefficient of viscosity of the medium, a the radius of the body, l the mean free path, v the constant velocity produced, and A' is a factor which varies with the density of the gas and the size of the particle and which is given by the equation

$$A'=A+Be^{-ca/l}$$

Thus A and $(A+B)$ give the limiting values of A' and a/l becomes infinity (vacuum) or zero (high pressure), respectively. An experimental study of the fall of oil drops in air leads to the empirical equation

$$F=6\pi\eta\, a\, v\left[1+\frac{l}{a}(.864+.290\, e^{-1.25\, a/l})\right]^{-1}$$

It is shown, both theoretically and experimentally, that the value of $(A+B)$ is not likely to vary more than 2 per cent or 3 per cent with the nature of the drop substance or the surrounding gas. This latter empirical equation "is of very general validity and may be taken as very nearly correct in the computation of the rate of settling of particles of any kind through the rarified regions of the upper air."

Further studies by the oil drop method, in which very large values of l/a were used confirm the previous conclusion and "demonstrate again the erroneousness of the work from which the existence of sub-electrons has been inferred." [R. A. Millikan. Proc. Nat. Acad. Sci., *9*, p. 67; March, 1923.] F. K. RICHTMYER

STAGES IN THE EXCITATION OF THE SPECTRA OF THALLIUM*

By F. L. Mohler and Arthur E. Ruark

ABSTRACT

Critical potentials of thallium vapor have been measured with the following results—first resonance potential 0.9 volts, first ionization potential 6.04 volts. A higher critical potential detected by the photoelectric effect of the radiation is at 12.4 volts.

Stages in the development of the spectrum were as follows. Below the ionization potential successive lines of the two subordinate series appear with increasing voltage Above 12 volts another line spectrum appears.

Comparison of the critical potentials with the doublet series system of thallium shows that the first ionization potential is determined by the limit $2p_2$ and the first resonance potential by the difference $2p_2-2p_1$. Since no radiation can result from this transition the orbit $2p_1$ must be meta-stable. Resonance potentials corresponding to frequencies $2p_2-ms$ and $2p_2-md$ give rise to the observed low voltage spectra. Corresponding critical potentials are computed for Al, Ga and In.

The 12.4 volt critical potential and the associated second line spectrum are ascribed to a second type of single ionization, the removal of one of the two 6_1 electrons.

INTRODUCTION

The arc spectrum of any metal of the group aluminium, gallium, indium, and thallium consists of a doublet series system quite similar to that of the alkali metals but with the important difference that $2p_2$ is the highest observed spectral term for the aluminium metals while $1s$ is the highest limit for the group I elements. The maximum valence of the third group metals is three though the heavier elements of the aluminium sub-group, particularly thallium, give stable monovalent compounds.

To account for these spectral and chemical properties Bohr[1] has modified his original scheme in which the three valence electrons are symetrically placed in orbits of azimuth number one and assumes that one electron occupies normally an orbit of azimuth number two while the two other electrons are in more firmly bound orbits of azimuth one.

Evidence for this assignment of orbits is given in a careful study of the absorption spectra of thallium and indium by Grotrian.[2] He finds that both subordinate series with the common limit $2p_{1,2}$ appear as absorption lines in contrast to the behavior of the first and second group metals where the absorption series are of the principal type.

*Published by permission of the Director of the Bureau of Standards of the U. S Department of Commerce.

[1] The Theory of Spectra and Atomic Constitution (Cambridge University Press).

[2] ZS. f. Phys., *12*, p. 218; 1922.

A direct test of the theory is afforded by a measurement of the critical potentials of these elements. Measurements have been attempted only with thallium[3] and apparently the results were not in accord with the theory. It was recognized, however, by Foote and Mohler that the interpretation of their results was open to question and in a recent communication[4] the source of error is pointed out and the data are shown to be in full accord with the assumption that $2p_2$ is the normal orbit of the third valence electron. We here give an account of further work with thallium which includes electrical measurements of critical potentials together with a spectroscopic study of the development of the spectrum with increasing voltage.

APPARATUS AND PROCEDURE

Thallium distills appreciably in vacuo at about 400°C but the vapor pressure is small (possibly .01 mm) at 600°C. The vapor is chemically active so that technical difficulties limit the accuracy and range of experiments. We have used Pyrex, fused quartz and porcelain containing tubes, and iron or nickel electrodes with incandescent tungsten cathodes. The methods have been described in detail elsewhere.[5] The discharge is in all cases maintained by the potential between the cathode and a wire gauze cylinder of about 8 mm diameter surrounding it. A second grid and plate at a distance of 4 to 15 cm. from the cathode were arranged either as cylinders surrounding the cathode or as plane circular electrodes set perpendicular to the axis of the containing tube and inner grid. The latter design made it possible to increase the electron path to any length desired, a convenient feature where vapor pressures must be small. The outer grid always completely shielded the plate which was so mounted that it was insulated by cold glass from the other electrodes.

The tubes used for spectroscopic observations contained three electrodes; a cathode and surrounding grid as above and a long coaxial metal cylinder in electrical contact with the grid. The discharge was concentrated into a beam along the axis by means of a magnetic field of about 300 gauss maintained by a copper helix around the tube. The radiation was viewed in a direction nearly parallel to the beam of

[3] Foote and Mohler, Phil. Mag. *37*, p. 33; 1919.

[4] Mohler, Foote and Ruark, Science, *57*, p. 475; 1923.

[5] Ionization and Resonance Potentials of Some Non-Metallic Elements, Mohler and Foote, Bureau of Standards, Scientific Paper 400.

Characteristic Soft X-rays from arcs in gases and vapors, Mohler and Foote, Bureau of Standards, Scientific Paper 425.

electrons, the incandescent cathode being shielded from the line of sight. Photographs were obtained with a small quartz spectrograph on ordinary unstained plates.

At the temperatures required, a gas pressure of a few ten thousandths mm was almost unavoidable and some of the spectra show the gaseous impurities.

ELECTRICAL MEASUREMENTS

The accelerating potential was always applied between the cathode and inner grid. To measure the potentials of inelastic impact the outer grid was kept at the same potential as the inner and the current reaching the plate against a retarding field of .5 volts was measured. Only a few measurements were made, using an electron path about 15 cm in length in vapor at 600°. The curve at the left of Fig. 1 is typical. It shows inflections at .6, 1.5 and possibly at 2.5 and 3.6 volts. The difference between the first two, 0.9 volts, is in good agreement with the predicted first resonance potential and the rather doubtful third and fourth points may correspond to the predicted second and third resonance potentials. However, the spectroscopic method offers a simpler and more conclusive method of showing the existence of these other resonance stages.

The first ionization potential was determined by measuring the positive ion current to the plate when it was negative with repect to all other electrodes. The correction to the applied potentias was found by measuring the electron current to the plate with a retalrding field of 5 volts between grids and plate. Fig. 1 shows the type of curves obtained. It will be noted that both ion current and electron current curves are nearly linear except for a rounding off at the bottom. The zero intercepts of the straight lines give definite criteria for the potentials at which the currents begin. This method of correction was checked by admitting mercury vapor into the tube and measuring the potential difference between the thallium and mercury ionization points.

An important and difficult phase of this study was to measure the photoelectric effect of the total radiation,—the most sensitive means of detecting higher critical potentials. The outer grid was negative with respect to the cathode and the plate positive with respect to all other electrodes. Thus photoelectrons either from the outer grid or the vapor reached the plate while all other ions or electrons were shielded from it. Since the temperature of the tube was over 650°C

the sensitivity of current measurement was limited. The two curves on the right of Fig. 1 show typical results. The increase at 11.5 volts applied potential is very sharp and definite but there is some uncertainty, possibly 0.5 volts, in the corrections to be added.

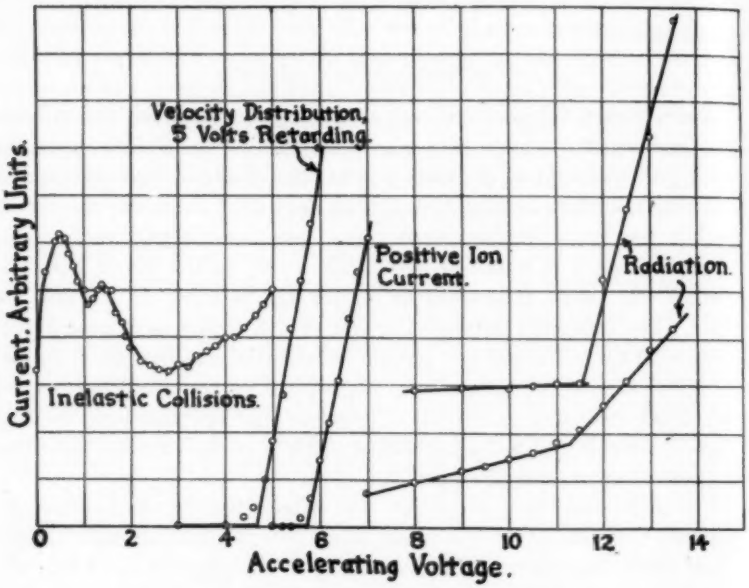

FIG. 1. *Current Voltage Curves in Thallium Vapor.*

Table 1 summarizes the electrical measurements described above.

TABLE 1

Summary of Critical Potential Measurements

1st resonance potential (2 curves)		0.9 volts
1st ionization potential		
Corrected from velocity distribution curves (5 curves)		6.04± .04
Corrected from mercury point (2 curves)		6.05± .15
	Mean	6.04 volts
Radiation potential		
Corrected from arc point (5 curves)		12.4 ± .2
Corrected from velocity distr.bution curves (2 curves)		12.4 ± .1
	Mean	12.4 volts

SPECTROSCOPIC RESULTS

Fig. 2 shows thallium spectra at different potentials which are typical of photographs taken throughout this voltage range. The

7 and 10 volt spectra show the first arc spectrum. All the thallium lines of these spectra are classified as arc lines and belong to the doublet series system. The 20 volt exposure shows a few additional lines.

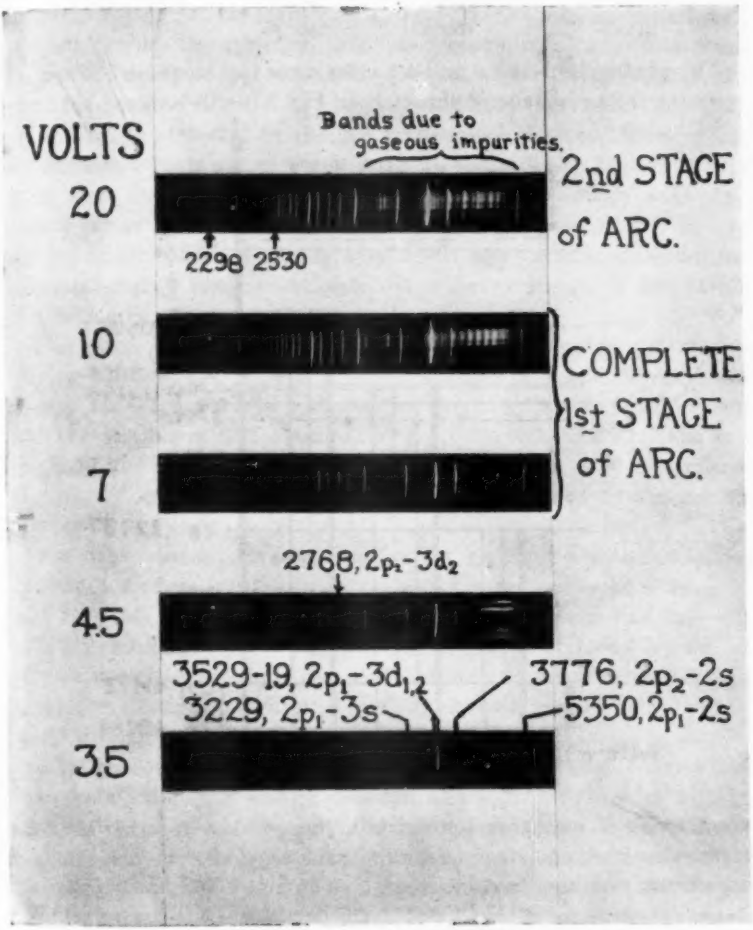

FIG. 2. *Stages in the Excitation of the Thallium Spectrum.*

These lines are entirely absent at 10 volts, quite faint at 12, and nearly as strong at 14 volts as at 20. They are listed in Table 2 and are evidently associated with the 12.4 volt critical potential.

TABLE 2

Thallium Lines Appearing Above 12 Volts

λ in Angstroms

4270.5	3091.9
3456.5	2530.9
3293.6	2394.7
3288.6	2298.2

The photographs at 3.5 and 4.5 volts show two stages in the spectra resulting from resonance collisions. In Fig. 3 it will be seen that there

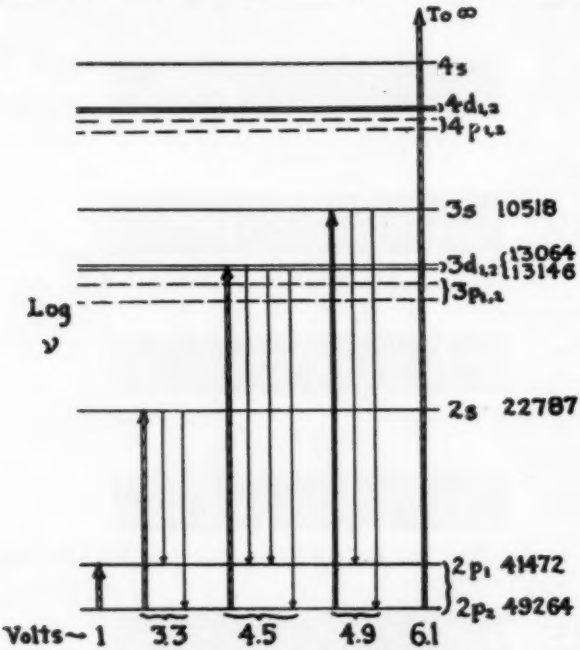

FIG. 3. *Energy Diagram of the Doublet Series System of Thallium.*

are a series of resonance potentials falling so close together that the transitions from one stage to another will be, under the conditions of experiment, apparently continuous.

INTERPRETATION OF RESULTS

Fig. 3 shows an energy diagram of the series system of thallium. Upward pointing arrows indicate possible excitation processes; downward, radiation transitions. The level of greatest negative energy, $2p_2$, gives an ionization potential of 6.082 volts. The agreement with

the observed value 6.04 confirms the view that $2p_2$ is a normal orbit of the atom. The least energy that this electron can receive is .962 volts in the transition $2p_2 \rightarrow 2p_1$. This corresponds to the observed first resonance potential .9 volts which was the most prominent type of inelastic impact. The transition $2p_1 \rightarrow 2p_2$ with emission of radiation is forbidden by the selection principle for azimuthal quantum numbers. No line $2p_2 - 2p_1$, λ12,832 is observed and we conclude that the state $2p_1$ must be metastable. On the other hand there is no detectable accumulation of atoms in the $2p_1$ state under the conditions of our experiment. Such atoms would have an ionization potential of 5.12 volts and the observed potential agreed almost exactly with $2p_2$. Hence metastable atoms must rapidly revert to normal. This can not occur by radiation but it may result from atomic collision, the potential energy being transformed into kinetic energy of translation of the colliding atoms.

The next possible energy exchange is the transition $2p_2 \rightarrow 2s$ requiring 3.269 volts. This is a true resonance potential in which the energy absorbed may be radiated as the line $2p_2 - 2s$, λ3776. But another possible radiation transition gives $2p_1 - 2s$, λ5350. Thus as a result of the resonance collision either of the lines may be emitted though the latter is not a "resonance line" absorbed by the normal atoms.

The next resonance potential 4.47 volts, giving rise to the transition $2p_2 \rightarrow 3d_{1,2}$, likewise results in emission of non-resonance lines $2p_1 - 3d_1$ and $2p_1 - 3d_2$, λ3519 and λ3529, as well as the resonance line $2p_2 - 3d_2$, λ2768. While the radiation process $3d_1 \rightarrow 2p_2$ is excluded by the selection principle for inner quantum numbers the possibility of the reverse excitation transition following electron impact is not necessarily excluded.

The spectra emitted below the ionization potential confirm this interpretation of the energy diagram although the range of velocity distribution of electrons prevented clear separation of the different stages. Thus the photograph at 3.5 volts applied potential shows the two lines λ5350 and λ3776 excited by 3.3 volts impacts and also λλ3519 − 29 resulting from a 4.5 volt collision. The 4.5 volt exposure shows the 4.5 volt excitation predominant but there are also lines associated with stages $2p_2 \rightarrow 3s$, $2p_2 \rightarrow 4d_{12}$ and higher stages.

A conspicuous feature of these spectra is the relatively great intensity of the non-resonance lines as compared with the resonance radiation. Thus the plates show λ5350 and λ3776 of nearly equal

photographic density though the sensitivity of the plate is much greater for the latter. The diffuse series shows the contrast even more strikingly. A reason for this difference quite apart from relative probability of transitions is found in the fact that the vapor is perfectly transparent to the non-resonance radiation but absorbs the resonance lines.

Though most of the prominent arc lines are visible in the 4.5 volt exposure there is a striking difference in relative intensity between this spectrum and the 7 volt photograph. One feature clearly shown in the original negatives is the change in relative intensity of the two lines $2p_1-3d_1$ and $2p_1-3d_2$. Below the ionization potential they are of nearly equal brightness while above, the former is decidedly the stronger. For this and other differences there is no evident explanation at present but such phenomena may with further study give valuable information on selection principles involved in radiation processes.

The production of metastable thallium is accomplished by resonance collisions at .96 volts or by any radiation process ending on $2p_1$. The absorption spectra obtained by Grotrian[6] show that the transition $2p_2 \rightarrow 2p_1$ is also accomplished by thermal excitation above 800°C. From 400°C to 800°C only lines originating in $2p_2$ appear in absorption while above 800°C the two series ending in $2p_1$ appear as well. Similar phenomena were found in indium.

These two metals are unique among elements so far studied in that they possess a metastable state differing from normal by such a magnitude that the vapor can be obtained either in the normal state alone or with an appreciable proportion in the excited state. The lighter metals of the group because of their higher boiling point and smaller value of $2p_2-2p_1$ will in the vapor state always consist of mixtures of stable and metastable atoms. The properties of the metastable atom can be seen from Fig. 3 if we consider p_1 rather than p_2 as the initial state. All excitation potentials will be reduced by an amount $2p_2-2p_1$ but the emission processes are presumably unchanged.

Since the arc spectrum of thallium is typical of the aluminium sub-group we can with safety predict from the known spectral terms the lower critical potentials of Al, Ga, and In. Table 3 gives critical potentials for the subgroup. The boron series are unknown but probably are of the same type, lying far in the ultraviolet. As to the other subgroup of group III containing scandium, yttrium and the rare

[6] Grotrian, l.c.

earths prediction is impossible as yet. Catalan[7] has found doublet groups in the arc spectrum of scandium suggestive of some similarity to the thallium type, but it is a consequence of Bohr's scheme that the spectra of elements in the rare earth subgroup may differ markedly from those in the thallium subgroup.

TABLE 3

CRITICAL POTENTIALS COMPUTED FROM DOUBLET SERIES

Element	Ionization		Resonance Potentials		
	$2p_2$	$2p_1$	$2p_2-2p_1$	$2p_2-2s$	$2p_2-3d_{1,2}$
Al	5.960	5.946	.014	3.129	4.004
Ga	5.973	5.871	.102	3.060	4.294
In	5.761	5.488	.273	3.009	4.06
Tl	6.082	5.120	.962	3.269	4.47

THE SECOND ARC SPECTRUM

The spectrum lines appearing above 12.4 volts which are listed in Table 2 are for the most part classified as enhanced in the spark. From the magnitude of the photoelectric effect observed it is safe to conclude that the strong lines of this spectrum lie far in the ultraviolet and indeed the thallium spectrum, which is known to λ1478, contains many strong lines beyond the range of a quartz spectrograph. The Bohr scheme suggests the significance of this second spectrum for according to this scheme the two 6_1 electrons correspond to the valence electrons of mercury. The removal of one of these will then require a potential a little greater than the ionization potential of mercury, 10.4 volts. The observed potential 12.4 is of the correct magnitude. Double ionization with removal of a 6_2 electron and one 6_1 electron, which would result in emission of a true spark spectrum, would require an energy greater than the sum of the two ionization potentials $6.1+12.4=18.5$ volts. This spark stage was not observed but here again we would expect to find the strong lines in the far ultraviolet. The spark spectrum would indeed be excited by successive impacts with 12.4 volt electrons but it seems improbable that the conditions of our experiments were favorable to such excitation. The evidence all indicates, though not conclusively, that the second line spectrum results from a single ionization process and is therefore a second arc spectrum and not a spark spectrum.

[7] Anales de la Soc. Espan. de Fis. y Quim, *20*, p. 606; 1922.

The classification of the spectrum resulting from the ejection of a 6_1 electron will require consideration of radiation processes that are as yet unknown in the field of optical spectra. Such would be the possible fall of the 6_2 electron into the vacant 6_1 orbit. The resulting radiation quantum is $12.4-6.1=6.3$ volts. The most intense line[8] in the ultraviolet is at λ1908.7 equivalent to 6.5 volts which falls within the experimental error of the predicted potential. Yet this identity is not conclusive for this is a process to which known selection principles may not apply. This hypothetical transition may be considered on the Bohr[9] theory as an X-ray emission process $P_1 \rightarrow P_2$ which is quite analogous to the transition $L_1 \rightarrow L_3$. No line of the latter type has ever been observed though it falls for heavy elements in a range easily studied, $(\nu/R > 260)$. The transition is not forbidden by selection principles for the azimuth numbers or the 'grund' numbers. However the 'grund' number restriction principle is an empirical

TABLE 4

Stages in the Excitation of the Thallium Spectrum

Type of Excitation	Critical Potential (Volts)		Radiation transition	Wave length emitted λ in A
	Computed	Observed		
1st Resonance $2p_2 \rightarrow 2p_1$	0.962	0.9	None	None
2nd Resonance $2p_2 \rightarrow 2s$	3.269	——	$2s \rightarrow 2p_2$ $2s \rightarrow 2p_1$	3776 5350
3rd Resonance $2p_2 \rightarrow 3d_{1,2}$	4.47	——	$3d_2 \rightarrow 2p_2$ $3d_1 \rightarrow 2p_1$ $3d_2 \rightarrow 2p_1$	2768 3519 3529
1st ionization $2p_2 \rightarrow \infty$	6.082	6.04	1st arc spectrum	limit 2030
2nd ionization	——	12.4	2nd arc spectrum	limit 995
1st double ionization	greater than 18.5	——	Spark spectrum	

[8] Saunders, Astrophys. Jour., *43*, p. 240; 1916.
[9] Bohr and Coster, ZS f. Phys., *12*, p. 342: 1923.

rule and though it predicts correctly the non occurrence of certain lines we can not be confident that allowed lines will actually appear.

Neither are we able to apply the inner quantum restrictions of optical spectra to the transition $P_1 \rightarrow P_2$ for while the state P_2 is assumed to be like the normal mercury state with inner quantum number zero we have no independent means of knowing the inner number for the P_1 state. This must of course be 1 if the transition in question actually occurs. A similar transition may occur when a metastable atom loses a 6_1 electron. Here again a line is known that falls in the proper position.

Table 4 summarizes the critical potentials of thallium and their relation to the stages in the excitation of spectra.

BUREAU OF STANDARDS,
MAY 15, 1923.

Studies of Smoke.—The methods which Whytlaw-Gray and Speakman employ for determining the size of smoke particles and the number of them per cc is fairly direct. But the surprising characteristic of the investigation is the definiteness of the work and the precision and consistency of the results when dealing with particles whose mass is of the order of 10^{-14} grams.

Clouds of NH_4Cl, CdO, CuO, and ZnO were studied. The oxide clouds were formed by striking an arc between electrodes of the metal in a large box (1 meter cube) containing air freed of dust by filtering through fine felt. To determine the number of particles per cc samples of these aerosols were drawn slowly and continuously through a specially constructed cell with glass windows, placed in the focal plane of a microscope. The particles were made visible ultramicroscopicly by focusing a highly illuminated narrow slit in the focal plane giving thus a thin "ribbon" of light the thickness of which (.0031 cm) was less than the depth of focus of the microscope. An area of this ribbon of .00041 cm^2 was viewed. There was thus a volume of $.0031 \times .00041 = 1.27 \times 10^{-6}$ cc visible in the field.

Conditions were so chosen that not more than 10 smoke particles were visible in this volume at any one time—a number which could by practice be "counted" at a glance. The method of counting consisted in observing the number of particles in the field at any given instant. These would slowly be drawn out of the field and as the last particle of the group disappeared the number in the next group would be observed. By making a large number of such observations the average number of particles in 1.27×10^{-6} cc is easily obtained, whence also the number per cc. In a certain experiment the average number of particles per cc in a Zinc Oxide cloud was 5.14×10^6.

It was found that the number of particles per cc decreased at first rapidly, then more slowly with time. The authors conclude that this is due to agglomeration of the small particles to form larger ones.

Having determined the number of particles per cc or per liter, it was necessary only to determine the total mass of smoke per liter to determine the average mass per particle. This was done by drawing the aerosal through a specially constructed filter consisting of "levigated white Gooch asbestos" packed in the moist state into a very thin walled glass tube 2 cm long and 3 mm internal diameter. To prevent loss during the filtering process the asbestos pad was treated in situ by a weak solution of collodion in acetone, after which the filter was dried in an oven and carefully weighed on a micro-balance sensitive to .0002 mg at a load of 200 mg. To insure complete deposition of the smoke in the filter a small platinum wire was sealed through the glass so as to project into the asbestos packing. During filtering the wire was connected to a small Wimshurst machine, producing a point discharge. The apparatus thus functioned as a combined filter and electrical precipitator.

Usually a volume of one liter was filtered for each determination, 5 minutes being required, and a mass of smoke of the order of .02 mg being collected. Simultaneous measurements of the number of particles per cc were also made, from which the average mass per particle is at once obtainable. The average mass per particle in a certain zinc oxide cloud was thus found to increase from 3.62×10^{-15} grams immediately after formation to 16.8×10^{-15} grams at the end of 5 hours.

The article discusses the behavior and appearance of the particles during and after agglomeration and also the evidence in favor of the presence of particles smaller than the limit of ultramicroscopic vision.

[Smokes: Part I. A Study of their Behavior and a Method of Determining the Number of Particles which they Contain. By R. Whytlaw-Gray, J. B. Speakman, and J. H. P. Campbell. Proc. Roy. Soc. Series A, *102*, p. 600; Feb. 1923. Part II. A Method of Determining the Size of Particles in Smokes. By R. Whytlaw-Gray and J. B. Speakman. Proc. Roy. Soc., Series A, *102*, p. 615; Feb. 1923.]

F. K. RICHTMYER

The K Absorption Limits of the Rare Earth Elements.—Measurements of these frequencies for all the rare earth elements, including Urbain's celtium, and comprising, with tantalum, all the atomic numbers from 57 to 73 (inclusive; except for the missing element 61, and assuming celtium to be 72). The square roots of the frequencies deviate perceptibly from a linear relation with the atomic number. [J. Cabrera, C.R. *176*, pp. 740–741; 1923.]

K. K. DARROW

INSTRUMENT SECTION

AN INSTRUMENT FOR THE TESTING OF PRISMS[1]

By G. W. Moffitt

INTRODUCTION

A number of ingenious and effective laboratory methods have been devised for the precise determination of the dihedral angles of a prism. In fact, it is now not at all difficult to set up apparatus of a fairly simple kind that will enable one to measure departures from the ideal in prism angles of most frequent occurrence, such as 30°, 45°, 60° and 90°, with a precision limited more by the imperfections of the prism surfaces than by the apparatus itself.

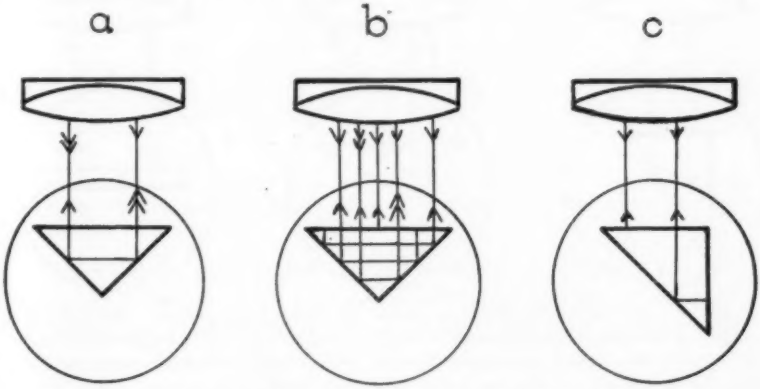

FIG. 1. *Auto-collimating methods of Chalmers and Ryland applied to the 45-45-90° prism: (a) representative rays of main image beams; (b) complete system of five beams; (c) position for measuring a 45° angle after the error in the 90° angle has been determined.*

Chalmers and Ryland[2] have described an auto-collimating method the principles of which have a number of interesting and useful applications. To measure the 90° angle of a 45-45-90° prism they placed it with the hypothenuse surface facing the objective of an auto-collimating telescope as shown in Fig. 1a. Two separate beams traverse

[1] The instrument as described in this article was shown at the Instrument Exhibit of the Optical Society at the meeting in Washington, D. C., October 1922.

[2] A Method of Testing Prisms, Trans. Opt. Soc. London, 1904–1905.

the prism in opposite directions, and, after two total reflections, emerge from the hypothenuse face. If the right angle be perfect the two emergent beams will be parallel to each other and to the original incident beam. But if the angle differs from a right angle the beams will be deflected from the ideal direction in opposite ways so that the angular separation of the two reflected beams while yet within the glass will be four times the error in the prism angle. If the errors dealt with be comparatively small the angular separation of the beams after emergence from the glass will be four times the error in the prism angle multiplied by the refractive index of the glass. This formula is sufficiently exact for practical purposes because angle errors in prisms need never be large.

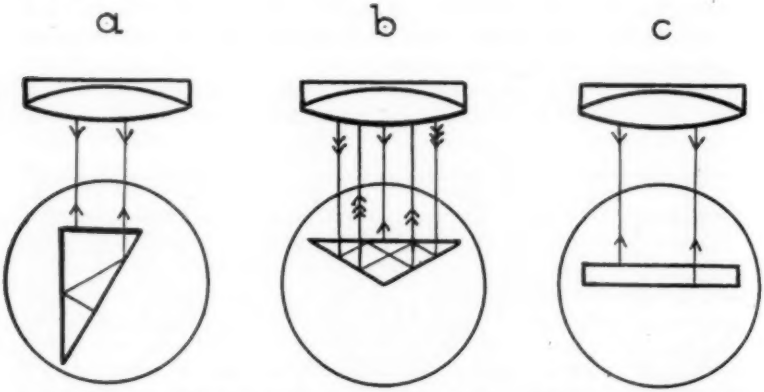

FIG. 2. *Auto-collimating method as applied by Chalmers and Ryland. Representative rays for, (a) reflection image beams with 30-60-90° prism, (b) reflection and main image beams with isosceles prism having equal angles less than 45°, (c) reflection beams with near-parallel plate.*

In all, there are five beams reflected from the 45-45-90° prism, as shown in Fig. 1b, and all of these will lie in the same plane provided the prism is free from pyramidal error.

These writers then show how the 45° angles may be studied (Fig. 1c) after having ascertained the error in the right angle. Mention is also made of the equilateral prism, the 30-60-90° prism (Fig. 2a), the isosceles prism when the equal angles are less than 45° (Fig. 2b), and the weak prism or near-parallel plate (Fig. 2c).

It will be pointed out in subsequent paragraphs of the present paper how the value of this method may be readily enhanced.

Guild[3] has suggested a way of avoiding the obvious limitations in the auto-collimating method of Chalmers and Ryland imposed by the zonal aberrations of the telescope objective and by the depth of focus of the telescope. In the case of the 45-45-90° he utilized the beams indicated in Fig. 3, but advocates the general use of comparison methods with a standard of known angle. He describes apparatus capable of high precision in a paper[4] published recently.

Wright[5] has given some of the relations existing between prism angle errors and deviation errors for a number of standard prism forms when light is incident in certain directions. The intention seems to have been to provide ways for determining prism angle errors from deviation measurements of certain beams, sometimes not those of normal use.

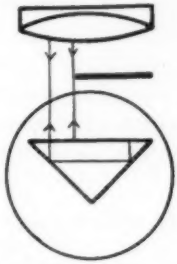

FIG. 3. *Auto-collimation as applied by Guild to the 45-45-90° prism. Since the two beams pass through the same portion of the objective the effects of zonal aberrations and depth of focus are eliminated.*

Thus while the purely geometrical problem of determining the dihedral angles of a prism has claimed consideration at various times, the important practical problem of determining the performance angle errors seems to have received less attention in print. In fact, one searches in vain for published information on methods for testing prisms that meet all the modern demands for efficiency, thoroughness and speed. Writers seem to have assumed that the ascertainment of precise measures of the dihedral prism angles is the ultimate goal. Sometimes it may be but more frequently information is desired concerning the characteristics that affect the performance of the prism when placed in its intended place within an optical instrument. Of course, if one were to make the unwarranted assumption that the surfaces were perfect

[3] Guild, Proc. Phys. Soc. London, *28;* 1916.
[4] Guild, Trans. Opt. Soc. London, *23;* 1921–1922.
[5] Wright, Journ. Opt. Soc. Amer. 1921.

and that the glass were strictly homogeneous, it would then be possible to deduce the performance angle errors from measured values of the prism angle errors. It would be difficult—perhaps impossible—to deduce any reliable measure of the definition given by a prism from measurements of the prism angle errors alone. If a proper measure of the definition afforded by a given prism is to be had, it is necessary to employ a method of examination in which the light will pass through the prism along the same general path as will be the case when the prism is housed in an instrument. Experience has shown that unless this is done good prisms may sometimes be rejected and poor prisms sometimes accepted. Therefore, in practical optical work where one is interested in obtaining the performance errors, and usually does not care what the individual prism angle errors may be, it is better to observe directly the things desired than to use the indirect methods by prism angle determination. This general plan of observing the performance errors does not limit the scope of applicability for one may readily deduce the prism angle errors from the measured values of the performance deviation errors in the few cases in which prism angle errors are of importance.

THE INSTRUMENT

In routine testing of prisms one desires to ascertain in the minimum of time reliable measures of the deviation angle error, the pyramidal deviation angle error, and the quality of the optical imagery afforded by the prism when light is passed through it as will be the case when it is seated in an instrument. If these characteristics are within the tolerances allowable for the instrument in question the prism is satisfactory optically for the use intended—and that is what the instrument assembler is interested in knowing. In addition to its capacity to yield the required information about a prism, the testing method must be amply sensitive and, at the same time, not unduly fatiguing when used continuously. It must also be so simple that persons of ordinary intelligence may be trained in a short time to use it. In view of these things the design of an instrument was undertaken in the hope of providing means for efficiently inspecting the majority of prisms and reflectors used in optical instruments. It has actually developed that the field of usefulness of the instrument finally evolved is even broader than planned in the designing, and that this little instrument is superior to a first-class spectrometer in the goniometry of certain prisms of common form.

Early in the preliminary study of methods in prism testing, it became apparent that an auto-collimating device would meet the requirements most readily. An auto-collimating telescope of moderate power will reveal the deviation angle errors of a prism and enable one to measure them. But its magnification is not sufficient for revealing the defects in the definition yielded by the prism. One may increase the magnification by substituting a microscope for the eyepiece of the telescope but the field of view will then become corresondingly smaller. It happens, however, that a magnification sufficient to reveal the defects in definition, even for prisms that are to be used in front of the objectives of telescopes magnifying from ten to twenty diameters, will still permit of the use of a field of view including the complete image system formed by a prism made with a reasonable amount of care as to its angles.

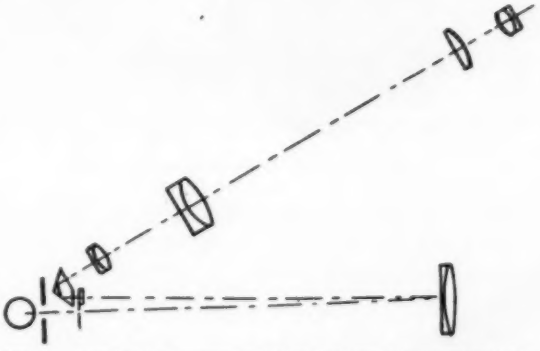

FIG. 4. *Showing the arrangement of optical parts in the prism tester.*

The optical system of the prism testing instrument is sketched in Fig. 4. Figs. 5 and 6 are general views of the instrument. Illumination is supplied by a small bulb of a form used extensively in automobile lighting. If the bulb is not frosted, a ground glass screen is interposed in the light path near it. This lamp illuminates both the pin-hole (diameter about 0.0013″) serving as an artificial star and also the rulings of the reticule. A screen having an aperture of suitable size stands between the lamp and the pin hole stopping useless light and controlling the illumination of the reticule without trimming the marginal illumination to the telescope objective. A very good objective, quite free from zonal aberrations and from coma, is required in this instrument, for it is obvious that defects in the lens might easily mask the charac-

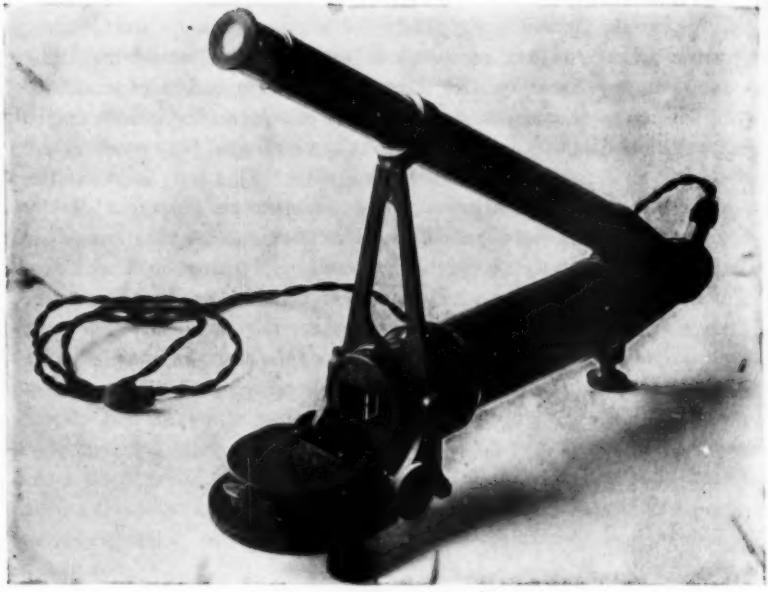

FIG. 5. *A general view of the prism testing instrument.*

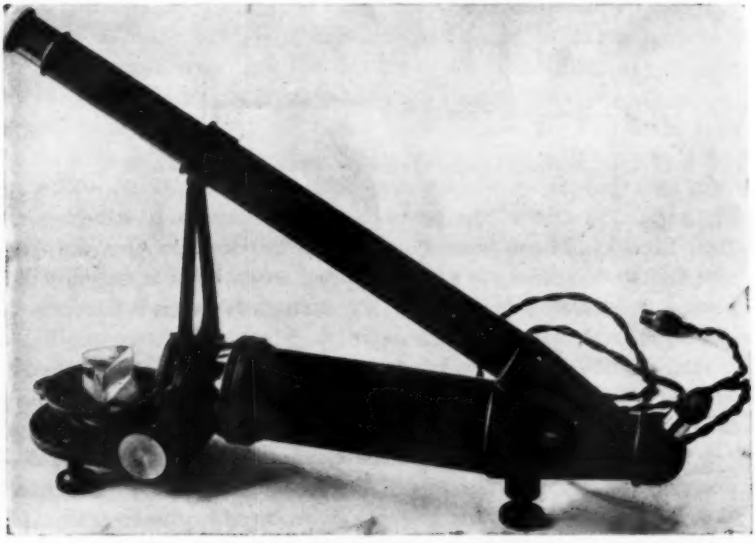

FIG. 6. *Side view of the prism testing instrument.*

teristics of a prism or even be ascribed to the prism in certain cases. Moreover, as already pointed out, zonal aberrations may result in an erroneous measurement of performance deviation angle errors. The light, after traversing the prism and returning through the objective is focused on the reticule held just above the artificial star and at the same distance from the lens. The remainder of the optical system is a compound miscroscope of magnification about sixty diameters, so arranged in conjunction with a change-direction prism that the eye-piece of the instrument stands at a point where comfortable observation is possible while operating the focussing ring or manipulating the control screws of the prism table. Considerable attention was given to the design of the prism table and the location of its controls in order that routine work might be carried on at the maximum rate with a minimum of fatigue. The prism table and all the controls were kept near the table level. As a result of this the hands and arms may remain in comfortable positions. Moreover, it is often desirable to record the results of the test on the end of the prism, and if this be done before the prism is removed from the table the location of the inscription serves to establish the positive direction of the pyramidal deviation error and there will be no chance of its being on the wrong end of the prism. For these reasons, as well as from considerations of stability and rigidity, a low position for the prism table is most desirable.

Fig. 7 shows the compactness of the design and the convenient placement of the controls. If the user is right handed the left hand will control the focusing ring while the right hand will place the prism in position against the adjustable stop provided on the prism table for that purpose. When once set for prisms of a given kind only slight readjustments of the table are required from prism to prism. While the left hand is focusing and the judgment of definition is being made, the thumb and fore finger of the right hand are bringing the image pattern into a portion of the field of view suitable for reading the performance deviation angle errors on the reticule scales. If the prisms are merely to pass a stated tolerance without record of the errors a reticule may be used showing a rectangle of the proper dimensions. One can then see at a glance whether the images fall within its boundaries.

The prism table may be set at any suitable height and securely clamped to the slow motion in azimuth, in order that the prism aperture may be placed centrally with respect to the objective. An adjustable and removable diaphragm plate is provided with which room light may be excluded from the unused portions of the objective. The small

rectangle of cylindrical lens on a vertical shaft in front of the objective provides a means for determining the sign of the deviation error in Porro prisms. Focal power of a prism may be read from the scale on the focussing ring. There is little use for any of this scale, however, except the zero mark which indicates when the collimator is set for parallel light.

FIG. 7. *Prism table controls and objective housing.*

While the instrument was made strong and rugged throughout, special attention was given to the design and construction of those hidden parts that make an instrument satisfactory in use. For example, the tube that carries the objective is practically as long as the body tube and slides in fitted rings at its ends. The focusing ring has broad bearing surfaces and adjustment to reduce backlash to a negligible amount. The focusing thrust is applied to the lens tube in line with the resistance. As a result of such precautions as these there is very little jumping or wandering of the images from mechanical causes as one passes to and fro through the positions of best focus.

THE TESTING OF PRISMS

While the original plan was to build an instrument suitable for the testing of Porro prisms a great variety of other forms may be examined with almost equal ease. The more important cases will now be discussed somewhat in detail. The treatment is not intended to be exhaus-

tive and many other cases might be given. But these will be sufficient to illustrate the use of the instrument and its adaptability to the work.

PROTECTIVE WINDOWS AND NEAR-PARALLEL PLATES

Protective windows of flat glass are used in front of the optical system in a number of instruments. Usually it does not matter if these windows have a slight amount of prism effect. In fact, as is the case with certain range finders, they are sometimes deliberately given a little prism action in order to accomplish certain adjustments of the instrument during assembly. The tolerances for these windows may be easily set for any given instrument both for definition and for prism action. Then it is simply a matter of determining whether a given window glass gives sufficiently good definition and shows a prism action within the prescribed limits. The determination of both these char-

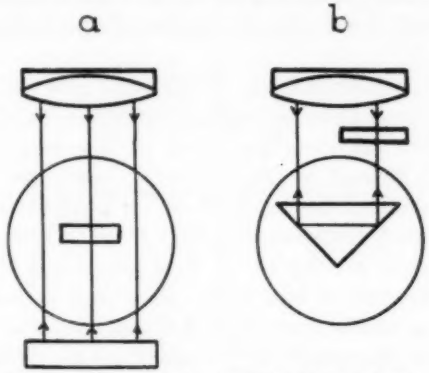

FIG. 8. *Arrangements for inspecting plates and wedges.*

acteristics is a simple matter with the prism tester. A high grade mirror, preferably of the front silvered kind, is supported on an arm extending from the base and is adjusted so that the light reflected back is focussed at a suitable point on the reticule. The glass to be examined is then held approximately perpendicular to the axis of the instrument so that a portion of the beam from the collimator traverses it twice (Fig. 8a). If a prism effect is present there will be a pair of images and the distance from the image formed by light from the mirror direct to the image formed by the light that has also traversed the glass is a measure of the deviation caused by the glass. This deviation is read directly on the divisions of the reticule scale. At the same time the character of the image formed by the light that has traversed the glass

indicates the optical quality of the window. The specimens may ordinarily be held in the fingers during the test. A deviation of about ten seconds of arc is easily seen.

If one wishes to determine the angle between the two surfaces of the plate this may be done by means of the well known formula,

$$D=A(n-1).$$

If no high grade mirror is at hand, or if one does not care to take time to attach and adjust it, a large Porro prism of known good quality may be used directly on the prism table instead; and this, being a constant deviation prism in the horizontal plane makes adjustment by rotation in azimuth unnecessary. Levelling only will be required to bring the images into the field of view. The wedge to be tested is then inserted between the objective and either the right or the left half of the Porro prism whereupon *each* of the Porro prism main images is moved by an amount (as read on the reticule) equal to the deviation of the window (Fig. 8b).

One may also determine the wedge angle and the deviation— but with less assurance as to the optical quality—without the use of any auxiliary mirror or prism according to the method suggested by Chalmers and Ryland in the reference already mentioned. If the plate to be examined be "squared on" two reflection images will be found, one for each surface of the plate. That is, if the surfaces are not strictly parallel or are not so far from parallelism that both images cannot enter the field of view at the same time, in which last case the wedging may be readily detected with the unaided eye. The separation of the images on the reticule is An from which the deviation when used as a transmission wedge may be easily found. This last method is not recommended, for the images are formed by the light reflected from unsilvered glass and are therefore faint in comparison with the main transmitted beam images used in the other methods which permit much better judgment of optical quality because of their greater brightness. Moreover, considerable trouble will be had with the "squaring on" preliminaries.

THE PORRO PRISM

The errors that may be found in the performance of specimens of this prism are (1) deviation angle error, (2) pyramidal deviation error, and (3) faulty definition. The first of these is almost entirely due to a departure from 90° in the angle at C in Fig. 9, and is practically independent of the values of the angles at A and B. The second

error arises from the pyramidal error of the prism, which may be defined in general as the angle between the line of intersection of the two shorter faces and the trace of this line on the longest face. When the incidence is normal, the definition errors are practically unaffected by the presence of deviation errors. They are due to lack of homogeneity in the glass and to imperfect surfaces.

Let us designate the error in C by c, and, according to long established practice, assume that c is positive when C is greater than the ideal value. In like manner we may designate the errors in angles A and B by a and b respectively. The perfect Porro prism would produce a deviation, D, of exactly 180°. In conformity with the notation for the prism angles and their errors, let us designate the deviation angle error by d and assume it to be positive when the deviation is greater than the ideal, that is, when the emergent beam crosses the incident beam somewhere in the space from whence the incident beam came.

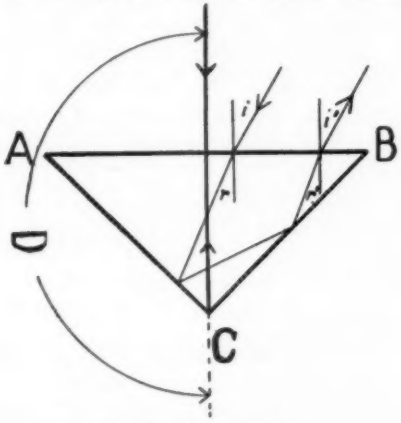

FIG. 9. *The Porro prism.*

Similarly we may designate the pyramidal deviation error by p, and if the prism is standing with principal plane horizontal—as when in position on the prism table—and the incident beam is also horizontal then the pyramidal deviation error is the amount by which the emergent beam departs from the horizontal. If this departure is in an upward direction we may assign the positive sign to the pyramidal deviation error. It will be noticed that the sign of this error changes on inverting the prism. This is not true of the deviation angle error.

To make the treatment more general, let i be the angle of incidence on the hypothenuse face as in Fig. 9. We desire to ascertain the

expression for the angle of emergence, i', from the hypothenuse face. Within the glass the angles made by the rays with the normals to the hypothenuse face are r and r', related by the expression

$$r' = r - 2c.$$

Now $$\sin i = n \sin r$$

And $$\sin i' = n \sin (r - 2c)$$
$$= n (\sin r \cos 2c - \cos r \sin 2c).$$

Combining to eliminate r,

$$\sin i' = \sin i \cos 2c - \sqrt{n^2 - \sin^2 i} \sin 2c.$$

Now, for any value of c that need be considered in a Porro prism as a result of difficulties in the forming of angle C, $\cos 2c =$ unity within practical limits. Therefore the equation may be written

$$\sin i' = \sin i - \sqrt{n^2 - \sin^2 i} \sin 2c$$

or $$\sin i' - \sin i = -\sqrt{n^2 - \sin^2 i} \sin 2c$$

If the values of i and i' ordinarily found in either axial or field pencils be substituted in this formula, the change in the deviation angle error from the case of normal incidence to the case of maximum value of i will be negligible. We may therefore assume that if the prism is satisfactory for normal incidence of a parallel beam, it will also be satisfactory under the conditions of actual use in instruments of ordinary characteristics.

If we assume perpendicular incidence and deviation errors and angle error sufficiently small to warrant taking the arc for the sine of the arc, we have

$$d = -2nc,$$

the formula usually given.

Now, when a Porro prism is placed with its hypothenuse surface perpendicular to the axis and facing the objective of the prism testing instrument, the complete image system of the artificial star consists, in general, of five separate and distinct images (see Fig. 1a), as follows:

1. The image by light reflected at the hypothenuse surface.
2. The image by light entering the right hand half of the hypothenuse surface and emerging from the left hand half of the hypothenuse surface after two total reflections.
3. The image similar to (2) formed by light passing around the circuit in the reversed direction.
4. The image by light that travels as in (2) as far as the second incidence on the hypothenuse surface where it is reflected back and retraces its path.

5. The counterpart of (4) formed by light passing around the circuit in the opposite direction.

If the prism were perfect all of these images would be superimposed. But in general all five are found grouped according to the magnitudes and signs of the two deviation errors. The main images (2 and 3), due to the transmitted light, do not move when the prism is rotated about an axis perpendicular to a principal section of the prism (rotation in azimuth) for in this respect the prism is one of constant deviation. The three reflection images, however, move laterally when the prism is rotated in azimuth but preserve their relative positions and actual spacings as they go. All the images may be moved at the same rate in the vertical direction by tipping the prism about a horizontal line perpendicular to the axis of the collimator.

Performance Errors.—Images 2 and 3 are formed by full aperture beams of light passing through the prism in a manner similar to that of an axial ray when the prism is in use in an instrument. If these images are small and round and without streamers, haze, nebulosity, or color, the definition is good. If not its defects may be measured on the reticule scales.

In the horizontal plane each one of these main beams deviates from parallelism with the incident beam by an amount which is the deviation angle error of the prism. Thus the angular distance between the two main images in the focal plane of the objective is equal to twice the deviation angle error of the prism. Therefore, the reticule carries a horizontal scale the divisions of which subtend angles of two minutes at the second principal point of the objective when it is focused for infinity, and thus each division of the scale represents one minute of deviation angle error in the prism.

In order to determine the sign of the deviation angle error the instrument is fitted with a small rectangle of cylindrical lens that may be easily introduced into the proper part of the light beams. This causes a line of light to cut diagonally across each main image in such a way as to form a cross in the field of view. If the intersection of the lines lies above the two main images in the field of view, the deviation angle error is positive, if below, negative.

In order to measure the pyramidal deviation error assume that the incident beam impinges perpendicularly on the hypothenuse surface—a condition not actually obtained in the instrument but not necessary, as tilting the prism table moves the whole pattern vertically as a unit without altering the spacings between the images. Then the

first, or hypothenuse reflected, beam would be thrown back upon itself while the main beams would return after traversing the prism. If any pyramidal deviation error were present they would rise out of the plane containing the incident beam or fall below it as the case might be. In the focal plane of the objective the vertical distance between the first, or hypothenuse, reflection image and a horizontal line joining the two main images subtends an angle at the second principal point of the objective equal to the pyramidal deviation error of the prism. Therefore, a vertical scale divided in minutes of arc subtended at the second principal point will enable one to read directly the value of the pyramidal deviation error. Or, since the two main images lie vertically half way between the single first reflection image and the pair of reflection images (4 and 5) it is obvious that the vertical distance from the single reflection image to the images (4 and 5) will be twice the pyramidal deviation error and if we rule a vertical scale with divisions equal to two minutes of arc at the second principal point of the objective each division will represent one minute of pyramidal deviation error. It is better to use the first mentioned measurement, however, for oftentimes the images (4 and 5) are too defective for satisfactory measurement owing to double passage through the prism. A coordinate ruled reticule may be used but it is better to have one with sufficient clear area within which the definition may be critically judged. Moreover, a Porro prism is a constant deviation prism in one direction and if a main image happens to fall behind a vertical line on the reticule it will be inaccessible for observation. The reticule would preferably have a clear area extending all the way across the field of view. The sign of the pyramidal deviation error is positive when the main images are above the first reflection image in the field of view.

It may be well to point out here that the values of the deviation angle error and the pyramidal deviation error do not afford a complete specification of the performance of a Porro prism with respect to collimation in an instrument if, as is customary, the Porro prism is seated with reference to its hypothenuse face. For while these errors are not affected in practice by the departure of the 45° angles from the ideal such a departure will cause a lateral shift of the axial ray when such a prism is placed in the image space of an objective. In order to insure a given degree of uniformity in this respect the prisms may be gaged by suitable mechanical means, or they may be checked on the prism tester according to the methods described in the para-

graphs on the subject of prism angle error determination of the right angled reflecting prism. Since it is advisable to gage prisms mechanically to insure proper fitting in their seat the mechanical method is sometimes preferred.

Prism Angle Errors.—Since the Porro prism is geometrically similar to the right angled reflecting prism, the description of the procedure in determining its angle errors will be given in the discussion of that prism.

THE RIGHT ANGLED REFLECTING PRISM

Angle errors in this prism are usually of considerably less importance than good definition, although there are certain instruments in which precision of angles, especially with respect to pyramidal deviation, is most desirable.

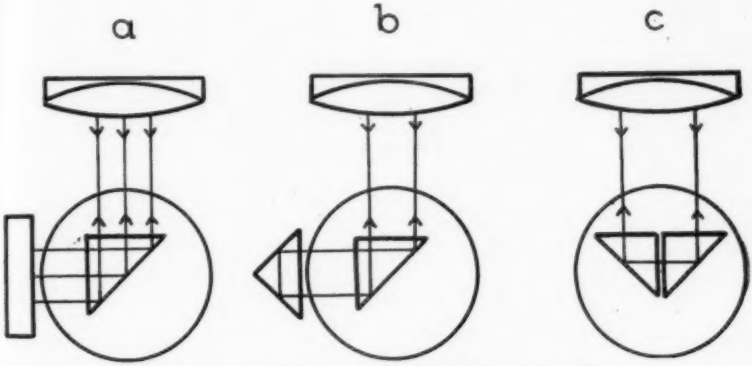

FIG. 10. *Arrangements for testing right angle reflecting prisms.*

Performance Errors.—Fig. 10 shows a number of arrangements suitable for judging the definition of the right angled reflecting prism. A high grade front surface mirror may be used to reflect the main beam back through the prism (Fig. 10a), the light thus completely traversing the prism twice. The imperfections of the definition are easily seen and judged. While but little trouble is experienced in finding the main images no doubt some would prefer a constant deviation arrangement requiring only a touch of one of the levelling screws to bring the main images into the field of view. A system of this kind is shown in Fig. 10b, in which the standard mirror is replaced by a standard Porro prism of high grade having a deviation angle error of a few minutes of arc. The standard Porro prism may be carried

directly on the prism table if desired. Two main images are seen in the field of view.

A third method not so good as the ones already mentioned is to employ a standard right angled reflecting prism on the prism table as shown in Fig. 10c.

Angle Errors.—In Fig. 11 let the direction of the incident beam be perpendicular to the face CA. Consider the two reflection images; the one formed by light reflected back from CA, and the other formed by light reflected back from CB. Let the angle errors in C and A be c and a respectively. Then the angle of incidence on CB is $2a+c$. Therefore the angle between the incident and the returning beam while yet within the glass is $2(2a+c)$ and outside the glass it is

$$d=2n(2a+c)$$

and is positive when the emergent ray lies nearer the normal to the hypothenuse than does the incident ray.

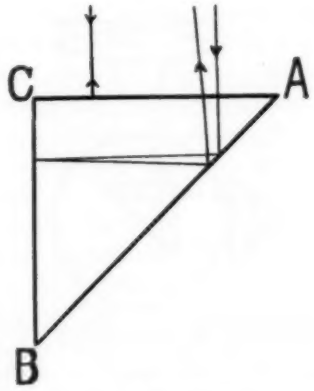

FIG. 11

If the prism be turned so that CB faces the objective, and if b represents the departure of the angle B from the ideal, a substitution of b for a in the above formula gives the relation of the observed deviation to the prism angle errors, b and c. The value of c may be determined by the method described in the discussion of the Porro prism, and then the values of a and b may be found with the aid of the formula.

The difference in height of the two images as seen on the reticule after the prism has been squared on for faces AC or BC is a measure of the pyramidal error of the prism.

REFLECTING PRISMS OF OTHER THAN 90° DEVIATION

One sometimes comes upon total reflection prisms intended to produce a deviation other than a right angle. Such prisms may be tested for definition by the methods described for the right angle reflecting prism by simply placing the auxiliary mirror or prism in the proper position. Whenever the ideal incidence and emergence angles are zero a measure of the prism angle errors may also be made.

THE ROOF PRISM

This prism would be handled precisely as in the case of ordinary reflecting prisms. The image system differs from that of such prisms, however, in that the main images are doubled in the vertical direction if the roof angle is not satisfactorily close to a right angle.

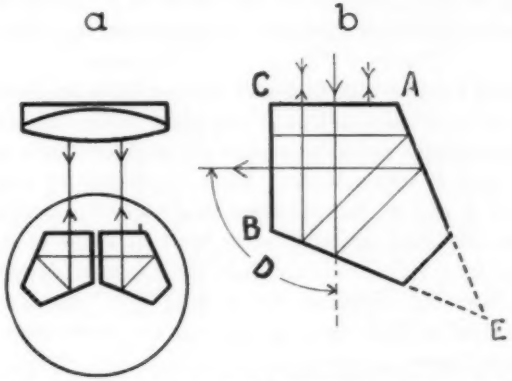

FIG. 12. *The penta prism. (a) A suitable arrangement for testing quality and pairing. (b) The angle errors of the penta prism.*

THE PENTA PRISM

Performance Errors.—The useful quadrilateral prism known as the *penta prism* may be tested on the auto-collimating instrument in a number of ways. For determining the definition and pyramidal deviation errors the procedure is similar to that for the right angled total reflecting prism, making use of an auxiliary reflector which may be either a front surface mirror, Porro prism, or a penta prism of excellent quality.

Small penta prisms may be tested in pairs as shown in Fig. 12a, either against one another or against a standard master prism. This is a convenient way of determining their deviation angle errors. It

is also very useful in pairing penta prisms for use together, as in a range finder.

Prism Angle Errors.—The angle errors of the penta prism present certain aspects not encountered in the triangular prisms. Ideal deviation may result even though all of the angles depart from the ideal values. However, in such cases, normal emergence and normal incidence are not obtained simultaneously, and on rotation of the prism in a principal plane the refraction effects at incidence and emergence are not quite identical. Therefore a slight lack of constancy in the deviation results. It is quite small, however. The condition for true constancy of deviation on rotation in a principal plane is that the angle at C shall be equal to the actual deviation, D, for the penta prism and not necessarily a right angle, Fig. 12b. When this condition is fulfilled, rotation of the prism in a principal plane will cause no variation in the deviation regardless of the values of A, B, and E.

It may be of interest here to derive the condition for ideal deviation in the case when C does not have the ideal value above mentioned. Assume perpendicular incidence on face BC, and let c and e be the angle errors of C and E respectively. Then, regardless of what may be the values of A and B, the emergent ray while yet within the glass departs from the ideal direction by $2e$, and its angle of incidence on the emergent face, AC, is $2e-c$. Thus the angle of departure of the main beam from the emergent face is $n(2e-c)$. But since AC fails to have the ideal position by c we have as the deviation error of the emergent main beam

$$d=n(2e-c)+c.$$

From this we deduce, when $d=0$,

$$2e=\frac{n-1}{n}\,c.$$

Assuming n to be 1.5 this means that we shall have $d=0$ whenever $6e=c$ approximately.

Since the measurements described under the heading of performance errors, while determining the deviation, do not give information on the question of simultaneous perpendicular incidence and emergence—on which the absolute constancy of deviation depends—it is necessary to make further observations if this point is to be determined. This may be done by observing the lateral separation on the reticule of the two reflection images, the one from AC the other from BC. It

will be noted that if the emergent beam reaches the face AC, the emergent surface, normal to this surface then that part of it reflected back and later forming the reflection image will exactly retrace its path. Thus, if perpendicular incidence and emergence simultaneously prevail the two reflection images will lie on the same vertical line—and if no pyramidal error is present will be coincident. A degree of freedom from pyramidal error sufficient to make it impossible to distinguish whether only one image is present or whether both are coincident will seldom occur. The departure of the images from a vertical line as measured on the reticule is equal to $2cn$, and from this simple relation it is possible to ascertain the actual departure of C from the ideal value.

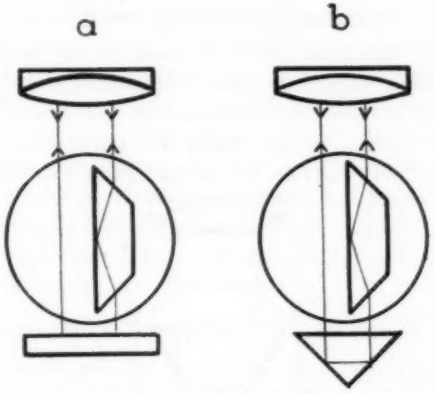

FIG. 13. *Convenient arrangements for testing inverting prisms.*

THE DOVE ERECTING PRISM

To examine this prism the auxiliary mirror is placed on the instrument and squared on with the collimator axis until the image is brought to a definite reference point on the reticule. The prism is then placed on the table in such a position that a portion of the beam traverses it twice while another portion passes alongside it as in Fig. 13a. If angle errors or performance errors are present, or if the prism is tilted, two images will be seen in the field of view, the one from the light reflected directly from the mirror (reference image), and the other by the light that has traversed the prism twice. Definition may be easily judged and the pyramidal error may be read directly from the scale on the reticule, it being the vertical distance between the two images.

Prism Angle Errors.—This prism is rather exceptional in that dihedral angle errors are of comparatively small importance while pyramidal angle error is of the utmost importance. Since it is not necessary, or even advisable in certain cases, that this prism be of the truncated 45-45-90° form, the prism angle error methods applicable to right angle reflecting or to Porro prisms do not always apply. But whenever it is desirable to determine the departure from equality of the two supposedly equal angles of the isosceles triangle, one may proceed as follows. See Fig. 13b. When the angles are less than 45° the method suggested by Chalmers and Ryland may be advantageously employed, as shown in Fig. 2b. This method gives a measure of the inequality of A and B, and also of the pyramidal error.

THE EQUILATERAL PRISM

The angles of this prism, so often used on the spectrometer, may be measured with surprising ease and precision by means of the auto-collimating method as employed in the prism tester. As in practically all cases already considered pyramidal error is easily seen and measured. In Fig. 14 assume perpendicular incidence on

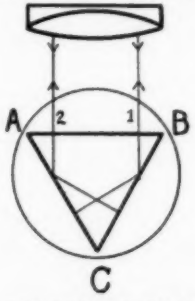

FIG. 14. *The equilateral prism polished on three faces.*

face AB. Consider ray 2. It is incident on BC at an angle of $2a+b$, and is reflected at the same angle. Therefore, the divergence of incident and returning ray while yet within the glass is $2(2a+b)$ and in the air after emergence it is

$$d=2n(2a+b)$$

the positive direction being that of crossing of the beams (as with the Porro prism).

Next consider ray 1. The angle of incidence on AC is $2b+a$, and the angle between the incident and the returning ray while yet within the glass is $2(2b+a)$, and after emergence

$$d=2n(2b+a)$$

Thus from these two observed deviations we obtain a pair of values for a and b.

By presenting each of the three faces of the prism in turn towards the collimator and observing the deviations, we obtain two independent values for each of the three angle errors of the prism.

Some idea of the precision of the instrument may be gained from the following trial. An equilateral prism of excellent quality was taken and the readings necessary for the determination of a, b, and c according to the method just described were made. The time required to take the readings and solve the three pairs of simultaneous equations was not more than ten or fifteen minutes. This prism had previously been measured a number of times on a high grade spectrometer under conditions insuring results accurate to the limit of precision of the instrument. The values for two of the angles, as determined with the prism tester, agreed to the second of arc with the mean of the spectrometer determinations for the same angles, while the value for the third angle agreed with the spectrometer value within the uncertainty of the spectrometer determination. Thus a little instrument weighing less than ten pounds and carrying no divided circle at all did the work in much less time and just as accurately as a first class spectrometer could do it in this special case of the equilateral prism.

CONCLUSIONS: HIGH POWER VERSUS LOW POWER TESTING

In conclusion it may be of interest to give some idea of what may be reasonably expected from an instrument of this kind in the work for which it was primarily intended, namely, the inspection of Porro prisms. In a number of actual trials the examination of one hundred prisms for definition and performance deviation errors required about twenty-five minutes of time when no record of the results was made. There was no attempt at speed in these tests and the inspectors had had but little experience with the instrument. This would indicate that an inspector may be relied upon to test two hundred prisms per hour and spend six or seven hours a day at the instrument without experiencing undue fatigue. If the prisms are to be numbered and a record kept, then, of course, the rate will be reduced, perhaps to one third or one fourth of the rate when no record is made.

With an instrument of this kind, capable of analyzing the performance of prisms for high power instruments carrying the prisms in the object space—or near the objective in the image space—judgment

must be exercised in the inspection of prisms intended for lower power instruments—or for those of moderately high power in which the prisms are carried near the focal plane. Imperfections of the images are so critically revealed that one may find himself judging too severely. In other words, the degree of perfection required of a prism depends upon the characteristics of the instrument for which it is intended. The question as to the advisability of employing high power tests to a prism of moderate requirements arises here. In this matter experience has shown that it is advisable to so arrange the tests that the visual acuity of the observer does not play a part. Unless this is done dlfferences of opinion as to what is seen are very apt to arise. Of course, this use of high power tests leaves the question open as to how defective a given optical part may be before it injures the performance of an instrument. But this is a matter for intelligent discussion whereas no logical reasoning will avail when two observers, say contractor and purchaser, do not agree as to what they see. Such situations have arisen with low power testing methods. Moreover, when the high power tests are employed the prospective purchaser may furnish tolerance limits in the form of actual prisms below which the quality must not fall. Such prisms may also be selected for each instrument, and preserved for the guidance of inspectors.

FRANKFORD ARSENAL,
PHILADELPHIA, PA.
APRIL, 1923.

The Eötvös Torsion Balance.—The theory and a description of the construction of the Eötvös torsion gravity balance for measuring small variations in gravity is given together with the results of some measurements preliminary to use in the field. The instrument is comparatively insensitive to vibration, the most serious source of disturbance being temperature differences in the apparatus, nevertheless variations in gravity of one part in 10^{12} can be measured in the field provided the work is done at night under the shelter of a tent. The instrument is apparently sufficiently sensitive and stable to be used in exploration work by oil companies.

The method of annealing the platinum-iridium suspension wire is described in some detail and curves are drawn showing the constancy of the suspension resulting from this annealing. The paper concludes with a complete bibliography. [H. Shaw and E. Lancaster-Jones, Phys. Soc. of London, *35*, p. 511; 1923].

L. BEHR

A SPECTROMETER TABLE

By B. J. Spence

For a number of years the writer has had in use a form of spectrometer table which differs quite radically from the divided circle type. It was designed primarily for rapid observations in spectro-radiometric work. The table with the divided circle and vernier is not well suited for most spectro-radiometric work, owing to the relatively long time required to make an angular setting and to read the vernier. The proximity of the observer's body to the radiometer, thermopile, or bolometer on making the vernier reading frequently causes a temporary zero drift in these instruments. It is usually desirable to cover or enclose the whole radiometric apparatus and this cannot be accomplished readily where it is necessary to read a vernier. With these points in view, it seemed feasible to attempt a radically different design of table giving more flexibility and also the accuracy of the divided circle instrument.

The following description with accompanying diagrams is of an instrument in use for the past two years. The spectrometer table consists essentially of a very carefully turned disc and cone of small taper fitted carefully into a vertical taper socket in a suitable tripod stand. The radius of the disc is 5.729 cm; its thickness 1 cm. The cone is truncated and is about 10 cm long with an angle of 9°. In order to prevent binding of the cone in its socket, the truncated end of the cone rests upon a 1 cm steel sphere at the bottom of the socket. A screw beneath the sphere allows the pressure of the surfaces in contact to be adjusted.

The disc is turned about the vertical axis by means of a thin steel strap fitting its periphery closely and attached to it at one point by means of a screw. One end of the steel strap is attached to a nut traveling on a carefully ground screw and the other to a counterpoise. The screw is attached to the tripod pedestal so that the motion of the nut is always tangent to the disc.

The screw is the most important feature of the apparatus. It has a 0.5 mm pitch, a diameter of 1 cm and a length of 6 cm. It was turned and ground with care according to the usual methods. Tests of the screw with the dividing engine revealed no periodic error. A more rigorous test was applied when the constant of the assembled instrument was determined. One bearing of the screw was an adjust-

able cone and the other a cylinder. The end of the screw, projecting beyond the cylindrical bearing, carries a circular disc divided into 100 parts. The screw mechanism, bearings, and divided head are similar to those found in the usual forms of Michelson interferometer. The pitch of the screw and diameter of the disc operated by the steel strap were so chosen that a rotation of the divided circle through one division produced rotation of the table through an angle of ap-

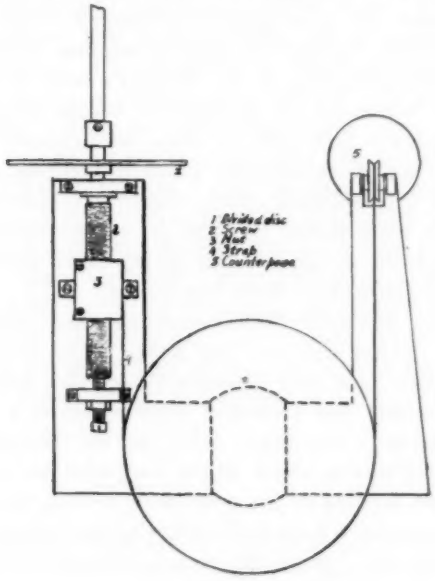

FIG .1

proximately 18 seconds. We have called the angular rotation in seconds produced by a rotation of 1 division of the divided circle the constant of the instrument. The divided circle is rotated by a long rod extending to the observer's table and the setting is viewed with an ordinary telescope.

The steel strap is kept under tension by means of a cord attached to the free end of the steel strap. This cord runs over a pulley supported from a projection on the tripod and carries a suitable weight. No lost motion could at any time be detected.

Above the disc operated by the steel strap was placed another brass disc 25 cm in diameter to serve as a table for grating or prism.

This disc is fitted over a truncated cone projecting from the upper surface of the lower disc. The upper disc can be rotated by hand independently of the lower disc. This arrangement makes it possible to adjust the position of the central image produced by a grating or prism train as observed at the receiving end of the apparatus to correspond with the zero of the divided circle.

In order to determine accurately the constant of the instrument several methods suggest themselves. The method giving the desired accuracy was a spectroscopic one, involving the use of a fixed telescope,

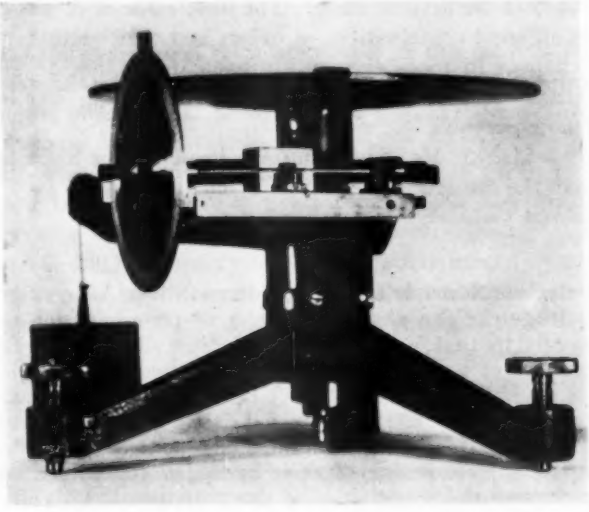

FIG. 2

fixed collimator, and a 15020 line per inch plane grating. The optical train was carefully adjusted according to the usual methods. The slit of the collimator was illuminated by means of a sodium flame. The settings for the central image and orders of the 5890 A. U. line up to the fourth order were carefully noted. The setting for example in the fourth order corresponded to $8846.2 \pm .1$ divisions of the divided circle. For the valuation of the constant the customary grating formula

$$n\lambda = 2d\cos\frac{\varphi}{2}\sin\frac{\theta}{2}$$

reduced to $$n\lambda = A \sin NK$$

where A is a constant involving the grating constant and the angle between the collimator and telescope. N is the setting on the spectrum line expressed in divisions of the divided disc and K the constant of the instrument. The constant A could not be determined experimentally with sufficient accuracy and was eliminated by using two orders and their corresponding settings. Hence

$$n_2 \sin N_1 K = n_1 \sin N_2 K$$

A direct solution of this equation for K is not readily obtained. A graphical solution gave a value of $17.962 \pm .001$ seconds corresponding to 1 division of the divided circle. The final value of K was obtained by using different combinations of orders and their settings. Effects due to changes in room temperature were found not to effect the experimental value of K. The tension of the strap was sufficient to allow no observable lost motion.

I am indebted to Mr. Küng, our mechanician, for his suggestions and care in the construction of the instrument.

NORTHWESTERN UNIVERSITY,
MARCH 15, 1923.

Photoelectric Sensitivity of Palladium Silver Alloys Saturated with Hydrogen.—The absorbing power of palladium for hydrogen is far exceeded by that of some of the palladium silver alloys; the maximum quantity of hydrogen occluded, when plotted against the percentage of silver in the alloy, reaches a relatively high maximum in the vicinity of 40% silver (although the data seem not to be as numerous as could be wished). As it has been suggested that the photoelectric sensitivity of metals is due to their hydrogen content, Krüger and Ehmer measured the sensitivities of the pure metals Pd and Ag and nine intermediate alloys, equally spaced in composition. The samples of the alloys were wires which they wound upon frames, and exposed successively to light from a mercury arc through quartz; the illuminated areas were probably not always equal. The photoelectric saturation-current was measured in a hydrogen atmosphere, after the metals and alloys had stood in hydrogen at about 160°C and 760 mm for about two hours. The curve of photoelectric current versus percentage of silver shows a very pronounced maximum at 40%, where the current is more than twice as great as for palladium and more than ten times as great as for silver. Less conspicuous maxima appear at 20% and 60%, but may be due to the inequalities in area suggested above. Unfortunately nothing is said about the sensitiveness of the substances when freed of gas. [F. Krüger and A. Ehmer, (Greifswald), ZS. f. Physik, *14*, pp. 1-5; 1923.]

K. K. DARROW

AN APPARATUS FOR TESTING THE PERCEPTION OF DEPTH

By Hermann Kellner

The problem of range finders on the stereoscopic principle which came to the foreground during the war led necessarily to the discussion of the accuracy obtainable with such instruments. One of the factors upon which this accuracy depends is the ability of the observer to distinguish by stereoscopic vision differences in depth. The apparatus herewith described was designed for determining the degree of this ability.

Any apparatus that was to be employed for this purpose had to be easy to handle and transportable. Therefore the usual methods which depend upon an object at a considerable distance from the observer for the purpose of obtaining small parallactic differences were out of question. The Zeiss stereoscope with micrometer (Wander Marke) could have been used were it not for the micrometer arrangement which, because of the minuteness of the displacements that have to be measured, must necessarily be of a delicate nature.

The apparatus here described combines simplicity of application with rugged construction. It consists of a simple lens stereoscope with a fixed distance of 63 mm between the optical axes. The focal length of the achromatic lenses is 180 mm. The object is placed in the focal plane of these lenses. This arrangement obviates, for an object of small extension, the necessity of an adjustment for different inter-pupillary distances, provided the observers have normal eyes or wear correction lenses. The stereograms represent two systems of parallel lines as shown in the upper part of Fig. 1. These lines are lined up somewhat like fence posts at equal distances from each other and the axes AA and BB which intersect under a small angle at C. For an eye looking squarely at the system AA the lines of BB at the left of C lie behind those of system AA, the lines of BB at the right of C lie in front of AA, and the lines of BB appear to bisect the spaces between the lines of AA. The center line of BB lies at the intersection of the axes AA and BB and lies, of course, in the same plane with the two adjacent lines of AA.

For the purpose of distinguishing the two series, the lines AA have a slightly pinkish color while the lines BB are of a faint greenish tint, all on a black background.

A green line between two red lines will lie apparently in front or behind the plane of the red lines and such a group represents one step in the depth scale.

The change of depth from one green line to the next one corresponds to a difference in parallactic angle of 5″, ten such steps being provided forward as well as back of the reference plane AA.

A right and left stereoscopic picture are mounted in a metal frame and placed in the stereoscope as will be described below.

To prevent prejudice in the observer an oblong diaphragm is placed in the middle of each field of the stereoscope which admits just three

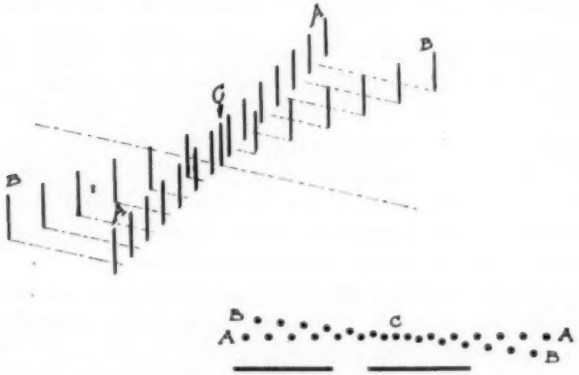

FIG. 1. *Perspective view of the object of which a stereogram is used in the instrument, also plan view of the object.*

lines, two pink ones with a green one between them. The diaphragm covers the top and bottom edges of the lines which may cause disturbances in fusion because they cannot be made exactly alike. In Fig. 2 are seen two sets of lines forming a stereoscopic picture as they appear in the stereoscope, also the difference between the two parallactic angles which causes the middle line to appear out of plane with the two others.

Fig. 3 shows schematically the general arrangement. Behind the diaphragms can be moved the metal frame carrying the stereograms of the test object so that the different triplets representing different parallactic angles can be brought into the field. A click work, not shown in the figure, stops the metal frame always in such a position that a green line appears in the center of the diaphragm. The corresponding parallactic angle may be read on the scale.

The observer starts with the scale at zero—the green line in the same plane with the two adjacent red lines—moves the object step by step away from the zero till the green line is appreciably out of plane,

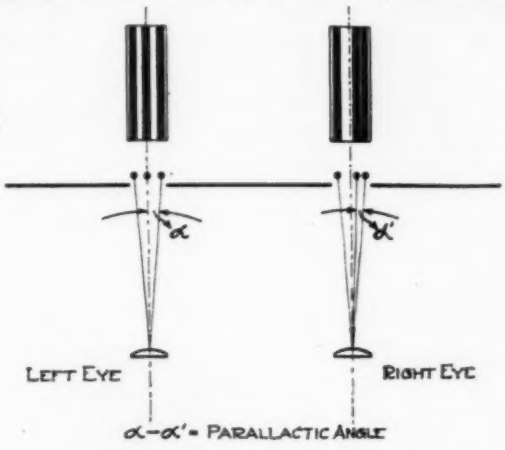

FIG. 2. *Showing a stereoscopic pair of triplets as viewed by the stereoscope.*

and notes the scale. Hereafter, for checking, the procedure is repeated by moving the scale across the zero position till the green line appears to be out of plane in the opposite direction.

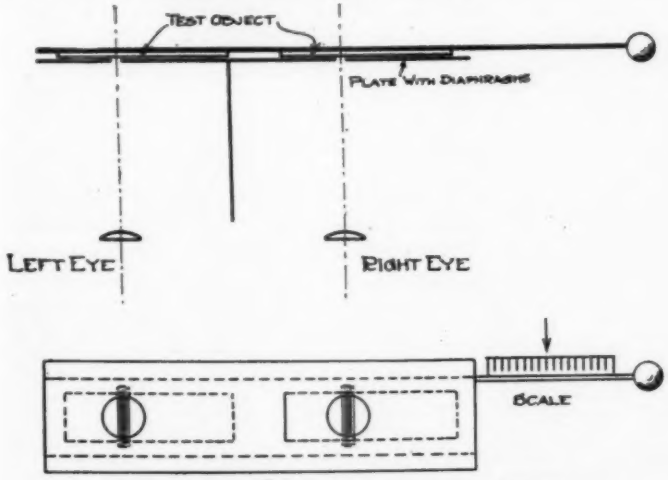

FIG. 3. *Schematic plan and elevation of the apparatus.*

Fig. 4 gives a view of the stereoscope as it was made.

The shifting of the test object, reading of the scale, etc., is preferably done by a second person as to avoid any influencing of the observer by the manipulation of the scale.

Although this apparatus does not provide for a continuous variation of parallactic angle, it has the advantage of simplicity, is easy to operate and quite immune against mechanical disorders. If the steps are made small enough, corresponding to a difference in parallactic angle of 5″, as in the instrument shown here, perfectly satisfactory results are obtained. Observers who can distinguish differences as far down as 2″, as Dr. E. Howard has found them in one or two cases among Army observers, are very rare exceptions.

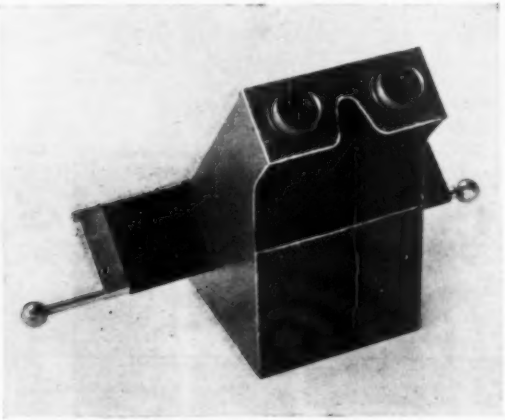

FIG. 4. *Photograph of the instrument.*

The tints used for distinguishing the two series of lines are faint, just deep enough to show a difference between them. Because of the possible objections to two different tints within the same triplet an attempt was made to distinguish them by difference in form. This, however, was found to be nearly impossible because of the great difficulty of producing a number of objects of such small dimensions so closely alike as not to cause disturbing stereoscopic effects and give the observer the chance to remember certain triplets.

. SCIENTIFIC BUREAU,
BAUSCH & LOMB OPTICAL COMPANY,
ROCHESTER, N. Y.
OCTOBER, 1922.

LONGITUDINAL ABERRATION IN ASPHERICAL OPTICAL SYSTEMS

By Irwin Roman

ABSTRACT

I. *Introduction.* Various references have been made to the use of aspherical lenses for reducing defects and new methods of analysis have been devised for studying such systems. The present paper extends certain well-known formulas from the case of spherical lenses to those not spherical, but symmetrical.

II. *The Coefficient of Form.* The general surface of revolution generated by the curve $x=x_0+\gamma_1 y^3+\gamma_2 y^4$ is characterized for present purposes by the coefficient of form $B=1-\gamma_2/\gamma_1^3$, which reduces to zero for the case of a sphere.

III. *Longitudinal Aberration.* Since the longitudinal aberration is the only second order defect affected by the departure from sphericity, the results are restricted to this defect. Several formulas are derived, each depending on the coefficient of form.

IV. *Conclusion.* The amount of retouching necessary to change a sphere of radius $1/k$ into a surface whose coefficient of form is B is $(1/8)\ B\ k^3h^4$, where h is the optical "height" i.e. distance from axis of the point concerned. For a Dallmeyer "Rapid Landscape" lens of focal length 102. 88 mm and semi-aperture 4.52 mm, the maximum amount of retouching necessary to completely remove the second order longitudinal aberration is found to be about 0.0026 mm, whether the initial or final surface is retouched.

I. Introduction

In the literature of geometrical optics, there have been numerous references to aspherical surfaces for lenses as a means of reducing defects. The practical optician apparently has known for a long time that a slight amount of longitudinal aberration could be removed by retouching locally. But little seems to have been done in the way of a study of aspherical surfaces. Taylor[1] remarks that second order aberration can be removed by parabolizing the surface. Various new methods have been devised for attacking the problem of aspherical lenses[2] and numerous attempts have been made to extend the ordinary theory to terms of order higher than the second in the case of spherical surfaces.[3]

In an abstract previously published,[4] it was stated that the curvature of the field, the relative error in zonal magnification, and the angular coma as seen from the diaphragm were not affected if the spheres were

[1] H. Dennis Taylor. "A System of Applied Optics," p. 107; London, 1906.

[2] Martin Linneman. "Über nicht-sphärische Objective." Göttingen, [thesis, 1905], Roman, Phys. Rev., *18*; pp. 62-77; 1921.

[3] For a partial list of references see S. Czapski. "Grundzüge der Theorie der Optischen Instrumente." Leipzig 1904. p. 122. E. H. Smart discusses fourth order terms in Phil. Mag., *20*, p. 82; 1910.

[4] Roman, Phys. Rev. *15*, p. 221; 1920.

replaced by quadrics of revolution about the axis of the instrument, but that the longitudinal aberration was affected. In a later abstract,[5] it was shown that every surface of revolution without cusps could be replaced by an equivalent quadric of revolution so far as the second order defects were concerned. In the present article, formulas for longitudinal aberration of the second order will be derived for a general system of revolution. Incidentally, the amount of retouching necessary to obtain a desired surface will be calculated, showing that it is proportional to the fourth power of the optical height, or of the paraxial angle, the variables most frequently used in discussions of the defects.

The methods used in the present article will be based mainly on the optical invariant introduced by Abbe and will follow, so far as convenient, the treatment of this method as given by Czapski,[3] for the corresponding spherical case. All formulas will reduce to the usual formulas for the case of spherical surfaces. Free use will also be made of unpublished methods of Professor A. C. Lunn, of The University of Chicago. Thanks is here offered for the use of these suggestions.

It will be assumed that all surfaces of the system are of revolution about a common axis, the axis of the system. This axis will be selected as the x-axis and the paraxial rays of light will be selected as going in the positive sense of this axis. Thus a single typical surface will furnish the necessary formulas. All surfaces will be assumed regular in those portions affecting the imagery, thus avoiding cusps.

II. THE COEFFICIENT OF FORM

Consider a surface generated by revolving a curve SP around an axis SC. Let PC be normal to the surface at P and cut the axis at C. Let PC make the angle ϕ with the positive x-axis, the axis of

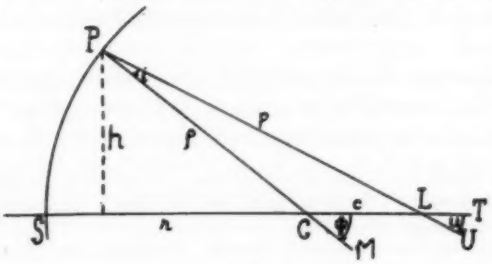

FIG. 1

[5] Roman, Phys. Rev. *18*, p. 126; 1921.

revolution coinciding with this axis. Let the distance SC be r, taken positive when the abscissa of C is greater than that of S. Let PC be ρ, taken positive in the same sense. If the surface is a sphere, $\rho = r$ and C is the center of the sphere. Let the curve SP have the equation

$$x = x_0 + \gamma_1 y^2 + \gamma_2 y^4, \tag{1}$$

where terms of order beyond the fourth are neglected and where γ_1 is finite, to avoid cusps at the axis; then, the surface generated by SP will be normal to the axis at S. The fourth order term is retained because it affects the second order aberration. The odd order terms are missing because of the symmetry.

Let the coordinates of P be (x_1, h), h being the "optical height" of the point P. Then

$$x_1 = x_0 + \gamma_1 h^2.$$

The slope of the normal at P is

$$-\left(2\gamma_1 h + 4\gamma_2 h^3\right) = -2\gamma_1 h\left(1 + \frac{2\gamma_2}{\gamma_1} h^2\right).$$

Thus the equation of the normal is

$$2\gamma_1 h\left(1 + \frac{2\gamma_2}{\gamma_1} h^2\right)\left(x - x_0 - \gamma_1 h^2\right) + \left(y - h\right) = 0.$$

Hence the abscissa of C is

$$x_0 + \gamma_1 h^2 + \frac{h}{2\gamma_1 h\left(1 + \frac{2\gamma_2}{\gamma_1} h^2\right)} = x_0 + \frac{1}{2\gamma_1} + B\gamma_1 h^2, \tag{2}$$

where $B = 1 - \dfrac{\gamma_2}{\gamma_1^3}$

may be called a "coefficient of form" for the surface. Since the abscissa of S is x_0, we have

$$r = r_0 + B\gamma_1 h^2,$$

where $r_0 = \dfrac{1}{2\gamma_1}$ is the axial radius of curvature. The horizontal distance from P to C is

$$\frac{1}{2\gamma_1} + (B-1)\gamma_1 h^2$$

so that

$$\rho^2 = \frac{1}{4\gamma_1^2}(1 + 4\gamma_1^2 B h^2)$$

and $$\rho=\frac{1}{2\gamma_1}+B\gamma_1 h^2.$$

Hence to terms of the second order in h, $\rho=r$, the value differing from the axial value of the radius of curvature by the term $B\gamma_1 h^2$, involving the coefficient of form. If we expand in terms of ϕ, we have, neglecting powers beyond the second,

$$\left.\begin{aligned} h&=\rho\sin\phi=\rho\phi \\ r-r_0&=\rho-\rho_0=\frac{Br_0}{2}\phi^2 \end{aligned}\right\}. \tag{3}$$

Let us evaluate the coefficient of form for a few special surfaces.

Case I. For a sphere, with center at the origin, taking a portion near the axis at the negative side of the center, we have for the equation of SP,

$$x^2+y^2=a^2 \quad \text{or} \quad x=-a+\frac{1}{2a}y^2+\frac{1}{8a^3}y^4,$$

so that $B=1-\frac{\gamma_2}{\gamma_1^3}=0$.

Thus B is a measure of departure from sphericity. To change a sphere of radius a into a surface with a given value of B, we may retouch the surface locally. Remembering that the axial radius of curvature is $1/2\gamma_1$, the general surface under discussion may be written

$$x=-a+\frac{1}{2a}y^2+\gamma_2 y^4$$

where a is the radius of the osculating sphere, at the axis. If the abscissa of the sphere for the same value of y is $\bar{x}$, we have, as the amount of retouching necessary, measured parallel to the axis,

$$\bar{x}-x=\left(\frac{1}{8a^3}-\gamma_2\right)y^4=\frac{B}{8a^3}y^4. \tag{4}$$

If B is positive, the surface is flatter than the sphere. In any case, the amount is proportional to the fourth power of the optical height.

Case II. For a paraboloid of revolution, the value of B is 1.

Case III. For a quadric generated by the curve

$$(1-e^2)x^2+y^2=a^2(1-e^2)$$

the value of B is e^2. The foci are on the axis of revolution, e is the eccentricity.

Case IV. For a quadric generated by the curve

$$x^2+(1-e^2)y^2=b^2(1-e^2)$$

the value of B is $e^2/(e^2-1)$. The foci are on a line perpendicular to the axis of revolution; e is the eccentricity.

Case V. For the surface generated by the catenary

$$x=-(e^{y/a}+e^{-y/a})$$

the value of B is $2/3$ so that such a surface is equivalent, in this sense, to a prolate ellipsoid of revolution of eccentricity $(1/3)\sqrt{6}$. This illustrates the general proposition that every surface of revolution, without singular points, can be considered equivalent to some quadric of revolution, neglecting powers of the optical height beyond the third. The truth of the general proposition follows from the fact that $e^2/(e^2-1)$ may vary from $-\infty$ to $+\infty$. In case B is positive, two quadrics are possible, except for $B=1$.

The coefficient of form in reality is a property of the generating curve, but we are interested only in its effect on the surface generated.

III. Longitudinal Aberration

In passing through a lens surface, a bundle of rays usually undergoes various changes, chief of which is a loss of homo-centricity, if present before refraction. The point at which a ray crosses the axis varies with the point at which it crosses the lens surface. If the system is symmetrical, we may take as the measure of the longitudinal aberration, the length of the axis cut by the extreme rays of the bundle. For ordinary surfaces, the marginal rays will cut the axis at one point, the paraxial rays will cut at another, and all the other rays will cut between. This is true even when the bundle is not homo-centric.

To calculate the longitudinal aberration, let us refer to Figure 1. Let $PL=p$, $SL=s$, $CL=c$, $<TLU=u$, $<TCM=\phi$ and $<LPC=i$. Then it follows that $c=s-r$ and $\phi=i+u$. We shall (as usual) call a quantity invariant if it has the same value before and after the ray passes (a) through the lens, for refraction, or (b) through the medium, for propagation without refraction. Since the problem of pure propagation is comparatively simple, being the theory of parallel surfaces, we shall be concerned primarily with the invariants of refraction. By the ordinary law of refraction, we have the optical invariant $I=n \sin i$. By the law of sines, $\sin u=(\rho/c)\sin i$ and so $p \sin u=I\rho(p/nc)$ giving the invariant $p/nc=p/n(s-r)$.

Remembering that we want only the second order aberration terms, we may write

$$s = s_o + b\phi^2 \tag{5}$$

so that $s - s_o = b\phi^2$ is the second order longitudinal aberration. We then have

$$c = (s - r) = (s_o - r_o)\left(1 + \frac{b - \frac{1}{2}Br_o}{s_o - r_o}\phi^2\right).$$

Also $p^2 = r^2 + c^2 + 2rc\cos\phi = (r+c)^2 - 2rc(1-\cos\phi)$

$$= s^2 - 2rc(1-\cos\phi) = s_o^2[1 + (2b/s_o - r_o/s_o + r_o^2/s_o^2)\phi^2]$$

whence $$p = s_o[1 + (b/s_o - r_o/2s_o + r_o^2/2s_o^2)\phi^2].$$

Further $$r = r_o(1 + \tfrac{1}{2}B\phi^2).$$

Hence the invariant

$$Q = \frac{nc}{pr} = \frac{n(s_o - r_o)}{s_o r_o}\left[1 + \frac{b - \frac{1}{2}Br_o}{s_o - r_o}\phi^2\right]\left[1 - \left(\frac{b}{s_o} - \frac{r_o}{2s_o} + \frac{r_o^2}{2s_o^2}\right)\phi^2\right]\left[1 - \tfrac{1}{2}B\phi^2\right]$$

$$= n\left(\frac{1}{r_o} - \frac{1}{s_o}\right)\left\{1 + \left[\left(\frac{1}{s_o - r_o} - \frac{1}{s_o}\right)b - \left(\frac{r_o}{s_o - r_o} + 1\right)\frac{B}{2} + \frac{r_o}{2s_o}\left(1 - \frac{r_o}{s_o}\right)\right]\phi^2\right\}$$

$$= n\left(\frac{1}{r_o} - \frac{1}{s_o}\right) + \left[\frac{bn}{s_o^2} - \frac{Bn}{2r_o} + \frac{r_o^2 n}{2s_o}\left(\frac{1}{r_o} - \frac{1}{s_o}\right)^2\right]\phi^2.$$

From this, we obtain the two invariants

$$Q_o = n(1/r_o - 1/s_o), \tag{6}$$

$$Q_1 = \frac{bn}{s_o^2} - \frac{Bn}{2r_o} + \frac{r_o^2}{2ns_o}Q_o^2. \tag{7}$$

If we use Δ to denote the increment due to passage through the surface, we have from these

$$\Delta\frac{bn}{s_o^2} = \frac{B}{2}\Delta\frac{n}{r_o} - \frac{r_o^2 Q_o^2}{2}\Delta\frac{1}{ns_o}, \tag{8}$$

while

$$\Delta\frac{n}{s_o} = \frac{1}{h}\Delta nu = \frac{1}{r_o}\Delta n.$$

The invariant Q_o enables us to compute the new value of s_o from the old, while Q_1 enables us to compute the new value of b from the old. Starting from a particular pair of values of s_o and b, we can calculate their values for each of the following media, since n, r_o and B depend on the media and lens surfaces entirely.

We can also express the aberration in terms of the angle u. We can write

$$s - s_o = au^2 \tag{9}$$

Since $\rho \sin \phi = p \sin u$, we have, to the second order,

$$u = \phi r_o / s_o$$

and $$au^2 = a\phi^2 (r_o/s_o)^2 = b\phi^2.$$

Hence $$b = ar_o^2/s_o^2 \quad \text{and}$$

$$Q_1 = \frac{ar_o^2 n}{s_o^4} - \frac{Bn}{2r_o} + \frac{r_o^2}{2ns_o} Q_o^2 = r_o^2 \left[\frac{Q_o^2}{2ns_o} + \frac{an}{s_o^4} - \frac{Bn}{2r_o^3} \right]. \tag{10}$$

Finally[6]

$$\Delta\left(\frac{an}{s_o^4}\right) = \frac{B}{2r_o^3}\Delta n - \frac{Q_o^2}{2}\Delta\left(\frac{1}{ns_o}\right). \tag{11}$$

One measure of the blurring due to longitudinal aberration is the optical height of the marginal ray as it crosses a plane normal to the axis at the intersection of the paraxial rays. If we call this height $\frac{1}{2}z$, it follows that we have

$$z = 2(s_o - s) \tan u = -2au^3. \tag{12}$$

Hence

$$nuz = -2anu^4 = -2h^4 \frac{an}{s_o^4} \tag{13}$$

where h is the optical height of the marginal ray at the lens. Then[7]

$$\Delta nuz = Q_o^2 h^4 \Delta(1/ns_o) - \frac{Bh^4}{r_o^3}\Delta n. \tag{14}$$

The quantity $nu = n \sin u$ (to the present degree of approximation) is the Abbe "numerical aperture."

Since the longitudinal aberration is $l = au^2$, we have

$$\Delta\left(\frac{an}{s_o^4}\right) = \Delta\left(\frac{nl}{s_o^4 u^2}\right) = \Delta\left(\frac{nlu^2}{h^4}\right) = \frac{B}{2r_o^3}\Delta n - \frac{Q_o^2}{2}\Delta\left(\frac{1}{ns_o}\right). \tag{15}$$

If the initial bundle is homo-centric, and if the system is used in air, the final longitudinal aberration is

$$l_k = \frac{h_k^4}{2u_k^2} \sum_{i=1}^{k} \left\{ \frac{B}{r_o^3}\Delta n - Q_o^2 \Delta\left(\frac{1}{ns_o}\right) \right\}_i = \frac{h_k^4}{2u_k^2} \sum_{i=1}^{k} \left\{ \frac{B}{r_o^3}\Delta n - \frac{Q_o^2}{h}\Delta\left(\frac{u}{n}\right) \right\}_i. \tag{16}$$

We also have

$$\Delta nlu^2 = \frac{Bh^4}{2}\Delta n - \frac{Q_o^2 h^4}{2}\Delta\left(\frac{1}{ns_o}\right),$$

[6] Czapski. *loc. cit.* p. 111.

[7] Czapski. *loc. cit.* p. 113.

so that

$$l_k=\frac{1}{2u_k^2}\sum_{i=1}^{k}\left\{\frac{Bh^4}{r_o^3}\Delta n-Q_o^2h^4\Delta\left(\frac{1}{ns_o}\right)\right\}_i=$$
$$\frac{1}{2u_k^2}\sum_{i=1}^{k}\left\{\frac{Bh^4}{r_o^3}\Delta n-Q_o^2h^2\Delta\left(\frac{u}{n}\right)\right\}_i. \qquad (17)$$

It is possible to get other formulas for the longitudinal aberration. Thus, we may proceed as follows. Let

$$c-c_o=\tfrac{1}{2}E\phi^2. \qquad (18)$$

Then

$$l=(r-r_o)+\tfrac{1}{2}E\phi^2.$$

By the law of sines,

$$\frac{1}{c}=\frac{\sin u}{\rho\sin i}=\frac{1}{\rho}\left\{\frac{\sin\phi\cos i}{\sin i}-\cos\phi\right\}=n\cos i\left\{\frac{p}{\rho cn}-\frac{\cos\phi}{\rho n\cos i}\right\}$$
$$=n\cos i\left\{\frac{1}{r\rho Q}-\frac{\cos\phi}{n\rho\cos i}\right\}$$

Hence

$$\frac{1}{nc\cos i}=\frac{1}{r\rho Q}-\frac{\cos\phi}{n\rho\cos i}$$

so that

$$\Delta\left(\frac{1}{nc\cos i}\right)=-\frac{\cos\phi}{\rho}\Delta\left(\frac{1}{n\cos i}\right)$$

and

$$\Delta\left(\frac{1}{n\cos i}\right)\left[\frac{1}{c}+\frac{\cos\phi}{\rho}\right]=0.$$

Since

$$\frac{\sin i}{c}=\frac{\sin u}{\rho}=\frac{\sin\phi}{p},$$

we have, to the second order,

$$i/c_o=u/r_o=\phi/s_o.$$

Thus

$$\begin{cases}\rho=r_o(1+\frac{1}{2}B\phi^2)\\ c=c_o(1+\frac{1}{2}E\phi^2/c_o)\\ \cos\phi=1-\frac{1}{2}\phi^2\\ \cos i=1-\frac{1}{2}c_o^2\phi^2/s_o^2,\end{cases}$$

whence

$$\Delta\left(\frac{1}{n}\right)\left[1+\tfrac{1}{2}\frac{c_o^2}{s_o^2}\phi^2\right]\left[\frac{1}{c_o}\left(1-\frac{1}{2}\frac{E}{c_o}\phi^2\right)+\frac{1}{r_o}\left(1-\tfrac{1}{2}\phi^2\right)\left(1-\tfrac{1}{2}B\phi^2\right)\right]=0,$$

and

$$\Delta\left(\frac{1}{n}\right)\left(\frac{1}{c_o}+\frac{1}{r_o}\right)+\frac{\phi^2}{2}\Delta\left(\frac{1}{n}\right)\left[\frac{c_o}{s_o^2}+\frac{c_o^2}{s_o^2 r_o}-\frac{E}{c_o^2}-\frac{1}{r_o}-\frac{B}{r_o}\right]=0.$$

Since

$$\Delta\left(\frac{1}{n}\right)\left(\frac{1}{c_o}+\frac{1}{r_o}\right)=\Delta\left(\frac{1}{Qr_o^2}\right)=0,$$

we have

$$\Delta\left(\frac{1}{n}\right)\left[\frac{c_o}{s_o^2 r_o}(r_o+c_o)-\frac{E}{c_o^2}-\frac{1+B}{r_o}\right]=0,$$

so that

$$\Delta\left(\frac{E}{nc_o^2}\right)=-\Delta\left(\frac{1}{ns_o}\right)-\frac{B}{r_o}\Delta\left(\frac{1}{n}\right). \tag{19}$$

Since $Q_o=n(1/r_o-1/s_o)$ we have $1/s_o=1/r_o-Q_o/n$ and hence

$$\Delta\left(\frac{E}{nc_o^2}\right)=Q_o\Delta\left(\frac{1}{n^2}\right)-\frac{B+1}{r_o}\Delta\left(\frac{1}{n}\right). \tag{20}$$

Thus if the initial bundle is homo-centric and if the system is used in air, the final longitudinal aberration is

$$l_k=\tfrac{1}{2}\sum_{i=1}^{k}(B\phi^2)_i+\tfrac{1}{2}(c_o^2)_k\left[\sum_{i=1}^{k}\left\{Q_o\Delta\left(\frac{1}{n^2}\right)-\frac{B+1}{r_o}\Delta\left(\frac{1}{n}\right)\right\}_i\right]\phi_k^2. \tag{21}$$

The value of c_o can be traced through the system by means of $c_o=s_o-r_o$ and $Q_o=n(1/r_o-1/s_o)$. ϕ_k is calculated with little difficulty. B, n and r_o depend on design.

Another form is sometimes useful. If we let

$$c-c_o=\tfrac{1}{2}Du^2=\tfrac{1}{2}E\phi^2, \tag{22}$$

then $E=(r_o^2/s_o^2)D.$

Since $Q_o=n(1/r_o-1/s_o)=nc_o/r_o s_o$

we have $1/nc_o^2=n/Q_o^2 r_o^2 s_o^2$

so that

$$\Delta\left(\frac{E}{nc_o^2}\right)=-\left(\Delta\frac{1}{ns_o}+\frac{B}{r_o}\Delta\frac{1}{n}\right)$$

becomes

$$\Delta\frac{nD}{s_o^4}=-Q_o^2\left(\Delta\frac{1}{ns_o}+\frac{B}{r_o}\Delta\frac{1}{n}\right). \tag{23}$$

Since $h=s_o u$, we have[8]

$$\Delta nDu^4=-Q_o^2h^4\left(\Delta\frac{u}{nh}+\frac{B}{r_o}\Delta\frac{1}{n}\right)=-Q_o^2h^3\left(\Delta\frac{u}{n}+\frac{Bh}{r_o}\Delta\frac{1}{n}\right). \tag{24}$$

[8] It has been shown that this formula and formula (20) are equivalent but the proof is omitted. The reader interested in this equivalence may prove it readily.

Since $r-r_0=Bh^2/2r_0$, we have for the final aberration,[9]

$$l_k=\tfrac{1}{2}\sum_{i=1}^{k}\left(\frac{Bh^2}{r_0}\right)_i-\frac{1}{2u_k^2}\sum_{i=1}^{k}\left\{Q_0^2h^3\left(\Delta\frac{u}{n}+\frac{Bh}{r_0}\Delta\frac{1}{n}\right)\right\}_i. \tag{25}$$

Further, since

$$u=h/s_0=h/r_0-hQ_0/n$$

we have

$$\Delta\frac{u}{n}=\frac{h}{r_0}\Delta\frac{1}{n}-hQ_0\Delta\frac{1}{n^2},$$

so that we can write the above formula

$$l_k=\tfrac{1}{2}\sum_{i=1}^{k}\left(\frac{Bh^2}{r_0}\right)_i-\frac{1}{2u_k^2}\sum_{i=1}^{k}\left\{Q_0^2h^4\left(\frac{B+1}{r_0}\Delta\frac{1}{n}-Q_0\Delta\frac{1}{n^2}\right)\right\}_i, \tag{26}$$

IV. CONCLUSION

We have thus derived several formulas for the longitudinal aberration of the second order. Other formulas might be derived, but it does not seem desirable to do so at this time. The formulas all involve B, the coefficient of form and hence by the proper selection of the value of B for one or more surfaces, the final aberration may be reduced or even eliminated. The amount of retouching necessary is of the fourth order in the optical height of the ray passing through that part of the lens. This amount of retouching is given by

$$\xi=\eta h^4 \text{ where } \eta=B/8a^3=Bk^3/8.$$

As an example of the method, let us consider the Dallmeyer "Rapid Landscape" lens.[10] This is a cemented triplet with the curvatures, indices of refraction and axial thicknesses given in the table. Let the incident beam be from the left and be parallel to the axis of the system. To trace the rays through the system we shall use the formulas

$$\left.\begin{array}{ll}\text{Refraction:} & n_i\kappa_i'=n_{i-1}\,\kappa_i+k_i\Delta n\\ & s_i'=\dfrac{1}{\kappa_i'}\\ \text{Transfer:} & s_{i+1}=s_i'-l_i\\ & \kappa_{i+1}=\dfrac{1}{s_{i+1}}\\ & h_{i+1}+h_i\,(1-\kappa_i'\,t_i)\end{array}\right\} \tag{27}$$

[9] Phys. Rev., *15*, p. 221; and *18*, p. 126.

[10] Moritz von Rohr; "Theorie und Geschichte des Photographischen Objectivs," Berlin, p. 178, 1899.

For the aberration, we have, (see Eq. (16)).

$$l=\frac{h_4^2\ s'_4{}^2}{2}\left\{\sum_{i=1}^{4}\lambda_i B_i-\sum_{i=1}^{4}Q_i^2\Delta_i\frac{\kappa}{n}\right\}\text{ where}$$
$$\lambda_i=k_i^3\,\Delta_i n \tag{28}$$

We then have, by these formulas, the values given in Table 1.

TABLE 1

i	1	2	3	4
k_i	−0.016556	−0.057803	−0.02079	−0.039063
κ_i	0	−0.005576	−0.0075010	−0.0068418
n_i	1.521	1.581	1.514	1
n_{i-1}	1	1.521	1.581	1.514
κ_i'	−0.005671	−0.0075581	−0.0069129	0.00972
s_i'	−176.34	−132.31	−144.63	102.88
t_i	3.0	1.0	1.5	
h_i	1	1.017	1.0247	1.0353
Q_i	−0.016556	−0.079437	−0.02101	−0.048783
$Q_i^2\Delta_i\kappa/n$	−0.000001022	−0.00000703	0.00000007879	0.000033886
λ_i	−0.00000236	−0.000011588	0.00000060203	0.000030637

The focal length is 102.88. For the longitudinal aberration, we have

$$l=5672\ \{\Sigma\,\lambda B-2.59\times10^{-5}\}$$

per unit aperture. For purely spherical surfaces, the aberration is −0.1469 per unit aperture. For an aperture 1/11 of the focal length, we have 4.52 for the initial value of h; in this case the aberration is −3 units.

To remove the aberration, we have merely to solve the equation

$$\Sigma\,\lambda B=2.59\times10^{-5}$$

Because of the nature of the lens, we shall retain the cemented surfaces as spherical and merely study the effects of retouching the initial and the final surfaces, respectively. Then $B_2=B_3=0$ and hence

$$30.637\,B_4-2.36\,B_1=25.9.$$

If only the first surface is retouched, $B_4=0$ and

$$B_1=-10.97 \qquad \eta=6.223\times10^{-6}.$$

If only the last surface is retouched, $B_1=0$ and so

$$B_4=0.8454 \qquad \eta=-6.299\times10^{-6}$$

In the former case, we must retouch negatively, i.e., most at the center, the maximum amount being $6.223\times10^{-6}h^4$, measured parallel to the

axis. In the latter case, the retouching is positive, the new surface being flatter than a sphere. In this case the maximum amount is $6.299\times10^{-6}h^4$. For the initial value of $h=4.52$, just mentioned, the two amounts are 0.00259 and 0.002622 units, respectively.

If we wish to correct for two colors, the two longitudinal spherical aberrations being l and l', the cemented surfaces may still be left spherical. In this case, we must solve the pair of equations

$$\left.\begin{aligned}\lambda_1B_1+\lambda_2B_2&=l\\ \lambda_1'B_1+\lambda_2'B_2&=l'\end{aligned}\right\} \tag{29}$$

If it is not necessary to remove the aberration, but is sufficient to reduce it to a value l_o, we have merely to solve the equations

$$\Sigma\lambda_iB_i=\Sigma_i\, Q_i^2\Delta_i\frac{\kappa}{n}+2l_o/h_k^2S_k'^2$$

for B_i. Other applications are apparent.

One distinct advantage of this method lies in the fact that so far as second order effects are concerned, a lens system may be designed with only secondary regard to longitudinal aberration and this then removed by retouching in a definitely known manner. In camera systems, where large apertures are needed, the higher order terms may make this method of questionable value. In telescope systems, where second order terms are sufficient, the method should prove valuable.

NORTHWESTERN UNIVERSITY,
EVANSTON, ILLINOIS,
FEBRUARY, 1923.

Measurement of Power Factor and Effective Resistance in Alternating Current Circuits.—Null methods are described for the measurement with the aid of a quadrant electrometer, of the power factor and the effective resistance of alternating current loads, including those operating at high voltages. The methods are especially suitable for low power factors and are independent of variations of the line voltage except of course in so far as the voltage alters the characteristics of the load itself. In addition to the usual Maxwell formula, the effect of electrical control on the electrometer is considered and the advantage in such a case of the null methods proposed is emphasized. Illustrative tests together with the discussion at the conclusion of the paper bring out the accuracy of measurement attainable. [D. Owen, Phys. Soc. of London, *35*, p. 140; 1923.]

L. BEHR

SOME PROPERTIES OF ATOMS AND ELECTRONS AS MEASURED BY STUDENTS[1]

By Frederic Palmer, Jr.

In the following article it is not the author's purpose to present any new scientific material, but merely to call attention to the frequent failure of teachers of physics to make the subject inspiring to their students either through lack of appreciation of the possibilities contained in a given experiment, or through the belief that certain experimental work described in text-books is too elaborate or too difficult for students to attempt, and adapted only to skilled research workers equipped with all the facilities of a large research laboratory.

In general a student's interest in his experimental work depends largely upon the object of the experiment as stated in his laboratory manual. He cares little for experiments purporting to familiarize him with scientific instruments and their calibration; such as, "Vernier Caliper," "Potentiometer," "Calibration of a Set of Weights," "Calibration of an Ammeter." He cares little more for those designed to teach him important methods of measurement; such as, "Method of Mixtures," "Timing by the Method of Coincidences," "Double Weighing by the Method of Vibrations." He responds much more keenly when his object is the examination of some physical phenomenon which he has already studied from his text-book but now for the first time manipulates with his own hands in the laboratory; such as, "Surface Tension," "Electrolysis," "Polarization." Fundamentally the average student is not thrilled by learning how to use or to calibrate scientific instruments, how to employ scientific methods, or even how to examine scientific phenomena, any more than the carpenter is thrilled by learning how to use a hammer, how to sharpen a saw, or how to put shingles on a roof. The carpenter's main interest is in building houses. All

[1] Interest in research, whether in pure or applied science, and the large volume of scientific material offered for publication has crowded out of our scientific journals discussions of a pedagogical nature, particularly where collegiate teaching is concerned. This is unfortunate, even if one considers only the advancement of Science. For the caliber of the scientists of the next generation depends in large part on how effectively we teach the students of the present generation. And further, scientific discovery, just as any other product, is of no value unless it can be properly distributed. In publishing this article by Dean Palmer, we wish to take occasion to say that the pages of this Journal are open to the teachers of the universities and colleges of the country for presenting herein the results of their pedagogical researches in the teaching of science. Editors.

else is but a means to that creative end. Similarly the natural interest of the student is in *doing* something, in measuring something. If the quantitive measurement of some property involved in the experiment is stressed as its object, use of the proper instruments and methods of measurement fall into their proper place, and a maximum of interest is immediately obtained from the student. To this end some of the objects mentioned already as examples might be changed so as to read "Volume of a Regular Solid," "Electromotive Force of a Dry Cell," "Value of the Acceleration due to Gravity in this Latitude," "Amount of Pure Sugar Contained in a Sample of Unknown Concentration."

In accordance with the principle just stated the title, "The Number of Molecules in a Cubic Centimeter of a Gas and the Mass of an Atom," takes hold of the student's imagination and stimulates his interest in a manner which is impossible when the same experiment is entitled "Coulomb-meter" ' "Calibration of an Ammeter," "Electrochemical Equivalent of Copper," "Electrolysis." The minute the student realizes that he himself is about to count molecules and weigh atoms—feats of the masters of science that have left him still a bit incredulous—his eyes sparkle with enthusiasm. The simplicity of it all is a revelation. Obviously it would be a mistake to lead him to believe that he could perform these feats himself, unless it were possible, with ordinary care in the making of observations and in the manipulation of apparatus at his disposal, to obtain results correct within a reasonable degree of accuracy. The student's confidence in himself, in his instructor, and in the subject of Physics is greatly enhanced when he looks in the Physical Tables for the accepted values of the magnitudes he has measured and finds that in two hours time he has obtained results which are accurate to within two or three per cent.

I. The Number of Molecules in a Cubic Centimeter of a Gas and the Mass of An Atom

The experiment may be divided into two parts, the first requiring the use of a gas coulomb-meter (voltameter), the second that of a coppe coulomb-meter. These are of the usual type, the former graduated in cubic centimeters, with an outlet at the bottom; the latter with three detachable copper plates, deposition taking place upon the central plate. The solutions of sulphuric acid and of copper sulphate are made up with distilled water according to the usual specifications. The ammeter should have an accuracy of at least one per cent, and should be connected in series with a sliding rheostat. A standard barometer,

a 0-50°C thermometer graduated in fifths of a degree, a good chemical balance, and an ordinary watch complete the necessary equipment.

Part 1. The objects of this part of the experiment are to determine (1) the number of molecules in one cubic centimeter of hydrogen under standard conditions of pressure and temperature, and (2) the absolute mass in grams, of an atom of hydrogen.

From Faraday's Laws

$$M = kit \qquad (1)$$

where k is the electrochemical equivalent of the ion in question, that is the mass, in grams, liberated by one coulomb. For hydrogen ions $k = .000010$ grams per coulomb. Let n = number of hydrogen molecules per cubic centimeter under standard conditions; m = mass of a hydrogen atom; $2m$ = mass of a hydrogen molecule; V = volume of hydrogen liberated during the experiment corrected for temperature, pressure, and water vapor pressure. Then since the total mass of hydrogen liberated (M) during a known number of seconds (t) equals the total number of molecules times the mass of one,

$$M = nV \times (2m) \qquad (2)$$

The theory of electrolysis leads to the belief that the passage of the measured quantity of electricity (Q) through the electrolyte is brought about by the motion of positively charged hydrogen ions (H) to the cathode and that of negatively charged sulphions (SO_4) to the anode. At the cathode each hydrogen ion (positively charged atom) extracts one electron, and hydrogen molecules are liberated. At the anode an equal number of electrons is given up by the sulphions, and molecules of oxygen are liberated. The released electrons are driven around the circuit by the storage battery, forming an electron stream in the opposite direction to that in which it has been agreed that an electric current would flow. The total quantity of electricity passing through the electrolyte in t seconds is thus made up of the total number of electrons times the charge on each. Since each hydrogen atom-ion extracts one electron from the cathode, each hydrogen molecule liberated must have extracted two; and the number of these liberated molecules has already been shown to be nV.

$$\text{Therefore} \qquad Q = 2nV \cdot e \qquad (3)$$

where e = electric charge of an electron in electromagnetic units, and Q must be measured in the same units. From the experimental work of Millikan it is known that $e = 4.77 \times 10^{-10}$ electrostatic units (1.59×10^{-20} electromagnetic units). Furthermore 1 ampere = 0.1 e.m.u. The sub-

stitution of the measured values of Q, V, and e in (3) thus give n, the number of molecules of hydrogen in one cubic centimeter of that gas under standard conditions. Attention should also be drawn to the fact that this number is the same for any gas under the same conditions, and is known as Avogadro's number.

The mass (M) of liberated hydrogen is calculated from the observed values of i (amperes) and t (sec.) and the given value of k in (1). Substitution of M, n and V in (2) gives m, the mass of a hydrogen atom in grams.

If (3) is divided by (2), the result is

$$e/m = Q/M$$

and substitution of the observed values of Q (e.m.u.) and M give the ratio of the charge to the mass for the hydrogen ion in electrolysis, the largest value of e/m for any ion, and a value which will be referred to in discussing another experiment.

Part 2. The objects of the second part of the experiment are to determine (1) the electrochemical equivalent of copper, (2) the mass, in grams, of a copper atom, and (3) the atomic weight of copper. The gas coulomb-meter is replaced by the copper coulomb-meter, and the gain in weight of the central copper plate is carefully measured, to milligrams, on a chemical balance. Special care is needed in drying and handling the copper plate.

As before

$$M = kit \qquad (1)$$

but now the ion liberated is the copper ion instead of the hydrogen ion. Since M (grams), i (amperes), and t (secs.) have all been measured, k, the electrochemical equivalent of copper may be calculated at once.

Equation (2) becomes

$$M = m\ N \qquad (2)$$

where N is the total number of copper ions liberated in this particular experiment.

Equation (3) becomes

$$Q\ (\text{e.m.u.}) = 2\ e\ N \qquad (3)$$

since each copper ion of mass m carries a charge of $2e$, that is it has lost two electrons; for in copper sulphate copper is divalent. The value of N is obtained from (3), and substituted together with that of M in (2). The resulting value of m is the mass of the copper atom sought.

By definition the atomic weight of an element is the ratio of its mass to the mass of an atom of hydrogen. (Within the limits of accuracy of

an experiment of this kind the atomic weight of hydrogen may be taken as 1). Therefore dividing the mass of the copper atom by that of the hydrogen atom obtained above gives the atomic weight of copper.

That students taking a college course in General Physics are capable of carrying out this experiment as outlined and obtaining good results has been amply demonstrated by several years experience. Furthermore the enthusiasm with which they vote it to be one of the most fascinating pieces of work of the year is of a very different order of magnitude from that evinced toward the same phenomena when looked at from the point of view of the calibration of an ammeter!

The results given below were obtained by a student within the past month.

Part 1

Time = 13 min 0 sec
Current = 0.3 amp
Pressure = 75.19 cm
Temperature = 25.2°C
Volume of liberated gas (observed) = 31.88 cm^3
Volume of liberated hydrogen (corrected) = 28.07 cm^3
Mass of liberated hydrogen (calculated) = 2.34×10^{-3} g
Avogadro's number (n) = 2.62×10^{19}
Mass of hydrogen atom = 1.59×10^{-24} g

Part 2

Time = 20 min 0 sec
Mass of copper deposited = 0.389 g
Electrochemical equivalent of copper = 3.24×10^{-4} g per coulomb.
Mass of copper atom = 1.03×10^{-22} g
Atomic weight of copper (H = 1) = 64.79

Should the carrying out of such an experiment as this lead the student to inquire after further easily obtained first-hand information concerning atoms and molecules, in particular as to their magnitude, it might be advisable to place in his hands the simple apparatus needed for measuring the diameters of some complex molecules by Langmuir's method. This consists of a large photographic tray partly filled with water; a burette with a stop-cock which will release a known number of drops per cubic centimeter; a solution of stearic acid ($C_{17}H_{35}$ COOH) in benzene of known concentration; and some finely powdered talc contained in a handkerchief for a sifter.

When a drop of such a solution is placed upon a talc-covered water surface it immediately spreads out pushing the talc before it. Langmuir has shown that as the benzene evaporates at once, there is left a film of stearic acid only *one molecule thick*, outlined by the talc. The area of such a film, though somewhat irregular, may be quickly measured with sufficient accuracy by a meter-bar. From the density of stearic acid, its concentration in the solution, and the volume of a drop from the burette, the mass of stearic acid per drop of solution is readily calculated.

Let m = mass of stearic acid per drop
ρ = density of stearic acid
n = number of drops from burette in film
a = area of film
d = diameter of stearic acid molecule, or thickness of film

then $$nm = da\rho$$

or $$d = \frac{nm}{a\rho}$$

A student obtained the following results:—.032 g stearic acid was dissolved in 33.00 cm³ of benzene making a solution of concentration = .00097g/cm³. The burrette released 50 drops per cm.³

Therefore $\frac{.00097 \text{ g/cm}^3}{50 \text{ drops/cm}^3} = .00002$ g per drop.

$m = .00002$ g; $\rho = .84$ g per cm³

$n = 4$; $a = 600$ cm² ; $d = \frac{4 \times .00002 \text{ g}}{600 \text{ cm}^2 \times .84 \text{ g/cm}^3}$

Therefore $d = 1.6 \times 10^{-7}$ cm.

Thus has been obtained the diameter of a large molecule. The diameter of a hydrogen molecule has not been measured; but the complexity of the stearic acid molecule leads the student to infer that the former is much smaller, and when told that it is about one-tenth of the above value he readily grasps the comparative magnitude. Therefore 10^{-8} cm is endowed with a real meaning to him which it could not possibly possess if he had not had the experience of measuring the diameter of a molecule for himself.

II. The Ratio of the Charge of an Electron to its Mass

Thomson's method of measuring the value of e/m for cathode rays is familiar enough, but how many teachers of physics have actually measured the ratio for themselves? Or, still more, how many have

placed the apparatus in the hands of their students? As a whole we possess a large amount of inertia when it comes to devoting much time to any project which has *only* teaching value. It is the object of Part II to point out that the determination of the value of e/m for cathode rays may be accomplished in any moderately equipped laboratory, without an undue expenditure of time either by instructor or by students, and with results which satisfy by stimulating interest and inspiring confidence.

Thomson's method of measurement requires the simultaneous deflection of the cathode beam by an electrostatic and by a magnetic field. The quantitative measurement of the strength of each of these fields to the necessary degree of accuracy is a difficult matter. Therefore, after some experience in the employment of this procedure it was abandoned in favor of the method of Kaufmann. His method possesses two advantages; first, the magnetic field is produced in such a way that its value may be calculated instead of being measured. Second, the electric field is dispensed with, and in its place is substituted the value of the potential drop between the anode and the cathode in the tube; Kaufmann's assumption being that at the low gas pressure existing in the tube, most of the electrons of mass m and charge e will fall through the whole potential V applied between the anode and the cathode without colliding with gas molecules, thereby acquiring the maximum kinetic energy, and the maximum velocity v. Under these circumstances,

$$V e = \tfrac{1}{2} m v^2. \tag{1}$$

The other condition is expressed in the usual way, that the centripetal force of the magnetic field of strength H (in gauss) acting upon the charge e moving with the velocity v is just balanced by the centrifugal force of the mass m moving with velocity v in the resulting circular path of radius r. Then

$$Hev = \frac{mv^2}{r} \tag{2}$$

Eliminating v between these two equations gives

$$\frac{e}{m} = \frac{2V}{H^2 r^2} \tag{3}$$

Also dividing (1) by (2) gives

$$v = \frac{2V}{Hr} \tag{4}$$

In carrying out this experiment it is necessary to use two pieces of apparatus of a rather special nature. The first is a storage battery capable of giving 1000 to 1500 volts. The second is a modified Braun or Thomson tube containing as a cathode a platinum strip with a spot of lime in the centre which may be heated by a current of 5 to 8 amp, and as an anode a metallic diaphragm very nearly filling the entire cross-section of the tube, but pierced through the centre with a small hole. At the end opposite to the cathode there is fixed the usual fluorescent screen with millimeter divisions marked upon the back. When the tube is in operation with +1000 volts or more applied to the anode a thin blueish thread of cathode rays traverses the length of the tube making a small bright spot on the screen, the displacement of which by a magnetic field is readily measured. The storage battery, mentioned above, may be readily constructed out of lead strips and test-tubes mounted fifty to the rack with the proper double-throw switches on the front to connect in parallel for charging and in series for discharging. Such a battery may be built very compactly, and is found exceedingly useful for many laboratory purposes where a fairly high potential and low current strength are demanded.

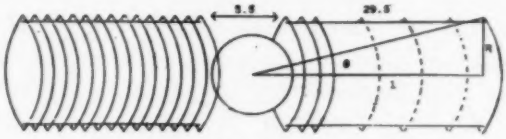

FIG. 1. *Solenoids and cathode ray tube.*

It is convenient to produce the magnetic field by means of a couple of solenoids wound in a single layer of no. 16 insulated wire upon cardboard tubes six inches in diameter and a foot long. The solenoids are placed one on either side of the screen end of the cathode ray tube, as in Fig. 1, so that, the current through them will generate a magnetic field that deflects the cathode beam up or down. The strength of the field within each solenoid (assuming the field to be practically uniform from axis to circumference) is readily calculated from the usual expression

$$H_S = 4\pi nI \cos\theta \qquad (5)$$

where n = no. of turns per cm of length, I = current in e.m.u., and θ is the angle subtended at the cathode beam by the radius of the solenoid (see Fig. 1). On account of the insertion of the tube between the two solenoids a certain amount of leakage of magnetic lines of force will take

place so that the magnetic field at the cathode beam (H_B) is less than H_S calculated above. H_B may be found from the following procedure. The solenoids are placed as close to the tube as possible and the current through them adjusted to give the maximum observable deflection of the cathode spot. With the current maintained constant, the solenoids are moved off parallel to their common axis a few centimeters at a time, and the resulting deflections of the spot are observed. Upon plotting spot deflections against distance between solenoids a practically straight line relationship is found. The point at which this line extended cuts the axis of zero distance gives the value of the spot deflection which would have been produced by the calculated field H_S.

In Fig. 2 is represented the circular path AB of the cathode beam through the magnetic field. The spot deflection is d, and the distance

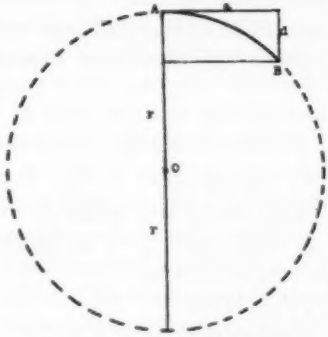

FIG. 2. *Path of cathode beam.*

from the point where the beam enters the field to the screen is a. More uncertainty attaches to the measurement of a than to any other of the observed quantities due to the uncertainty as to the exact boundary of the magnetic field. The most satisfactory method tried thus far is to look along the axis of the solenoids noting the point at which the cathode beam begins to bend as the solenoid current is thrown off and on. This point can then be located within about one millimeter. It is readily seen that the radius of curvature of the circle is

$$r = \frac{a^2+d^2}{2d}. \tag{6}$$

Since the value of e/m is independent of H and r, it is evident from equation (3) that the product $H\,r$ is constant; therefore

$$H_S r_S = H_B r_B, \tag{7}$$

where the subscripts have the same significance as before.
Substituting (6) and (7) gives

$$\frac{H_B}{H_S}=\frac{d_B}{d_S}\left(\frac{a^2+d^2_S}{a^2+d^2_B}\right), \tag{8}$$

where H_B is the strength of the field sought, H_S is the strength of the field calculated, d_B is the spot deflection observed, d_S is the spot deflection extrapolated.

The value of H_B as obtained thus is then substituted in (3) together with the value of r_B obtained from the observed spot deflection d_B. The only remaining quantity V may be measured on an electrostatic voltmeter of range 0 to 1500 volts.[2] Both e/m and v may therefore be calculated. Variation of V from 1000 to 1500 volts leads to differing values of v but constant values of e/m.

The following observations and calculations were carried out by a small number of advanced undergraduates with the assistance of the instructor:

$$l=29.5 \text{ cm}+\frac{5.5}{2} \text{ cm}=32.25 \text{ cm}$$

$$R=8.6 \text{ cm}, \qquad \cos\theta=.967$$

$$H_S=4\pi\times5.2\times.093\times.967=5.88 \text{ gauss}$$

$$a=11.4 \text{ cm}; \quad d_B=2.8 \text{ cm}; \quad d_S=3.48 \text{ cm (from graph)}$$

$$H_B=4.878 \text{ gauss}; \quad r_B=24.59 \text{ cm}$$

$$H_B r_B=120.0; \quad H^2_B r^2_B=14400$$

$$V=1260 \text{ volts}=1260\times10^8 \text{ e.m.u.}$$

$$e/m=\frac{2\times1260\times10^8}{14400}=1.75\times10^7 \text{ e.m.u.}$$

$$v=\frac{2\times1260\times10^8}{120}=2.10\times10^9 \text{ cm/sec.}$$

V (volts)	$v\left(\frac{\text{cm}}{\text{sec}}\right)$	e/m (e.m.u.)
1260	2.10×10^9	1.75×10^7
1140	1.95×10^9	1.75×10^7
1020	1.85×10^9	1.78×10^7
	mean	1.76×10^7

A comparison of this value of e/m may then be made with that of the hydrogen ion in electrolysis (see Part I) which shows that on the assumption that both kinds of particles carry the same charge the mass

[2] Note. Made by the Central Scientific Co.

of the cathode ray particle, or electron, must be more than eighteen hundred times less than that of the hydrogen atom.

III. THE ELECTRONIC CHARGE e

When we read Millikan's description of his ingenious oil-drop experiment, by means of which an accurate determination of the electronic charge e was first made possible, the arrangement of apparatus appears complicated and difficult to handle with its pressure gauges, constant temperature bath, and 5000 volt battery. We are likely to put it down as one of those elaborate pieces of work requiring the genius of a Millikan to carry through with success. That all the refinements employed are necessary for the exact evaluation of the constant e is plain enough. But without these elaborate refinements, using merely what appear to be the essentials of the apparatus, which are easy to construct and not difficult to manipulate, I have found that results within two or three per cent of Millikan's value may be obtained by advanced undergraduates, working in pairs, without any preliminary training in the technique of this particular apparatus. To watch the star-like drops rain across the field of view is fascinating in itself; but when one drop has been singled out and kept moving up and down for several trips until it finally captures an ion and suddenly changes its velocity under the electric field, the student experiences a thrill not surpassed in laboratory experience. The excitement of the chase is contagious.

The apparatus consists essentially of two parallel brass plates (P P, Fig. 3) 15 cm in diameter, with plane faces held 8 mm apart by ebonite rings nn surrounding three ebonite screws no one of which is in line with W_1W_2. The plates are cast with three vanes on the unused side to prevent them from warping. Through the centre of the upper plate is a hole .5 mm or less in diameter through which the oil-drops fall from the dome D, into which they have been sprayed from an atomizer through the opening C. The dome rests upon a wooden ring RR surrounding the plates and containing three windows, W_1, W_2, W_3 (W_3 is not shown in the figure). Light from a small right-angle arc lamp is passed through a lens, reflected from a plane mirror into W_1 focussing on the drops, and out again through W_2. A low power microscope with micrometer eye-piece is used for observation of the drops through W_3 at an angle of 15° to the line W_1W_2. One plate is connected to ground, while the other is connected through a rocking switch to one terminal of the 1500-volt storage battery previously described (Section 2), or to ground.

When "vacuum oil" is sprayed into the dome the heaviest drops fall first through the hole passing rapidly across the field of view. With an electric field of only 1500 volts per centimeter it is impossible to catch and hold such large drops; but very soon smaller ones begin to meander along, and it is a matter of only a few moments, rocking the switch back and forth, to pick out a drop of convenient size to fall say 3 mm in six or seven seconds under gravity, and of convenient charge to rise the same distance in about the same time under the electric field. The

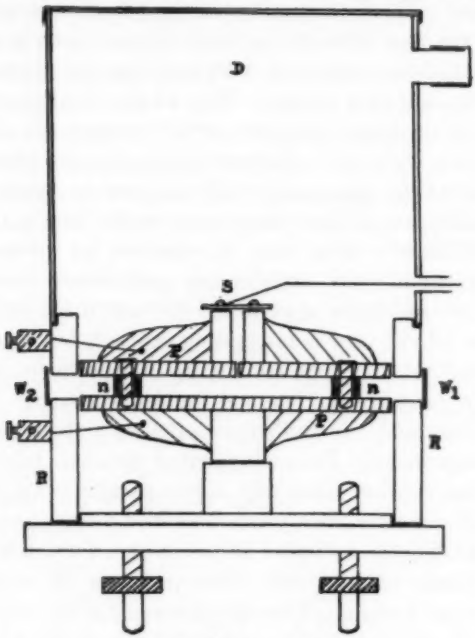

FIG. 3. *Oil-drop apparatus.*

ebonite shutter S is then moved so as to close the drop hole, and after a few switch reversals the chosen drop alone usually remains in the field of view.

The time of passage of the drop over a known distance between microscope cross-hairs may be taken by means of a stop-watch. One observer pays strict attention to the drop, while the other reads and sets the stop-watch after each observation, replacing it ready to snap in the hand of the drop observer. When the drop gets a little out of focus, due to wandering with the air convection currents, the microscope

may be moved slightly so as to produce a sharp focus once more. Either very weak X-rays or some radio-active material brought near the apparatus may be employed to force the drop to pick up an ion with resulting change in velocity under the electric field. The ion picked up is more frequently of opposite sign to that of the oil-drop than otherwise, so that the velocity under electric field becomes less and less until the available field is no longer able to reverse the direction of the drop and it slowly falls to the lower plate, thus ending the series of observations on that particular drop.

The students work up such a series of readings into a table similar to those given by Millikan, calculating the whole number of electronic charges captured with each ion, and the total number contained on the oil-drop. Substitution in the usual equation gives a value for e_1, which is then corrected for the failure of Stokes' Law giving the electronic charge e which is sought.

Below is a table made from a series of recent observations with the apparatus as described. The values of the time of fall of the drop under gravity t_g, and of the time of rise under the electric field t_f, are not single observations, but the means of several readings each. The actual change in velocity of the drop brought about by the capture of an ion is $v'_F - v_F$, and n' is the number of electronic charges thereby added to or subtracted from the total drop charge. The change in

Determination of Smallest Possible Velocity of Oil-Drop.

t_g	t_F	v_F	$v'_F - v_F$	n'	$\frac{v'_F - v_F}{n'}$	$v_g + v_F$	n	$\frac{v_g + v_F}{n}$
7.4	5.2	.05766				.09826	25	.00393
	6.7	.04485	.01281	3	.00427	.08545	22	.00387
	11.4	.02631	.01854	5	.00371	.06691	17	.00394
	27.8	.01080	.01551	4	.00388	.05140	13	.00395
	44.4	.00677	.00403	1	.00403	.04737	12	.00395
	27.8	.01080	.00403	1	.00403	.05140	13	.00395
	20.7	.01449	.00369	1	.00369	.05509	14	.00394
	16.5	.01818	.00369	1	.00369	.05878	15	.00392
	20.7	.01449	.00369	1	.00369	.05509	14	.00394
	13.2	.02272	.00823	2	.00412	.06332	16	.00395
	20.7	.01449	.00823	2	.00412	.05509	14	.00394
$V_g = .0406$	27.8	.01080	.00369	1	.00369	.05140	13	.00395
	121.4	.00246	.00834	2	.00417	.04306	11	.00391
	Means				.003924			.003934
	Mean of both					.003929 = v_0		

velocity of this particular drop produced by a change in charge of *one* electron is therefore $\frac{v'_F - v_F}{n'}$. Since the electric field must be able to give the drop a velocity v_g upwards in order to just prevent it from falling, the total equivalent velocity of the drop in the field (i.e. the velocity which it would have were gravity eliminated) must be $v_g + v_F$, and the total charge on the drop (n electrons) must be proportional to this. The smallest possible velocity this particular drop could experience in this particular electric field is therefore $\frac{v_g + v_F}{n}$, which should give the same value as that obtained above. The mean of these two is taken as the best determination of this velocity and is called v_0.

Drop fall distance = 0.3 cm; oil density = 0.90 gr/cm^3 = ρ
Plate potential = 1250 volts; plate distance = 0.8 cm
Coef. of viscosity of air = $1.824 \times 10^{-4} = \mu$
Temperature = 23°C; barometric pressure = 74.20 cm of Hg
Millikan's equation is

$$e_1 = \frac{4\pi}{3}\left(\frac{9\mu}{2}\right)^{\frac{3}{2}}\left(\frac{1}{g\rho}\right)^{\frac{1}{2}}\frac{v_0\, v_g^{\frac{1}{2}}}{F}$$

Putting all but the last term equal to a constant K, $e_1 = K\frac{v_0\, v_g^{\frac{1}{2}}}{F}$

$K = 3.32 \times 10^{-6}$; $v_g^{\frac{1}{2}} = .202$; $v_0 = .00393$ cm/sec

$$F = \frac{1250}{.8 \times 300} = 5.21 \text{ e.s.u.}$$

$$e_1 = \frac{3.32 \times 10^{-6} \times .00393 \times .202}{5.21} = 5.04 \times 10^{-10} \text{ e.s.u.}$$

From Stokes' Law

$$v_g = \frac{2gr^2\rho}{9\mu}, \qquad \therefore\ r^2 = \frac{9\mu\ v_g}{2\ g\rho}$$

$$\therefore\ r = 1.93 \times 10^{-4} \text{ cm}$$

which is the radius of the observed drop. There is a correction to be applied on account of the small dimensions of the drop, resulting in a greater velocity than that calculated on the assumption that the drop is continuously in contact with air molecules. Millikan shows that the correct value of the electronic charge e may be obtained from e_1 by the equation

$$e = \left(\frac{1}{1 + b/pr}\right)^{\frac{3}{2}} \times e_1$$

where r = radius of drop, p = pressure in centimeters of mercury, and $b = .000625$. Substituting the above values, we have

$$e = .935\, e_1 = .935 \times 5.04 \times 10^{-10}$$

$$\therefore\ e = 4.71 \times 10^{-10} \text{ e.s.u.}$$

HAVERFORD COLLEGE,
HAVERFORD, PA.

Measurement of Projectile Velocities by Means of the Johnsen-Rahbek Effect.—Johnsen and Rahbek found that very considerable electrostatic forces could be obtained by applying a comparatively small voltage to a metal plate and a leaky insulator which are in good contact. The present paper describes a recorder built on this principle which, although designed primarily for high speed telegraphy, is here used to measure the velocity of projectiles.

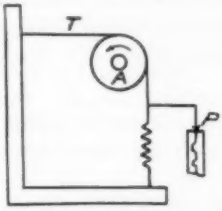

In the figure, which diagrammatically illustrates the recorder proper, the agate cylinder A is driven in the direction of the arrow by means of a motor. In frictional contact with the cylinder is the steel tape T, which is stretched taut by a spring fastened to the base. Any motion of the tape is transmitted through a pivoted link to the recording pen P. The application of a suitable potential difference between the steel shaft on which the agate cylinder is mounted and the tape, increases the frictional force sufficiently to cause an upward displacement of the tape and a corresponding movement of the pen. Ample motion is apparently secured with 100 volts and a current of from one to ten microamperes.

In measuring the velocity of a projectile it is shot through two or more coils of wire, each of which is connected in series with a battery and the primary of a transformer. The voltage induced by the passage of the bullet is stepped up by the transformer and still further increased with the aid of a three electrode vacuum tube. The output side of the vacuum tube is connected directly to the recorder.

No details as to speed of rotation, magnitude of the electrostatic forces or the like are presented which might give some notion of the speed of operation attainable. In the one record of performance which is mentioned, the velocity of the bullet was measured for a time interval of approximately .03 second. [By ZS.f. Phys. *4*, p. 63; 1924.]

LEO BEHR

Synopsis of Applicable Mathematics. L. Silberstein, G. Bell and Sons, 1923, pp. xi+250.

The author of this synopsis has succeeded admirably in bringing within the compass of a single volume practically all tables and formulae having a reasonably wide range of utility among physicists and practical mathematicians, and withal he has managed to weave his facts on each subject into a terse but interesting discourse.

The first 68 pages are given over to 4- and 5-place logarithmic, trigonometric and reciprocal tables, very well arranged. The body of the book begins with all the topics usually treated in higher algebra and theory of equations. There are sections on matrices, interpolation, and finite differences. Formulae involving central differences might well be given here.

Then come complex numbers and infinite series and products, after which the most important transcendental equations are tabulated. (Lagrange's expansion is not given, but Dr. Silberstein recognizes that *intelligent* trial and error is the practical way for getting the roots of these equations.) Next, the elementary functions are discussed for both real and complex values of the argument, the hyperbolic functions are tabulated, and calculus is put into 7 pages, with tables of definite and indefinite integrals.

The study of special functions which ensues shows excellent choice of subject matter. It includes the sine, cosine, and exponential integrals, the Γ-function, Fresnel's integrals, the error function, spherical harmonics, Bessel functions, elliptic functions and integrals in both Jacobian and Weierstrassian form, and θ-functions. There are tables galore, including even the complete elliptic integrals, [Legendre's $F(\phi, k)$ and $E(\phi, k)$]. Fourier series and integrals are not forgotten, nor are rules for approximate quadrature and for transformation of multiple integrals, while space is found for explanation of the nature of a function of $x+iy$, residues, and complex integration.

Trigonometry, plane and spherical, is followed by analytics, plane and solid, and then we are surprised with easily readable sections on differential, projective and non-Euclidean geometry. Reciprocal polars are spoken of, but space does not allow a discussion of inversive geometry. Finally, we encounter the notation and formulae of vector analysis, given in considerable detail, a much too condensed section on quaternions, and an explanation of the more important processes of tensor algebra.

The author states in the preface that a future edition will contain sections on differential and integral equations, and perhaps collections of physical formulae. A treatment of calculus of variations, difference equations and functional equations would prove very acceptable also. Suffice to say, this work will fill a great need for the practical physicist, and is wonderfully well adapted to give graduate students a comprehensive view of useful mathematics.

ARTHUR E. RUARK

A NEW OCULAR MICROMETER

By Hermann Kellner

In the usual type of reading microscope or telescope an image of the scale which is to be read is formed by means of an optical system. The intervals of this scale image are then subdivided either by a line or wire which can be moved over the scale image by a micrometer screw, or by means of a transparent scale which is superimposed on the scale image and may be ruled, etched or photographed upon glass.

The glass scale superimposed upon the image of the main scale has the advantage of mechanical simplicity and gives a complete reading at once for one position of the eye. It has the disadvantage that the lines of the two superimposed scales are crowded over each other and generally not easy to read.

The screw micrometer is easy to read but has to be made with great precision and is, therefore, expensive. It is slower to use and requires two positions of the eye, one for looking through the ocular for setting the movable wire in coincidence with the next fixed one, the other one over the drum for making the reading. Here frequently a magnifier has to be employed.

The micrometer herewith presented seems to be free from these objections and possesses the advantages of both the other types. In place of a micrometer screw a sliding measuring wedge is employed. We see in Fig. 1 the image of a vertical scale whose graduation is to be subdivided. A fixed wedge is attached to the ocular box and carries on a strip of glass the index line. Along the fixed wedge slides a movable wedge which by gentle pressure is always kept in contact with a fixed wedge. The movable wedge carries a glass plate on which is etched a double line running parallel to the lines of the main scale. It is obvious that this double line moves up and down over the image of the main scale when the movable slide is pushed along the fixed wedge, and can, therefore, be used for setting upon the image of the lines of the main scale. The glass plate which carries the double line is also provided with a scale allowing the position of the movable wedge to be read by the index which is fastened to the fixed wedge. The length of this scale is such that a shift of the movable wedge amounting to the length of this scale corresponds to a movement of the double line over one interval of the image of the main scale.

Fig. 1 pictures the field as it would appear in the ocular with the double line between 7 and 8 of the main scale and the ocular scale at zero. Fig. 2 shows the movable slide pushed to the left, till line 7 is

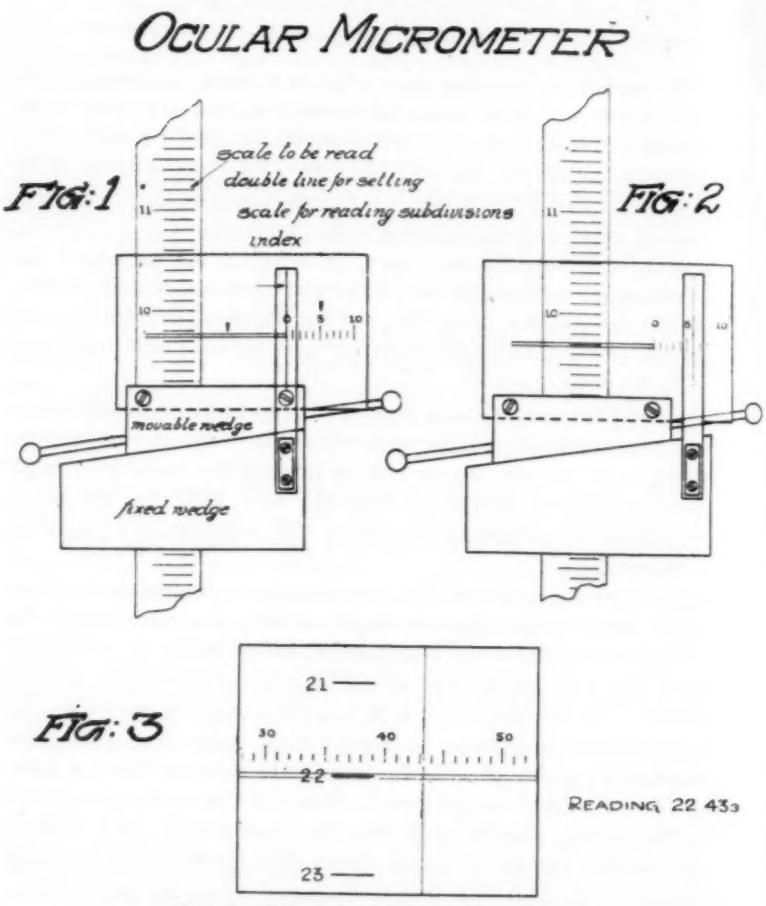

FIGS. 1 and 2. *Schematic views of the micrometer.*
FIG. 3. *Micrometer as it appears in the field of the eyepiece.*

between the double lines of the movable wedge. The index line is now at 6 on the ocular scale indicating a reading of 7.6.

It is a matter of course that the image of the main scale, the ocular scale, and the index line must all lie in the same plane, a condition which

can be easily fulfilled with sufficient approximation. Figs. 1 and 2 are of course only schematic. Fig. 3 represents the field of one of our shop instruments as it actually appears. Each interval of the main scale is here subdivided into 100 parts. Fig. 4 shows a depth gauge reading to

FIG. 4. *Depth gauge equipped with the new micrometer eyepiece.*

0.01 mm which is equipped with this micrometer. A number of such gauges have been used with good success in our plant.

SCIENTIFIC BUREAU,
BAUSCH & LOMB OPTICAL COMPANY,
ROCHESTER, N. Y.
MAY, 1923.

The Quantum Theory of Radioactive Disintegration.—Gamma-ray spectra are easily explainable on the assumption that the nucleus can exist in several stationary states; Rosseland has conjectured that electrons in heavy atoms may approach so close to the nucleus as to cause large disturbances by mechanical resonance. (Nature *3*, p. 357;

1923.) The present paper explains α- and β-ray emission by analogy with a new type of quantum transition in atoms robbed of an X-ray electron; a loose-bound electron may fall into the vacant X-ray level without emission of radiation, while another loose-bound electron is ejected from the atom. β-ray groups with energies K—L, K—M, etc., are explained by Ellis as due to absorption of K-radiation by looser-bound electrons, but may also be explained as above. If swift *nuclear* β-rays are to be explained by Ellis' idea, γ-rays of wave length 10^{-11} cm must exist to produce them; if such γ-rays do exist, there is no evidence that they ever get out of the nucleus.

Rosseland's explanation seems to require that α- and β-particles could have only a discrete set of velocities, in contradiction to experiment. But the correspondence principle shows that these particles must give rise to a continuous γ-ray spectrum as they move away from the nucleus; their motion is aperiodic, and can be resolved into harmonic components only if we assume a continuous distribution of frequencies (Fourier integral). The γ-spectrum is produced at the expense of the energy of the α- or β- particle, so continuous velocity distribution of the particles is attained. α-particles must move away from the nucleus almost in a straight line, starting with small velocities; i.e., electrostatic repulsion accounts for almost all their energy; but β-rays can move on spirals with infinitely many turns. Classical dynamics is used to get estimates of the radiation from α- and β-rays moving away in straight lines. Such α-rays lose less than 1% of their energy, but electrons lose energy equivalent to that of a low-velocity β-ray ($v/c=0.47$). These ideas are being applied by Kramers to continuous X-ray spectra. [S. Rosseland, ZS. f. Phys. *14*, p. 173; 1923.]

ARTHUR E. RUARK

Vector Calculus. By Professor James Byrnie Shaw, Professor of Mathematics at the University of Illinois. Published by the D. Van Nostrand Company, 8 Warren St., New York. 5+314 pages. $3.50 net.

This volume, which embodies "the lectures given on the subject to graduate students over a period of four repetitions," forms a welcome addition to the existing textbooks on vector analysis. The author has followed Joly and Tait in his preference for quaternions the use of which he believes to be the simplest of the different vector methods. The great diversity of notations at present in use by various writers is displayed in comparative form and is very useful for cross reference.

After discussing scalar and vector field, addition and multiplication of vectors and quaternions, differential and integral vector calculus is treated. This is followed by chapters on linear vector function, elasticity, and hydrodynamics. Very extensive applications are given to problems in physics and mathematics. All terms used are carefully defined and all physical ideas are clearly interpreted.

H. PORITSKY

A PHOTOMETRIC SECTORED DISK, VARIABLE AND ELECTRICALLY READABLE WHILE IN ROTATION

By Enoch Karrer

Considerable interest is attached to the photometric sectored disk both from the standpoint of theory and of practice. In this paper my interest lies in the latter, in that the present object is to describe such a disk that is variable and readable while in operation.

Pfund[1] has recently described a variable sectored disk, whose relative opening may be read stroboscopically, that surpasses all the earlier designs. There are several stroboscopic methods that may be used. In addition to those of Pfund and of Lummer[2] I may point out several others in a future paper, in which certain other forms and new uses of the sectored disk may also be described.

The new features in the disk which I am now describing are essentially two. Firstly, the manner of reading the relative opening electrically by means of an ordinary milliammeter at any distance, has never been employed in this connection; secondly, the manner of adjusting the displaceable disk is different from others.

Referring immediately to Fig. 1, one disk 1, is mounted directly and immoveably upon the shaft 7, by means of the cap 3. The second disk 2, is mounted upon the sleeve 4, which for a portion of its length bears snugly on the shaft 7. The manner of mounting the disk 2, upon the sleeve 4, is by means of a hub consisting of a portion of brass 5 and a portion of hard rubber 6, which composite construction merely allows for certain matters connected with the electrical reading device to be described later. The sleeve 4, has a shank which receives the rotar of the ball bearing 8. The rotor of the second ball bearing 9 is similarly attached to the shaft directly. The sleeve 4 holding the second disk 2, has four spiral grooves cut through and along it, while for an equal distance the shaft 7, has also four longitudinal grooves 10. Hardened steel pins 11, screwed securely into a brass collar 12, pass tightly through the spiral grooves of the sleeve 4, and into the straight grooves 10, in the shaft 7. It is obvious now that when the pins 11, move to and fro the shaft and sleeve undergo an angular displacement, and so too, the disks attached to the sleeve and shaft respectively glide over each

[1] Pfund, A precision Rotating Sector. Aperture Variable and Measurable While in Motion. Jour. Fr. Inst. *193*, p. 641; 1922.

[2] Brodhun, ZS. f. Instrk. *24*, p. 313; 1904; or Liebenthal's Praktische Photometrie.

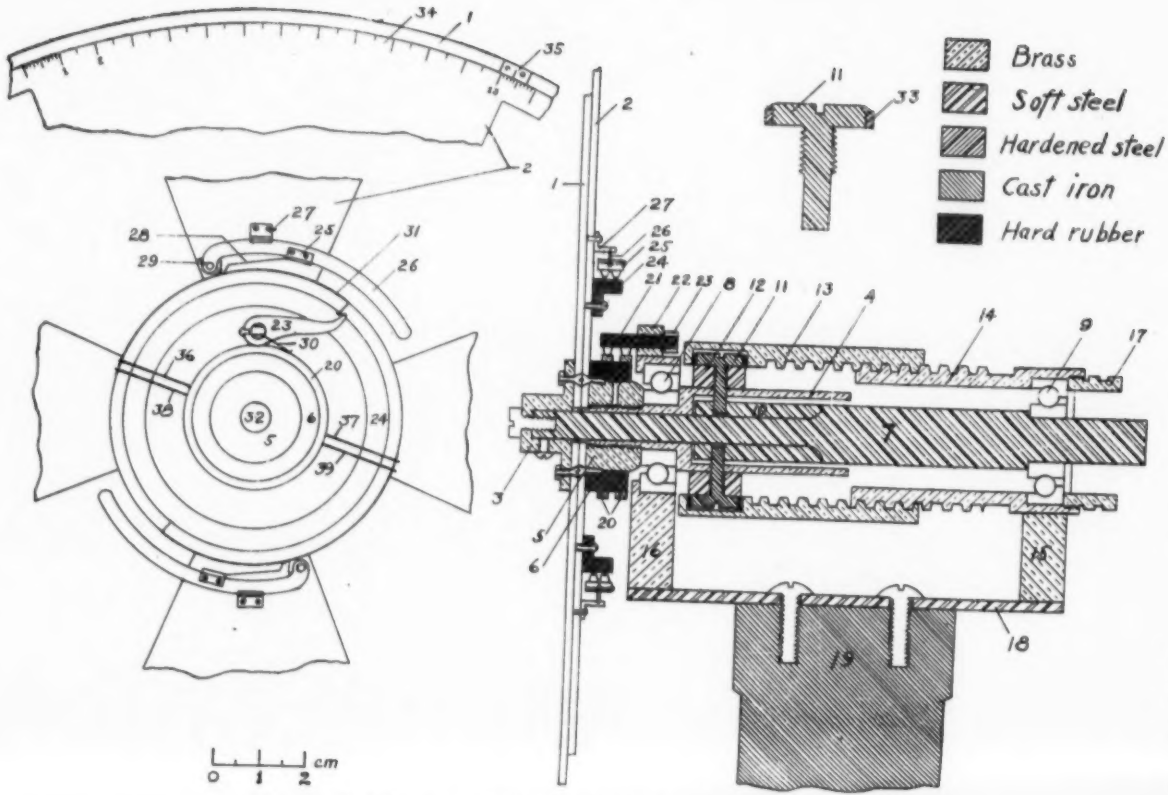

FIG. 1. *Variable sectored disk detailed drawing to show mechanical parts.*

other. To move the pins back and forth one turns the nut 13, through the threads of a hollow stock 14 attaced to and a part of the bearing mount. The steel pins which are moved along the grooves in the shaft and along the spiral grooves in the sleeve whenever the opening of the double disk is adjusted, are equipped with a soft steel roller bearing 33, see (insert); and may to advantage be slightly offset in the carrying collar 12, so that two of the pin rollers bear effectively against the adjusting nut 13, when the latter is turned in one direction and two bear thus when the nut is turned in the reverse direction.

It remains now to describe the device which enables one to read the relative opening electrically. The electrical circuit is shown schematically in Fig. 2. The branched circuit due to Wheatstone is employed. One branch of the circuit consists of a fine nichrome wire (B.S. No. 28) mounted upon a hard rubber flange 24 secured to one of the disks 2. The ends 36, 37, of this wire are attached to two insulated rings 20, Fig. 1, 2, encircling the hard rubber rim of the composite hub already referred to, whence they are extended by means of spring silver brushes 30, to the rest of the Wheatstone circuit consisting of three resistances[3] 40, 41, 42, one at least of which is adjustable; a storage battery 43, and a milliammeter (0-10 ma) 44. As one disk glides over the other the effective length of the wire resistor is changed. The accompanying change of resistance may be determined in one of the usual methods with the Wheatstone circuit, and by calibration related to the relative sectored disk opening.

The electrical and mechanical details involved in this scheme of reading may be briefly traced through. The disk wire 31, which is the variable branch of the Wheatstone bridge, is double and is extended on opposite radii in order to preserve symmetry and to increase the range of the deflections of the milliammeter for a given current in the bridge. The extension across the center of the disk is made by a copper ring concealed behind the flange 24. To this ring the two ends 38, 39, of the fine wire are attached. The effective length of the nichrome wire that for any opening of the disk is in the circuit, is determined by the position of a short circuiting contact 28 carried by the other disk. These contacts are mounted upon a stiff strip of phosphor bronze 26, whose bearing 29, is secured to one of the disks and whose restraining guide is on

[3] E. Karrer and A. Porritsky, An Improved Slide Wire Resistance, J. O. S. A. & R. S. I. 7, p. 277, 1923. (We have recently provided this resistance with a rack and pinion for better regulation. Such improvement may also to good advantage be made in the ordinary slide wire rheostats.)

FIG. 1. *Variable sectored disk detailed drawing to show mechanical parts.*

the other disk. This construction allows easy access to the brush 28 carried on a hard rubber block 25, by the phosphor bronze strip. The brushes 30, which connect the terminal rings 20, to the Wheatstone bridge are mounted upon a block of fibre 21, with a bearing at 22, and a lever 23, which allows the brushes to lie in or out of contact as de-

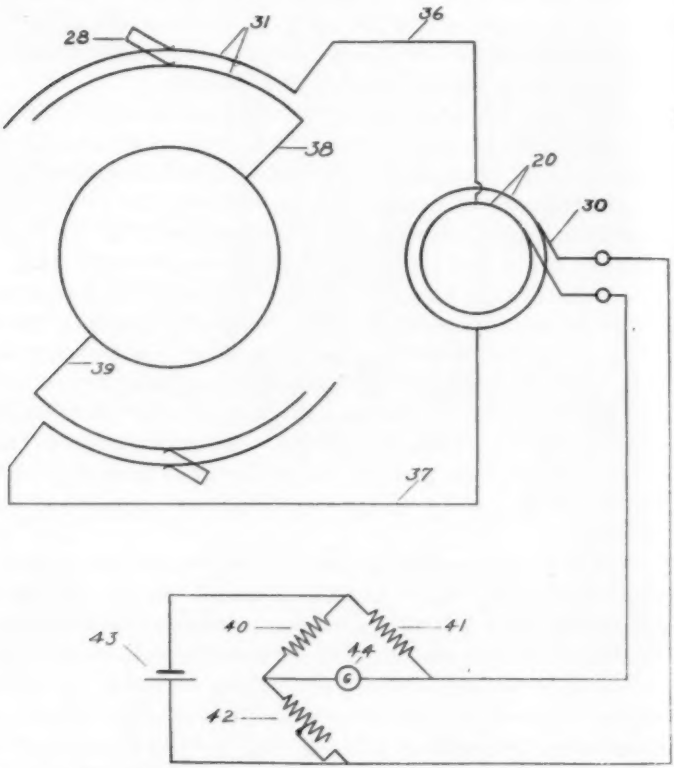

FIG. 2. *Schematic drawing to show the electrical circuits required to make the variable disk readable electrically while in motion.*

sired. To facilitate this a piano wire stud in the lever rubs against a tall notched screw head.

The disk which is mounted upon the spirally slotted sleve is graduated over one eighth of its circumference into thousandths of the whole circle. Upon the other disk is mounted the fiducial line. This is suggestively indicated in 34, 35, Fig. 2. This scale may be read stroboscopi-

cally also by one of several means. For this the screw 17, binding the bearing 9, is extended so that parts of any stroboscopic device may be mounted upon it.

The disk may be rotated as shown in the photograph of Fig. 3 by a 1/100 H.P. motor. For larger disks a larger motor will be necessary. For compactness the disk may in the latter case be mounted above and upon the motor. The disks in the present case are 27.9 and 29.2 cm in

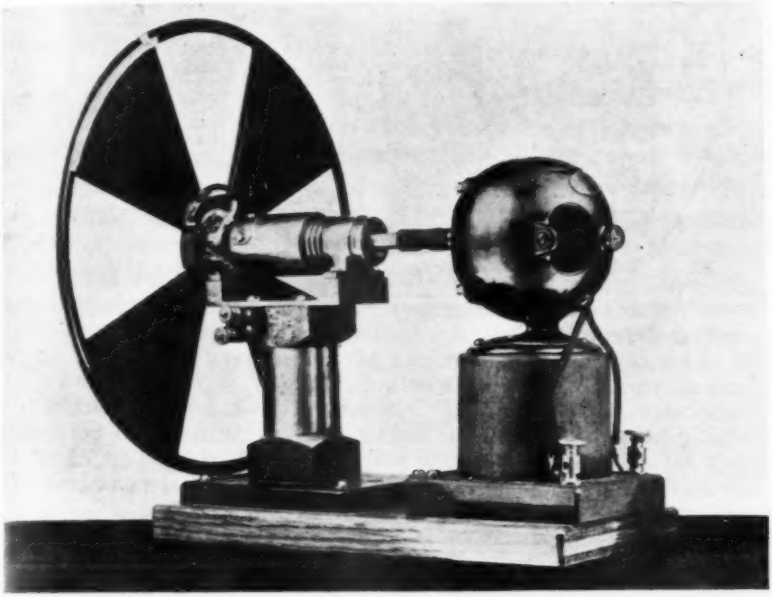

FIG. 3. *Photograph showing the variable disk assembled. Auxiliary resistances and milliammeter are not shown.*

diameter. The motor is attached to the disk shaft by a short rubber tube. The supports (brass blocks 15, 16, steel plate 18, and standard 19) for the two bearings 8, 9, need no mention.

An idea of what may be expected in the way of the size of the scale and the sensitivity of the electrical method of reading the relative opening of the disk may be obtained from the following practical case, where numerical values are only approximate. Single wire resistances and a common milliammeter for purposes of wireless telephony were used. About one volt across the bridge giving about 0.4 amp. in the circuit,

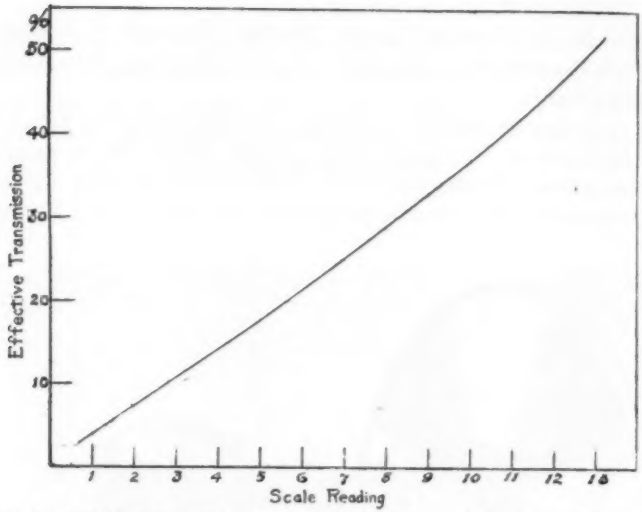

FIG. 4. *Relation between the scale reading and the transmission factor of the disk.*

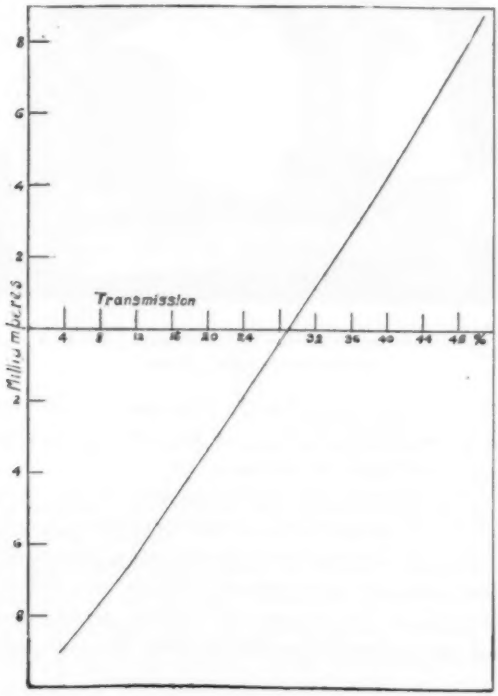

FIG. 5. *Relation between the transmission factor and the deflection of the milliammeter*

will allow the milliammeter to deflect twice the full scale (i.e. once for the negative and once for the positive direction) when adjustment is made from zero to full opening of the disk. The milliammeter has 100 scale divisions. The actual deflection obtained in a Wheatstone circuit set up are determined by several factors and it is perhaps safe to say that any accuracy desired for purposes as this is attainable.

The curves of Fig. 4 and Fig. 5 show the performance of the disk. The first gives the relation between the scale reading of the disk and the effective transmission determined photometrically; the second that between the transmission and the milliammeter reading. Of course the zero method may also be employed and will always afford a check of the milliammeter scale under any given conditions.

NELA RESEARCH LABORATORIES,
LABORATORY OF APPLIED SCIENCE,
NELA PARK, CLEVELAND,
JUNE 8, 1923.

Optical Properties of Long X-Rays.—Holweck performed the classical diffraction and reflection experiments with the X-rays excited from tungsten by 265 volt and by 1620 volt electrons; these X-rays are believed to be heterogeneous, the minimum wave lengths being 47 and 7.6A respectively, and the "effective wave lengths" being estimated by Holweck as respectively 60 and 10A. In the diffraction experiments the bombarded tungsten wire, .012 mm in diameter, is placed parallel to and 7 cm away from the diffracting slit, .0066 mm in diameter, 7 cm beyond which is placed the (Schumann) photographic plate. With the 1620 volt electrons, the image on the plate is merely the geometrical image of the source, but with the 265 volt electrons it is a band about four times as wide as the geometrical image, with a broad penumbra on either side. These magnitudes agree with the breadths of the theoretical diffraction patterns calculated in the classical way, using the wave lengths aforesaid; but the details of the theoretical pattern are absent from the observed image, presumably because the X-rays are not monochromatic. (Note that this might constitute a practicable method of determining the wave lengths of X-rays, independent of the Avogadro number). As for the reflection experiments, they were performed with a polished bronze mirror, the rays being received by an ionization chamber. The measured reflecting power, for rays incident at 78.3° (measured from the normal) attains values as high as 35% for wave lengths between 100 and 62A, being less on both sides of this range; for rays incident at 73.8° the reflecting power is smaller and decreases more rapidly with decreasing wave length. Gouy suggests that these rays might be used in a microscope with concave mirrors, or possibly with lenses if a suitable refracting substance could

be found; thus making details perceptible which are some 50 times smaller than those at which diffraction now imposes the limit. [Holweck, C. R. *176*, pp. 570–573; 1923. G. Gouy, C. R. *176*, pp. 807-808; 1923.]

K. K. DARROW

Emission and Absorption of Halogens in the Visible and Ultraviolet regions.—The emission spectra of chlorine and bromine were obtained with Geissler tube discharges, and also with discharges between platinum electrodes embedded in silver halides. They are line spectra, varying with the intensity of the discharge and the temperature of the tube. The absorption spectra of these and of iodine, observed by conventional methods, display bands with fine structure in the yellow and green, other bands with fine structure in the far ultraviolet, and between these two regions a deep continuous absorption band, which widens as the temperature is raised, and eventually, (at least with bromine and iodine) begins to shrink again. The emission and absorption spectra are not complementary, and Beer's law is not valid. [A. L. Narayan and D. Gunnayya, (Vizianagram); Phil. Mag. *45*, pp. 827-830; 1923.]

K. K. DARROW

Absorption Spectrum of Potassium Vapor.—The molecules of a gas maintained at a sufficiently low temperature and not excited by electrical or other agencies are mostly in their normal or equilibrium state, and the frequencies absorbed by such a gas are those belonging to quanta with just sufficient energy to lift the valence electron of the molecule from its normal orbit into one or another of the outer orbits. With atoms of potassium (and of the other alkali metals) these frequencies are those of the principal series ($1s$-mp). Narayan and Gunnayya (like many other investigators before them) heat potassium in a straight steel tube closed by quartz plates, and photograph the spectrum of light from a carbon arc transmitted through it. As the temperature is raised more and more of the lines of the principal series appear; the increasing temperature is supposed to act only by increasing the density of the vapor and hence the number of absorbing atoms, not to alter the proportion of atoms in the normal state; this simultaneous changing of density and temperature is, however, rather unfortunate. At and beyond 800° C thirty members of the principal series were observed—four more than ever before—and at 950° C there were hints of absorption lines of the diffuse series ($2p$—md) which would mean a perceptible number of atoms in an abnormal or excited state. A band spectrum was also perceived. [A. L. Narayan and D. Gunnayya, (Vizianagram); Phil. Mag. *45*, pp. 831-834; 1923].

K. K. DARROW

SOME LABORATORY NOTES

By H. W. Farwell

A Simple Experiment in Mechanics

A variation of some one of our hard-worked experiments for demonstration frequently does as much good for the teacher as it does for the students. The following illustration has been of no little interest to my classes and may serve some one else.

After some of the usual discussion on friction we measure the force necessary to move a weight along the top of the lecture table. Then we compute the velocity which the weight would have in falling from a height, say of one foot. Then the distance the weight will move along the top of the table if it starts with the given velocity can be found. The weight is then put on a swinging support at the end of the table so that the support can be lifted away from the table and dropped. The support strikes the end of the table, delivering the weight to the table with a horizontal velocity, very approximately that which it would have in free fall from the initial height.

The data for the experiment are all fairly direct and the whole procedure exceedingly simple, so that altogether the performance helps materially in the presentation of the subject at this point.

The Microscope on the Optical Bench

Probably a great many men are familiar with the procedure described below, but the comments upon it have so surprised me that I venture to offer it for publication, as something not new, but frequently overlooked.

Years ago we used a telescope on the optical bench, usually for the purpose of locating virtual images, but the accuracy was not high, since the observer's skill in eliminating parallax on the cross hairs was severely tried. While working with small spherical surfaces I have used a compound microscope with much greater success. The preliminary axial adjustment is quite important but is not difficult. The rest of the manipulation is fairly simple, and can be carried out by elementary students.

For example, in finding the back focal length of a lens, the microscope is suitably mounted on the bench, set in focus on the surface of the lens, then moved back until the image of a distant axial point is properly

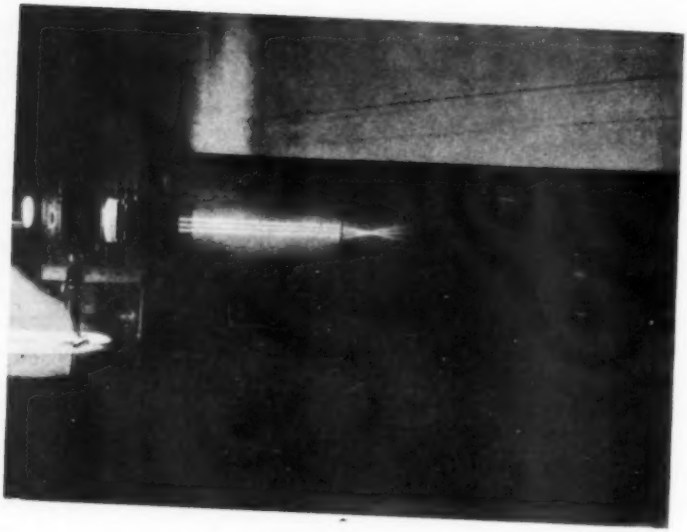

FIG. 1. *General arrangement.*

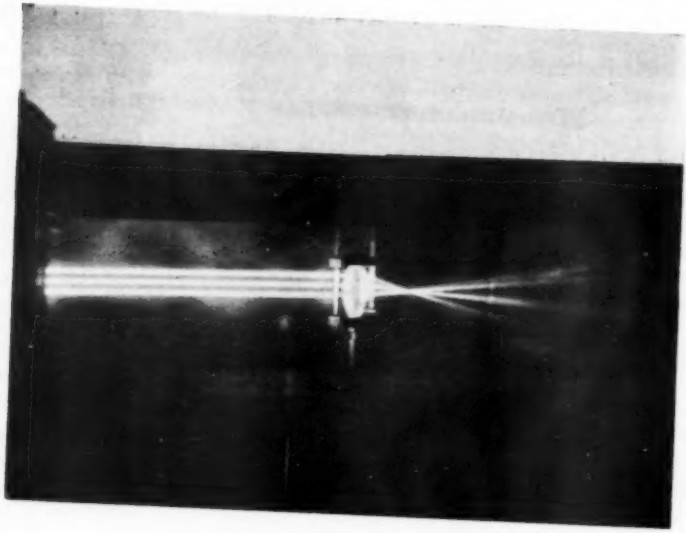

FIG. 2. *Close-up view.*

focused. The accuracy of setting depends on the microscope, of course, but settings within a tenth of a millimeter are not at all difficult. For a reflecting surface where the microscope would be in the way, a small right angle prism fastened to the objective enables one to set the miscroscope at right angles to the axis of the surface in question and the same procedure as before is employed.

ON THE USE OF THE OPTICAL BENCH IN THE SMOKE BOX

Those who have to deal with elementary students in optics probably realize the advantage in getting before these students the various ways of making visible the path of the energy stream. We find particularly advantageous an exercise in which the student actually studies the behavior of the rays when the whole bench is enclosed in a black box with glass front.

A small arc light outside gives a fair approximation for a point source, and in front of it can be placed a lens for obtaining a parallel beam or any other. A diaphragm with numerous small openings will permit separate "rays" to be examined. The results quantitatively are not accurate, and should not be called for, but qualitatively the exercise is well worth while.

This "smoke box" as we use it is simply a wooden box about four feet long, twelve inches high and six inches wide. (See Figs. 1 and 2.) An opening is cut in one end at the proper height for admitting the light from the source. It is essential that this and other openings be covered with glass, otherwise the air currents will greatly annoy the observer. The front of the box is glass, so arranged as to slide easily to permit of adjustment of the bench without too much disturbance. The bottom of the box is open so that it can be readily lifted from the table, leaving the bench free.

COLUMBIA UNIVERSITY,
NEW YORK CITY.

Annual Tables of Constants and Numerical Data—Chemical, Physical, and Technological (for 1913 to 1916 inclusive). Compiled and edited under the direction of the International Committee appointed by the Seventh Congress of Applied Chemistry. *4*, part I, xxxii+1–626 pages, 1921. *4*, part II, xxxiv+627–1377 pages, 1922. Each part $13.25 ($13.57 postpaid). The University of Chicago Press (Chicago), The Cambridge University Press (Cambridge, England), Gauthier-Villars and Co., (Paris). The publication of these important tables, discontinued during the war, has been

resumed and will be brought up to date in two volumes: Volume IV covering the years 1913 to 1916 inclusive, and Volume V, now in preparation, 1917 to 1921.

To those who are not familiar with the purpose and scope of these tables it may be remarked that they aim to present a compilation, properly classified and indexed, of all scientific data in Chemistry, Physics, Biology, and Technology, which has appeared during the period covered. There is no attempt to make the tables critical. This is left to the reader, who, by the aid of the references given, can readily trace all data to its source. The text, where text is needed, is in French. But this need not deter those who do not read French from using the tables. For the table of contents and of chapter headings, is in four parallel columns in French, German, English and Italian.

These tables are indeed a mine of information for those who are engaged in any phase of scientific or technological work. The material has been compiled from nearly three hundred and fifty journals in all branches of Chemistry, Physics and Engineering. There are forty-six chapter headings such as, to take several at random, Density, Specific Heats, Infrared Spectrum, Rotatory Power, Atomic Weights, Solubility, Colloids, Organic Chemistry, Animal Physiology, and Metallurgy. Under "Density" one finds some 53 pages of data, containing all the important determinations made during the four-year period. If, for example, one is interested in the density of Neon, one readily finds that two determinations were made, one by Aston in 1913, published in Proc. Roy. Soc., *85* A, p. 445, and the other by Leduc in 1914, published in Comptes Rendus, *158*, p. 864. Pages 708–712 contain atomic weight determinations on some forty elements, compiled from sixty-six different sources. Nine different series of determinations of Pb are quoted giving values which range from 206.046+.014 to 207.64. In the Chapter on Engineering one finds such sub-titles as "The Bursting Speed of Pulleys," "The Melting Point of Fire Bricks," or "The Physical Properties of Oils for Steam Turbines."

These illustrations may serve to show the scope of the work and the thoroughness with which the abstractors have completed their task. With the complete set of these tables at hand it is possible easily to ascertain what measurements have been made in any particular field since 1910, when the first volume was published, and to trace the data to original sources.

The international character of the work insures that it is without bias. The International Committee in charge is composed of over forty members from twenty-three countries. Financial support, in the form of subsidies, has been received from some sixty different sources (such as societies, industrial firms, individuals, and governments) in Belgium, Denmark, Great Britian, The United States, France, Holland, Italy, Japan, Argentine, Roumania, Russia, and Sweden. It is to be hoped that the political leaders of the world may ultimately learn, as have scientists, the value of international coöperation. F. K. RICHTMYER

DESIGN OF A KUNDT'S TUBE

By Otto Stuhlman, Jr.

The usual form of Kundt's apparatus for determining the velocity of longitudinal vibrations in metal rods has been found to be of such unsatisfactory design and construction that the above modification of a fool-proof, inexpensive and simple design has been constructed and is now in use in its fourth year, giving excellent results at minimum cost of up-keep.

It differs from the usual catalogued type, through the absence of breakable, non-alligned parts. The usual vise for holding the vibrating

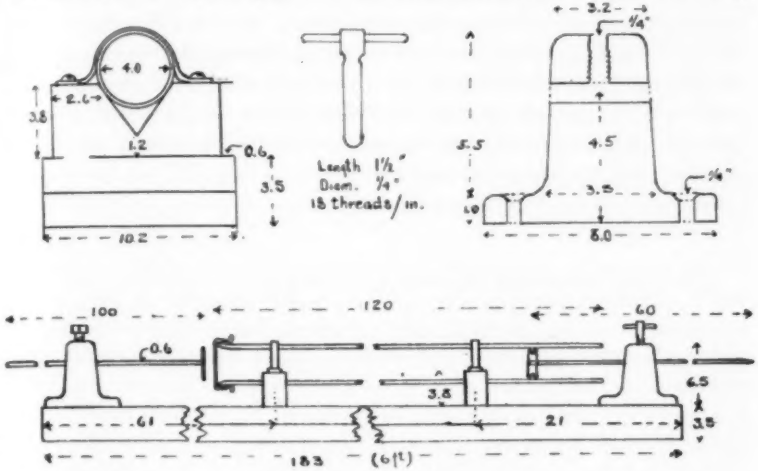

Fig. 1. *Kundt's tube design. Dimensions are in centimeters except where otherwise specified.*

rod, so susceptible to breaking loose from the frame is replaced by a truncated cone of cast iron, permanently and rigidly screwed to the wooden frame. The design is of a convenient size to afford a good hand-hold and is alligned with the tube and piston head when assembled.

The base is made of two pieces of hard wood to prevent warping. The four centimeter glass tube rests upon two wooden supports as sketched, the shoulders being about 2 cm thick. The tube is held in place by two metal strips as indicated. The vibrating rod is about 100 cm long and is held rigidly in place by the truncated cast iron support, fastened at its mid point with a quarter inch, square-headed standard bolt. The

2.54 cm disk at one end rests against the rubber diaphragm. This drum head (dentist's rubber dam) is held in place by rubber bands. They are prevented from slipping by the slightly flanged end of the glass resonance tube. This glass tube 120 cm long and 4 cm in diameter can be slightly flanged at both ends during the heat treatment for removing the sharp, broken cutting edge.

The piston head and rod rest in a similar cast iron support as the vibrating rod. It is interchangeable except for a thumb screw replacing the square headed bolt of the same dimensions. The piston head is made of wood, spool shaped, one cm thick, wound with cotton twine. A flat headed countersunk screw holds it to the rod, thus presenting a vertical, air tight reflecting surface. The thunb screw holding the piston rod in place allows one to change the length of the resonating air column and tune for maximum resonance with great ease.

For storage the rods are loosened, pushed into the glass tube, screwed down to prevent loss of rods and parts and reduced to the size of the wooden base 120×10.2 cm (6 ft×4″).

THE UNIVERSITY OF NORTH CAROLINA,
CHAPEL HILL, N. C.

The Mass-spectra of Chemical Elements.—By partially dissolving the gelatine, photographic plates have been produced with high concentration of grains at the surface, which are very sensitive to material rays. Six more elements have been analyzed with the mass-spectrograph:

	At. No.	At. Wt.	Isotopes		At. No.	At. Wt.	Isotopes
Al	13	26.96	27	Se	34	79.2	74, 76–78, 80, 82
Fe	26	55.84	56, (54?)	Sn	50	118.7	116–120, (121?), 122, 124
Ni	28	58.68	58, 60	Sb	51	121.77	121, 123

Isotope 39 of Cl does not exist; 124 and 126 are added to the seven previously known types of Xe. The masses 78, 80, and 82 are common to Se and Kr (isobaric nuclei). Small but definite deviations from the whole-number rule have been found in Sn as compared with xenon.

Metallic chlorides proved a failure for positive-ray work; free Cl liberated volatile compounds of every metal in the apparatus. A number of volatile metallic compounds are discussed. Iron and nickel carbonyl, lead ethide, zinc methide, tin tetramethide, tellurium chloride, beryllium acetate, and antimony methide may be of some interest to those working on critical potentials or absorption spectra.

A table of all known isotopes is included. [F. W. Aston, Phil. Mag. *45*, p. 934; 1923.] ARTHUR E. RUARK

A CONSTANT PRESSURE BLOWPIPE.

By H. G. Becker

Laboratory blowpipes have hitherto been largely designed with a view to being used with a foot bellows, since the latter has been the chief source of air pressure in the laboratory. However, in the modern well-equipped laboratory the tendency is to replace the bellows entirely by the use of power-driven blowers, either in the form of centrally situated large units or smaller portable sets.

This change has accentuated the defects inherent in the old form of blowpipe, which arise largely from the fact that it requires a continually varying air pressure when the size of the flame is being varied. The use of the foot bellows allowed the operator to adjust the pressure to some extent by the rate at which the bellows was worked, but when the power blower is used no such variation is possible. The only way to get over the difficulty is to keep the blower running so as to produce the maximum pressure required, and produce all lower pressure by regulation with a tap.

Each change in size of flame thus necessitates two distinct operations which must be made by trial until the correct result is obtained. When an ordinary blowpipe flame, correctly adjusted, has to be changed to a larger one the gas tap is first turned thus producing a semi luminous flame, and the air tap must then be adjusted until the flame is again correctly aerated. Both taps must be adjusted by trial and error, and two or three trials are sometimes necessary to obtain a flame of the desired size.

Attempts have been made to get over this difficulty by combining the regulation of the gas and air in one tap. The effect of this is to limit the instrument to a very narrow range of flame sizes, since, if the air jet is correctly proportioned for a small flame, opening the tap has the result of producing a luminous flame, as the small jet cannot supply sufficient air for the larger flame. Fig. 1 shows such an instrument with the small flame in use operating on air at constant pressure, and Fig. 2 shows the result of turning the tap to get a larger flame; the flame has become luminous and can only be made non-luminous by a greatly increased air pressure. It is clear then that a blowpipe, to be used efficiently on a constant gas and air pressure, must have a variable air jet, since each size of flame demands a suitably proportioned air jet.

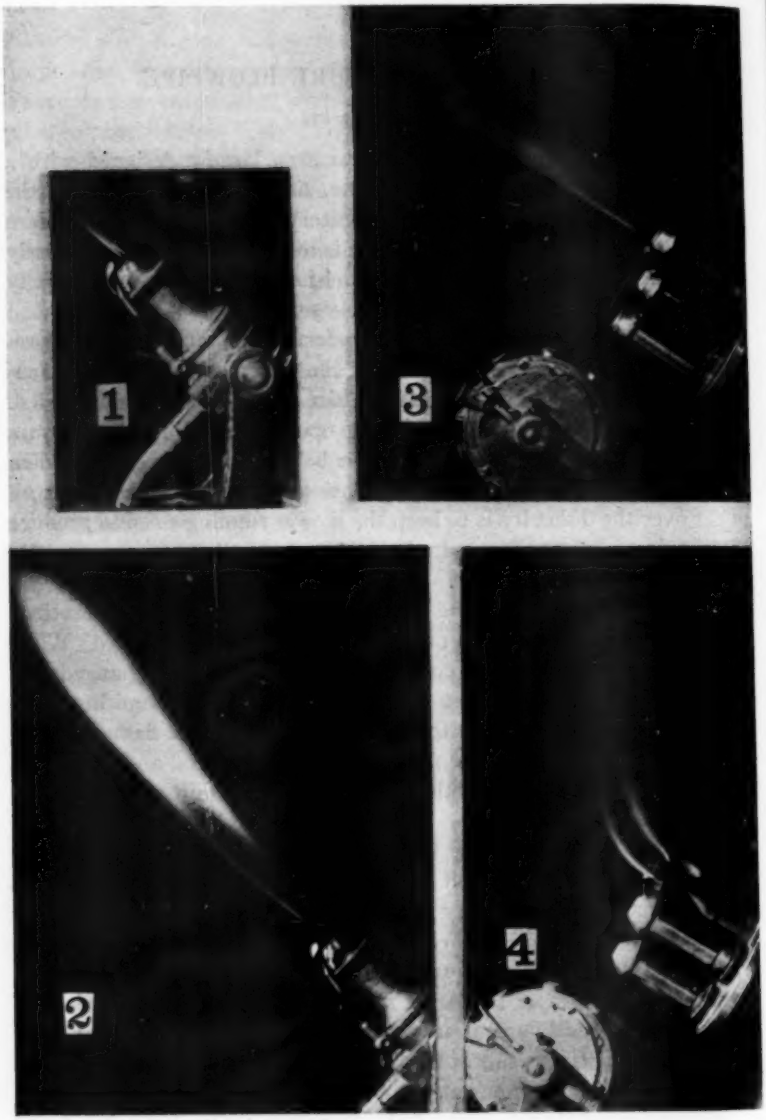

FIGS. 1-4. *Photographs showing alteration of character of flame with change in size or shape.*

The use of incorrectly proportioned jets has also led to the reproduction of the tubular form associated with the first blowpipe in all succeeding designs. Fig. 3 shows a modern blowpipe with interchangeable flame tubes of the usual type. The use of sliding tubes of this type is intended to get rid of the yellow tip which plays round the nozzle of the blowpipe when an incorrectly proportioned air jet is in use. With correctly proportioned air jets the yellow tip does not appear, and the sliding flame tube is consequently unnecessary. The use of four large flame tubes of this kind gives rise to a very large and awkward instrument, without any corresponding advantage, for the gas and air pressure have still to be controlled by taps. Fig. 3 shows the blowpipe operating correctly on the largest flame, and Fig. 4 shows the result of turning the disc to bring the flat flame into operation. It will be seen that the latter has become luminous, as it will not operate on the same air pressure without re-adjustment of the gas or air by taps.

The recognition of these two facts, namely, the necessity for a variable jet, and the superfluity of the flame-tube, has led to the design of a blowpipe which is specially adapted to use with power blowers. It consists of a number of small gas-chambers and air-jets arranged radially round a cylinder which can be rotated on a horizontal axis, each gas-chamber and air-jet being adjusted to produce a certain size and shape of flame. This secures that each size of flame is blown with an air jet correctly adjusted to its needs.

The photographs show the wide variety of sizes and shapes of flames which can be produced in this way by mere rotation of the cylinder without any alteration in the pressure of the gas or air supply. Fig. 5 shows the smallest flame in operation on an air-pressure of seven inches of water, Fig. 6 shows an intermediate size, and Fig. 8 the largest flame, while Fig. 7 shows the flat flame in which a piece of wire is held to indicate its width. All these flames are produced by the rotation of the cylinder and there is no element of trial and error in the process, as the proportion of gas and air is determined by the size of the air jet in each case.

A sectional drawing of the blowpipe is given in Fig. 9. The small gas chambers which replace the flame-tubes are formed by radial partitions in the body of the instrument, and have flame openings which are lined with steatite. The steatite prevents the blowpipe getting too hot with prolonged use, and it also prevents the corrosion of the usual brass tip which is caused by the impurities in the gas. The short air jets are screwed with a standard thread so as to be interchangeable, and each

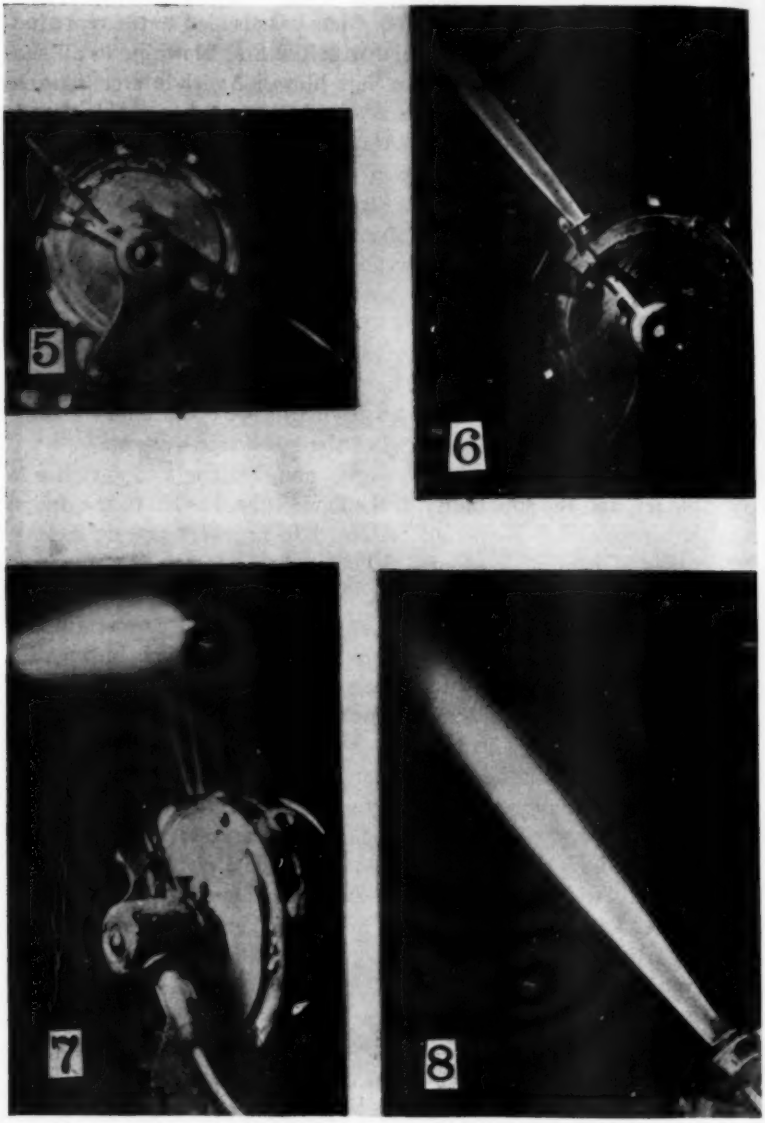

FIGS. 5-8. *Photographs showing constancy of character of flames of different sizes and shapes.*

one is bored with a hole of suitable size for the flame with which it is to be used, while the holes *m*, *m*, control the amount of gas admitted to the gas-chambers, thus regulating the size of the flame. Provision is made for eight different sizes of flame this number being found sufficient for all purposes, and the ninth gas chamber is modified so as to produce a flat flame by making the air-jet and the steatite tip of a particular shape.

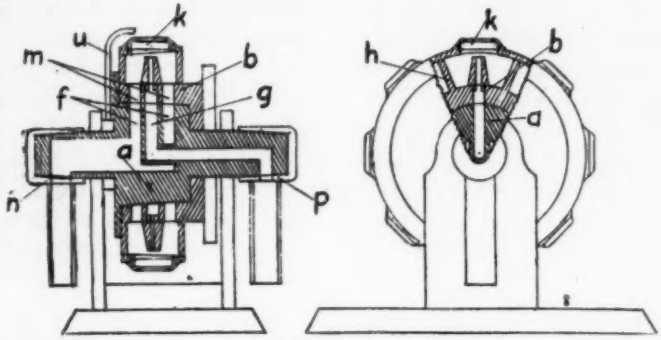

FIG. 9. *Sectional drawing of blowpipe.*

It will be seen that without the abandonment of the usual tubular flame tube the provision of a separate jet for each size of flame would not be possible, as an instrument with nine flame tubes projecting from it would be altogether too unwieldy. The same principle is readily

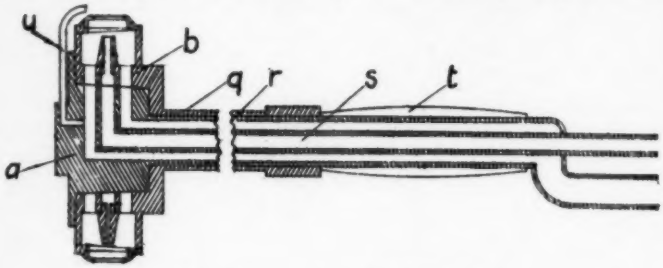

FIG. 10. *Blowpipe, as adapted for hand use.*

applicable to the hand blowpipe, as shown in Fig. 10 thus producing a convenient instrument for working in awkward positions. In this form the rotating member is fixed to a knurled sleeve which can be rotated with the finger and thumb, so that the blowpipe is completely controlled by one hand.

In addition to the correct regulation of the flames, the different sized jets have the advantage of producing standard flames, which can be reproduced at any time by using the same gas and air pressure. This enables the worker to note which flame is most suitable for some particular operation, and to use it whenever that operation occurs, thus leading to uniform results.

Owing to the fact that the gas and air passages are very short and straight, the blowpipe will give a larger flame than any other type on the same gas supply, the friction of the gas and air being reduced to a minimum. For the same reason the air pressure required to operate all the flames is very much lower than that commonly in use for blowpipe work. The instrument shown in Figs. 5 to 8 is adjusted to work on an air pressure of only seven inches of water while the pressure usually used to operate the ordinary blowpipes is about eighty-three inches (3 lbs. per sq. in.) This represents a considerable saving in the power necessary to compress the air for a number of blowpipes.

CHEMICAL LABORATORY,
COLLEGE OF SCIENCE,
DUBLIN.

Cathodo-Luminescence and its Relation to States of Molecular Aggregation.—Ewles subjected a number of salts to cathode ray bombardment, unfortunately in an old style gas filled X-ray tube with the salts spread on a target in the focus of a concave cathode. He gives for each salt the least voltage at which he perceived luminescence (by visual observation). While admitting that this must depend on the sensitiveness of the eye, he says "in many cases the luminescence came in so sharply as to leave no doubt as to the existence of a very definite minimum [voltage]." The values range from 350 for zinc oxide, prepared in a certain manner, to 5200 for tungsten trioxide. Some of the salts were prepared and treated in a variety of ways, and the threshold voltage and the color of the luminescence were found to differ considerably. For example, when zinc oxide was prepared by igniting zinc hydroxide precipitated from a hot solution, it gave a red and green luminescence beginning at 400 volts; but when precipitated from a cold solution, it gave a bluish-white luminescence beginning at 850 volts. Ewles also investigated fourteen salts which have transformation points in the range of temperature between room-temperature and 1200°, and which exhibit cathodo-luminescence at room temperature. In every case the luminescence ceases when the transformation to the higher temperature modification takes place. This indicates that luminescence is a property of molecules in groups, and so must absorption be if absorption and luminescence are correlated. [J. Ewles (Leeds Univ.), Phil. Mag. *45*, pp. 957-968; 1923.] K. K. DARROW